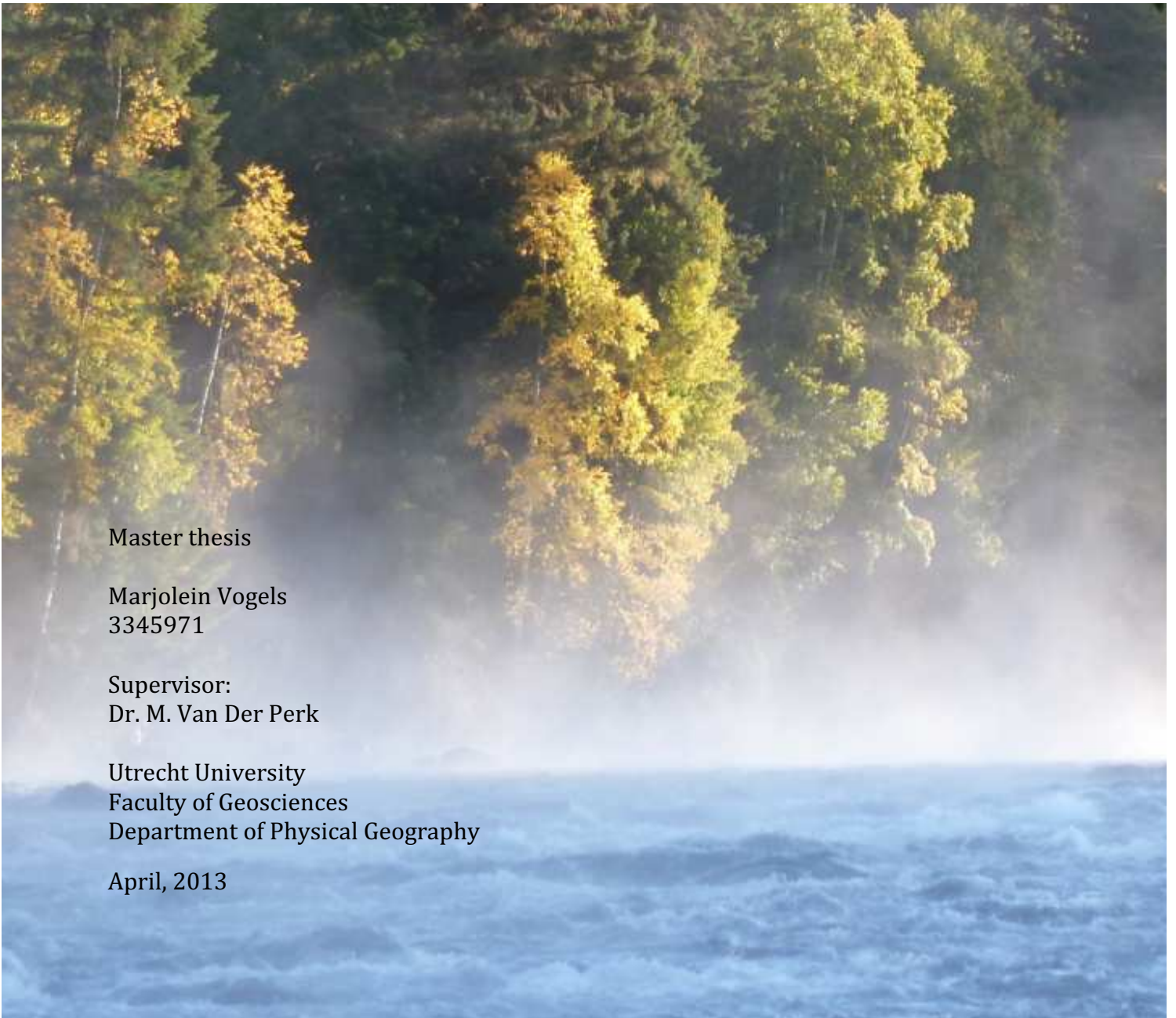




Effects of past and present mining on fine sediment geochemistry of floodplain soils, Horsefly River, BC, Canada



Master thesis

Marjolein Vogels
3345971

Supervisor:
Dr. M. Van Der Perk

Utrecht University
Faculty of Geosciences
Department of Physical Geography

April, 2013

Cover: Quesnel River, Likely, British Columbia, Canada (2012)



Abstract

Active and abandoned mine sites are known to be a dominant source of metal contamination in fluvial systems worldwide. Small-scale mining of minerals like gold, copper and zinc has been prevalent in interior British Columbia, Canada since the 19th century. The region is also characterized to provide an important habitat for wildlife of which the river gravel beds for several salmon species are a prime example. This thesis investigated the impact of past and present mining on floodplain soils of the Horsefly River, BC, Canada. The abandoned Black Creek placer mine was specifically studied.

Floodplain cores were analysed for metal distributions of arsenic, cadmium, zinc, lead, selenium and copper, elements often associated with gold placer mining. The anthropogenic part (residual part) of these metal concentrations was determined by subtracting that part stemming from local geology from the total concentration measured. The concentrations representing local geology were determined using a normalization procedure combined with regression analysis. The cores were also analysed for ²¹⁰Pb abundance from which age-depth profiles were established. Three floodplain cores were analysed this way: (1) upstream of the Black Creek inlet into the Horsefly River, (2) downstream of the Black Creek inlet, (3) at the Horsefly delta (55 kilometers downstream).

It was concluded that there were no present effects of the Black Creek mine on the fine sediment geochemistry of the Horsefly floodplain. A past mining response of this mine was reflected in a peak in arsenic related to the early 1930s. Present day elevated concentrations of selenium in the catchment indicated a further upstream located source unrelated to the Black Creek mine and this signal was also present in the Horsefly delta. Furthermore, elevated concentrations of lead, cadmium and zinc were present in the Horsefly delta, which were absent in the upper Horsefly catchment. These concentrations were not related to mining activities.

Contents

Abstract	3
List of figures	6
List of tables	8
Acknowledgements	9
1. Introduction.....	10
2. Sources, transport and fate of heavy metals	13
2.1 Mining, a source of heavy metals and associated contamination	13
2.1.1 Surface mining and underground mining.....	13
2.1.2 Acid mine drainage.....	14
2.1.3 The use of mercury in gold mining and associated environmental contamination.....	17
2.1.4 The use of cyanide in gold mining and associated environmental contamination.....	17
2.2 Dispersion of heavy metals in the environment	18
2.3 Sediment composition in floodplain soils	21
2.3.1 Grain size distribution and cation exchange capacity	21
2.3.2 Redox potential and pH.....	21
2.3.3 Correlations between metals	22
2.4 Quantification of the impact of mining.....	23
3. Study area.....	25
3.1 Geology.....	27
3.1.1 Regional geology	27
3.1.2 Horsefly geology.....	27
3.2 Geomorphology of the Horsefly River area.....	29
3.3 Climate.....	29
3.4 Mining history of the Horsefly River area	30
3.4.1 The Black Creek gold mine	30
4. Methods	32
4.1 Sample collection and analysis.....	32
4.1.1 Sample collection	32
4.1.2 Sample storage and preparation.....	33
4.1.3 Sample analysis	33
4.2 Data analysis.....	34
4.2.1 Lowest quantile regression	34
4.2.2 Calculation of residual concentrations.....	35

4.2.3	Establishing age-depth profiles	35
4.2.4	Manganese and iron cycles	36
5.	Results and discussion.....	37
5.1	Regression analysis.....	37
5.1.1	Assessment of the baseline concentrations.....	37
5.1.2	Assessment of the regression dataset used (lowest quartile)	38
5.2	Sediment characteristics	38
5.2.1	Organic matter and aluminum content.....	38
5.2.2	Particle size and aluminum content	41
5.2.3	Age-depth profiles and sedimentation	42
5.2.4	Manganese and iron depth profiles	43
5.3	Metal depth profiles.....	46
5.3.1	The upstream (E1) and downstream (B1) core	46
5.3.2	The delta core.....	52
5.4	Interpretation and discussion	58
5.4.1	Response of metal contamination to mining activities in the Horsefly floodplain	59
5.4.2	Response of metal contamination to mining activities in the Horsefly delta	62
6.	Conclusions.....	67
7.	References.....	68
8.	Appendices	73
A1	Metal depth-profiles	73
A2	Regression dataset	76
A3	Qualitative descriptions of core E1, B1 and D1.....	82
A4	Horsefly watershed map	85
A5	Geology of the Central Quesnel Belt map.....	86
A6	Grain size dataset.....	89
A7	Organic matter dataset	90
A8	Radionuclide dataset.....	92
A9	Geochemical data.....	93

List of figures

Figure 2.1: Mountaintop mining for coal extraction in Elk Valley, British Columbia. A clear example of how surface mining results in ecological degradation.

Figure 2.1: Rates of pyrite oxidation with and without iron-oxidizing bacteria in small columns maintained at different oxygen partial pressures.

Figure 2.3: A seep that discharges acid mine drainage at the Friar Tuck site near Dugger, India, illustrates the effect of iron oxyhydroxide precipitates on stream bed sediments.

Figure 2.4: Pre- and post-mining conditions of the Britannia mine and necessary pollution prevention measures.

Figure 2.5: Cu concentrations in fine-grained sediments in the Fal estuary system in southwest England decline progressively from the river, through the estuary and toward the sea, due to the process of mixing with uncontaminated sediment.

Figure 2.6: Basin diagram showing the visual terms used in the model to predict downstream dilution of contaminated sediment.

Figure 2.7: Concentrations of Cu and Pb in coastal zone sediments (USA) normalized by Al concentrations, which results in the baseline (local geology flux).

Figure 3.1: Drainage basin of Quesnel Lake from the National Topographic Survey 1:250,000 map 93A.

Figure 3.2: Horsefly River near Horsefly Bridge just below the confluent with McKinley Creek.

Figure 3.3: Map of the accreted terranes in British Columbia (Source: Ricketts, 2008).

Figure 3.4: A sketch from Lay (1932) showing the Miocene channels and location of the mines: Miocene shaft (1897-1900), Wards Horsefly (1864-1913) and Hobsons Horsefly mine (1890-1899). The Black Creek is also visible following the Horsefly River in the eastern direction.

Figure 3.5: Mean, minimum and maximum daily discharge for the Horsefly River above McKinley Creek (08KH010). Statistics correspond to 47 years of data from January 1955 to December 2006.

Figure 3.6: Left: Black Creek canyon with remnants of old sluice boxes. Right: Wall of the lower pit of the Black Creek mine.

Figure 4.1: The image shows the cores upstream and downstream (meander-bend-area) of Black Creek.

Figure 4.2: The image shows the location of the delta core on the Horsefly delta at Quesnel Lake, about 55 kilometers further downstream of Black Creek.

Figure 5.1: Organic matter content over depth for the upstream (E1), downstream (B1) and delta (D1) core.

Figure 5.2: Aluminum content over depth for the upstream (E1), downstream (B1) and delta (D1) core.

Figure 5.3: Correlation between aluminum and organic matter for the upstream (E1), downstream (B1) and delta (D1) core. The blue scatter plot represents the lower part of each core and the red scatter plot the upper part. The division between the upper and lower part of a core is based on sight i.e. where does the correlation between organic matter and aluminum change from positive to negative.

Figure 5.4: Aluminum and clay fraction for the downstream (B1), upstream (E1) and delta (D1) core.

Figure 5.5: Established age-depth profiles for the upstream (E1), downstream (B1) and delta (D1) core.

Figure 5.6: ^{137}Cs profiles for the upstream (E1), downstream (B1) and delta (D1) core. Note the significant peak in the delta core (D1) at 18.5 cm depth.

Figure 5.7: Observed manganese and iron concentrations in the upstream core (E1).

Figure 5.8: Observed manganese and iron concentrations in the downstream core (B1).

Figure 5.9: Observed manganese and iron concentrations in the delta core (D1).

Figure 5.10: Iron and manganese baselines from regression analyses for the upstream (E1) and downstream (B1) cores.

Figure 5.11: Iron and manganese baselines from regression analyses for the delta core (D1).

Figure 5.12: Left: Copper baseline and confidence levels in a scatter plot with total concentrations of the upstream (E1) and downstream (B1) core. Right: depth profile of the copper residual concentrations in the upstream (E1) and downstream (B1) core.

Figure 5.13: Left: Zinc baseline and confidence levels in a scatter plot with total concentrations of the upstream (E1) and downstream (B1) core. Right: depth profile of the zinc residual concentrations in the upstream (E1) and downstream (B1) core.

Figure 5.14: Left: Selenium baseline and confidence levels in a scatter plot with total concentrations of the upstream (E1) and downstream (B1) core. Right: depth profile of the selenium residual concentrations in the upstream (E1) and downstream (B1) core.

Figure 5.15: Left: Cadmium baseline and confidence levels in a scatter plot with total concentrations of the upstream (E1) and downstream (B1) core. Right: depth profile of the cadmium residual concentrations in the upstream (E1) and downstream (B1) core.

Figure 5.16: Left: Lead baseline and confidence levels in a scatter plot with total concentrations of the upstream (E1) and downstream (B1) core. Right: depth profile of the lead residual concentrations in the upstream (E1) and downstream (B1) core.

Figure 5.17: Left: Arsenic baseline and confidence levels in a scatter plot with total concentrations of the upstream (E1) and downstream (B1) core. Right: depth profile of the arsenic residual concentrations in the upstream (E1) and downstream (B1) core.

Figure 5.18: Left: Copper baseline and confidence levels in a scatter plot with total concentrations of the delta core (D1). Right: depth profile of the copper residual concentrations in the delta core (D1).

Figure 5.19: Left: Zinc baseline and confidence levels in a scatter plot with total concentrations of the delta core (D1). Right: depth profile of the zinc residual concentrations in the delta core (D1).

Figure 5.20: Left: Selenium baseline and confidence levels in a scatter plot with total concentrations of the delta core (D1). Right: depth profile of the selenium residual concentrations in the delta core (D1).

Figure 5.21: Left: Cadmium baseline and confidence levels in a scatter plot with total concentrations of the delta core (D1). Right: depth profile of the cadmium residual concentrations in the delta core (D1).

Figure 5.22: Left: Lead baseline and confidence levels in a scatter plot with total concentrations of the delta core (D1). Right: depth profile of the lead residual concentrations in the delta core (D1).

Figure 5.23: Left: Arsenic baseline and confidence levels in a scatter plot with total concentrations of the delta core (D1). Right: depth profile of the arsenic residual concentrations in the delta core (D1).

Figure 5.24: The percentage residual concentration of the total concentration for the downstream (B1) core for arsenic to compare the peak occurring at 17.5 cm depth to its age.

Figure 5.25: The percentage residual concentration of the total concentration for the downstream (B1) and upstream (E1) core for selenium. Included is a moving average of 15 and the age-depth profile.

Figure 5.26: The percentage residual concentration of the total concentration for the delta core (D1) including the age-depth profile.

Figure 5.27: Moving average of 15 of the percentage residual concentration of total concentration in the delta core.

List of tables

Table 4.1: Coordinates of the cores taken from the Horsefly River's floodplain.

Table 5.1: Regression coefficients and baselines for the upstream (E1) and downstream (B1) core.

Table 5.2: Regression coefficients and baselines for the delta core (D1). Note: Cd and Cu regressions are not statistically significant.

Table 5.3: Minimum, maximum and average organic matter content for the upstream (E1), downstream (B1) and delta (D1) core.

Table 5.4: Minimum, maximum and average aluminum content for the cores B1, E1 and D1.

Table 5.5: Minimum, maximum and average manganese concentration and iron content for the upstream (E1), downstream (B1) and delta (D1) core.

Table 5.6: Average total concentrations of Cd, Pb, Zn and Se are compared to literature and other research. Canadian sediment quality guidelines (CCME) are given for Cd, Pb and Zn. Included is a criteria for Se from Luoma and Rainbow, 2008. The comparison with other research in the area includes Clark (2013), Smith and Owens (2010) and Karimlou (2011). The average concentration in the upper 20.5 cm is chosen, since the concentration stagnates above this depth.

Acknowledgements

This MSc thesis would not have been possible without the guidance and the help of several people who in one way or another contributed in the preparation and completion of this study. First I would like to thank my supervisor Marcel van Der Perk from Utrecht University for his guidance and support while writing this thesis. The thesis was carried out at the UNBC Quesnel River Research Center, which is located in Likely, British Columbia (Canada). I would like to thank everybody from this research center for their help and making this project feasible. Phil Owens and Ellen Petticrew, thank you for your guidance, coordination of the project and also your visit to the Netherlands to assist me with the data interpretation. It was all much appreciated. I also thank the possibility of carrying out this project to my field partner, Deirdre Clark. Furthermore, I would like to express my gratitude for the financial support of the Association for Canadian Studies in the Netherlands and to Guy Nesbitt for his help and information.

Last but not least, it gives me great pleasure to finally be able to acknowledge my family for their support during all those years.

1. Introduction

Active and abandoned mine sites represent a major environmental problem for fluvial systems worldwide (Du Laing et al., 2007; Du Laing et al., 2009) and the pollution relating to mining is of particular concern for the effect on water and sediment quality (Luoma and Rainbow, 2008). Most of the sources of mining are point sources and examples are tailings and mill effluents. However, not only the point sources of active or abandoned mines are of concern: secondary contamination is the result of the release of heavy metals from alluvial deposits (floodplains). These deposits are diffuse sources of heavy metals for long periods of time (Vandecasteele et al., 2005; Grybos et al., 2007). Mining related pollution does ultimately leave the watershed after several deposition and erosion cycles. The key to understanding and predicting metal transport and environmental availability, as well as to identifying sources and sinks, lies in identifying and quantifying the metal associations in sediments and the reactions that occur between sediment, water, and biota (Horowitz, 1991). Since the environment is ever dynamically changing it is difficult to determine the anthropogenic part of a metal concentration as well as identifying the several natural aspects relating to that concentration. E.g. changing hydrologic conditions influences the amount of sediment deposited on floodplains and rainfall events in certain areas of the catchment result in different chemical compositions of sediment transported and likewise deposited. Also, in the floodplain sediments itself are a number of factors responsible for the way trace metals are distributed and related to the geochemical, physical and biological heterogeneity of the sediment column, such as biota, sediment composition and groundwater fluctuations. The metal mobility in floodplain soils is determined to a large extent by a range of factors, such as redox potential and pH, adsorption/desorption/precipitation-processes, metal content, salinity, clay content, plant growth, presence of organic matter, sulphur (S), and carbonates (Du Laing et al., 2007). To retain high levels of water quality, it is of vital importance to understand the transport mechanisms of sediment and associated contaminants. Key processes that determine the transport and the physico-chemical composition of sediments are the result of relationships between hydrology, erosion and transformation processes, but also climate, topography and geology.

British Columbia has been one of the major mining areas throughout the world since the mid-1800s and historically, British Columbia's vast mineral resources have contributed extensively to the province's growth and development (Ministry of energy, mines and natural gas, BC). Mining practices are generally characterized by its consumption, diversion and pollution of water and is one of the main sources of chemical threats to groundwater quality in British Columbia according to the 1993 British Columbia's State of the Environment Report. Enormous amounts of waste rock are generated for small amounts of gold, copper and other valuable metals. It was estimated that there were over 240 million tonnes of acid-generating waste rock and 72 million tonnes of acid-generated mine tailings in British Columbia in 1993 (BC State of the Environment Report, 1993). Examples of water pollution originating from such tailings and waste rock in British Columbia are: (1) the Britannia Copper mine north of Vancouver draining acidic water into the Howe Sound fjord network and (2) the Mount Washington mine on Vancouver Island where sulphide bearing ores lie exposed to water and air in open pits along with 130,000 tonnes of waste rock ultimately draining toxic copper into the whole Tsolum River watershed. As British Columbia is also known for its salmon habitat, the impact of mining can be devastating for its ecosystems and the entire food chain of which salmon is the backbone. Effects of metal mining effluents, and metals in general on fish are extensively studied and include behavioral changes, such as avoidance of effluent streams during migration runs, affect their

immune system and decreases survival, growth and reproductivity (Dubé et al., 2005). Especially copper is particularly harmful to the sensory systems of salmon and decreases the ability of young salmon to escape from predators and the ability of adult salmon to find their spawning grounds. In the study of Dubé et al. (2005) significant negative effects were also observed on the survival and growth of Atlantic salmon due to increasing concentrations of metal mining effluents. Another threat to the salmonid species in British Columbia (and other mining related regions) is that the excessive sediment generated by mining practices blocks the oxygen supply to salmon eggs in the gravel beds and therefore has a major impact on survival rates of salmon. Thus, not only the chemical alteration that heavy metals cause to ecosystems is of concern, but also the input of associated sediment.

This MSc research project is a pilot study of the Horsefly River area and was carried out at the UNBC Quesnel River Research Center, which is located in Likely, British Columbia. The aim of this study is to investigate the effects of the abandoned Black Creek mine on the Horsefly River system, British Columbia, Canada, which is part of the Quesnel watershed. The Black Creek, which drains the mine, enters the Horsefly River 55 kilometers upstream of the Horsefly delta in Quesnel Lake. Smith and Owens (2010) concluded that concentrations of selenium, copper and arsenic related to mining land use are elevated in parts of the Quesnel watershed area. The Horsefly river system is an important ecosystem as it is a major spawning habitat for several salmon species, which use the numerous gravel beds to bury their eggs. As the majority of metals have a strong affinity with particulates, especially the finer fraction (Horowitz, 1991; Loring, 1991; Luoma and Rainbow, 2008; Van der Perk, 2006), the downstream transport of metals is mainly in the particulate form under normal conditions (neutral pH) due to the low solubility of metals (Helgen and Moore, 1996). During floods these particulates will enter the floodplain and will be deposited over the years resulting in a diffuse source of contamination for long periods of time. The deposited sediment over the subsequent years will provide a history record of sediment geochemistry and possible contamination in the Horsefly watershed.

Objective

The objective is to identify the effect of mining on the fine sediment geochemistry on the floodplains of the Horsefly River using sediment coring. The sediment cores are processed, dated and analyzed for total concentrations of heavy metals. The most common heavy metals associated with gold are studied: arsenic, cadmium, lead, zinc, selenium and copper (LaPierre et al., 1985). Peaks in metal concentration are possibly linked to active mining periods. Upstream- and downstream cores of where the Black Creek enters the Horsefly River will be compared to assess the impact of this small and nowadays abandoned mine, for past, present and future times on floodplain geochemistry. As the delta receives sediment from the entire Horsefly catchment, it will be investigated whether the mining signal from the Black Creek mine is large enough to be traced back in the delta, or if other processes related to anthropogenic activity are going on in the catchment. A storyline is provided to assess the mining history of the Horsefly river system to identify active and abandoned mining periods and other mines in the catchment.

Research questions

1. Can active mining periods of the Black Creek mine be related to peaks in heavy metal concentration in the downstream floodplain and with which metals is the downstream floodplain core enriched?
2. In what way and in which metals does the mining impact manifest in the downstream floodplain sediments?
3. Is the impact of the Black Creek mine traceable in the delta of the Horsefly River?

Thesis outline

A short literature study is provided about mining as a source of heavy metals and the transport and fate of these metals. It discusses the various processes and mechanisms (natural and/or anthropogenic) that affect the metal distribution on floodplains, because chemical, biological and physical processes are able to alter concentrations. It will serve as an introduction and a guideline for the reader. This section is followed by: (1) detailed information about the study area and its mining history, (2) the methodology of how the impact of mining is assessed in this study, and, (3) the results, discussion and conclusion addressing the research questions and fulfilling the objective of this study.

2. Sources, transport and fate of heavy metals

2.1 Mining, a source of heavy metals and associated contamination

Areas that have been inhabited by humans for long times are prone to have serious metal contamination, because there are many anthropogenic sources of heavy metals, such as sewage sludge, manure, phosphate fertilizers, atmospheric fallout, leaching from building materials, deposition of contaminated river sediments, and direct domestic or industrial discharges and disposals (Van der Perk, 2006). One of the most important anthropogenic input of heavy metals is often related to mining practices in ore bodies. Exposing such ore bodies to oxygen ultimately results in an enhanced mobility of heavy metals and a widespread dispersion, which depends on the local hydrology and sediment transport. This section will explain the main sources of heavy metals related to mining.

Sulphide (more specifically pyrite or porphyry) ore bodies constitute more than half of the major source of several common metals, including copper, nickel, lead and zinc (Luoma and Rainbow, 2008). The highest concentrations of trace elements are generally found in areas near such ore deposits (often associated with volcanic activity) and they may give rise to a natural enrichment in soil, groundwater, stream water and stream sediment (Van der Perk, 2006). These deposits are often exploited in mines as they are economically very beneficial.

Mining generally involves six stages: (1) exploration, (2) development, (3) extraction, (4) concentration, (5) processing or refining and (6) closure and, historically each advance in mining technology increased the potential for dispersing contamination (Luoma and Rainbow, 2008). As exploration (1) is about orientating potential ore bodies, the main impacts are generally low. Development (2), however, includes the excavation of overlying waste rock, top soil and often, deforestation. Extraction (3), concentration (4) and smelting (5) are the operations that generate the most environmental contamination. Concentration (4) involves milling to a finer particle size and disposal of waste rock (tailings), which are potentially hazardous as sulphuric acid can be formed after oxidation (section 2.1.2). Tailings are potentially the most damaging for ecosystems, as large quantities of such waste rock are produced compared to the product needed. Especially surface mining results in severe ecological degradation (section 2.1.1). Separation of the desired product is usually done using chemical extraction, which can involve mercury or cyanide (section 2.1.3 and section 2.1.4).

2.1.1 Surface mining and underground mining

Surface mining is a much larger source of contaminated sediment compared to underground mining and results in large amounts of waste rock, in which oxidation processes lead to acid mine drainage. Surface mining takes place on the land surface and has therefore, compared to underground mining, also a more striking impact in visual terms (figure 2.1). Mineral exploitation, particularly surface mining, frequently involves extensive land disturbances, which create barren landscapes in mined areas and subsequent ecological degradation (Tong et al., 2005). Only a small part of the land surface is altered for underground mining structures and tailings disposal is often done by using it as backfill to provide support in the mines (Grice, 1998). This way less above ground storage is needed and the backfill also stabilizes mined-out areas.

Nowadays remediation of mining sites after closure is required. However, in many parts of the world (particularly in developing countries) while environmental legislation and policy related to mine site remediation are in place, their implementation is often incomplete (Tong et al., 2005).



Figure 2.1: Mountaintop mining for coal extraction in Elk Valley, British Columbia. A clear example of how surface mining results in ecological degradation (source: National Geographic, 2009 [online image]).

2.1.2 Acid mine drainage

Acid mine drainage is generated by the oxidation of sulfide minerals, which are commonly present in rocks associated with metal mining activity. This oxidation results in the release and mobilization of sulphuric acid when sufficient water is present. Prior to mining, oxidation of these minerals and the formation of sulphuric acid is a function of natural weathering processes. Oxidation of these undisturbed ore bodies and the release of acid and associated mobilization of metals, is slow. Aquatic ecosystems receive such small doses from these discharges they are not considered to be under threat. Mining, however, increases the exposed surface area of sulphur-bearing rocks allowing for excess acid generation beyond natural buffering capabilities found in host rock and water resources (Jennings et al., 2008).

The kinetics of acid formation depend on the availability of oxygen, the surface area of exposed pyrite, the activity of iron-oxidizing bacteria (figure 2.2), and the chemical characteristics of the influent water (Kleinmann et al., 1980).

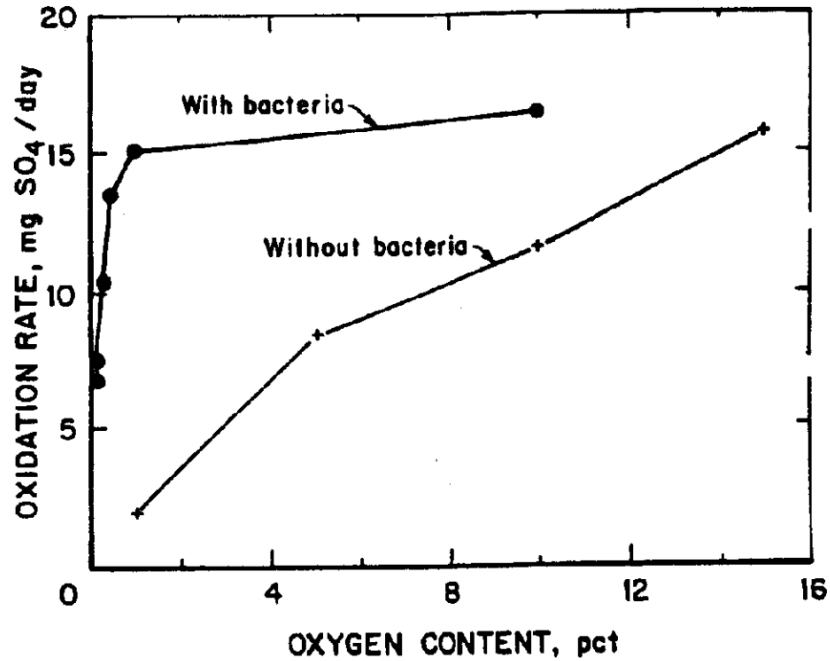


Figure 2.2: Rates of pyrite oxidation with and without iron-oxidizing bacteria in small columns maintained at different oxygen partial pressures (Source: Hammack and Watzlaf, 1990).

Streams affected by acid mine drainage typically have low pH, high concentrations of dissolved metals, and substrata coated with metal hydroxide precipitates (Hogsden and Harding, 2012) (figure 2.3). The formations of these iron (hydr)oxides are an ecological drawdown for salmon spawning rivers as they may physically coat the surface of stream sediments and streambeds. This destroys habitat, diminishes the availability of clean gravels used for spawning, and reduces fish food items such as benthic macro-invertebrates (Jennings et al., 2008). Also mining below the groundwater table has a pronounced effect as it provides a direct pathway of contaminants to aquifers.



Figure 2.3: A seep that discharges acid mine drainage at the Friar Tuck site near Dugger, India, illustrates the effect of iron oxyhydroxide precipitates on stream bed sediments (Source: PhysOrg, 2012 [online image]).

The use of sulphur-reducing bacteria and lime to create alkaline conditions, are few of many ways they treat acid mine drainage worldwide (Akzil and Koldas, 2006). Sulphur-reducing bacteria can persist in very toxic environments (Martins et al., 2009) and, together with the addition of lime, reduce the solubility, hence mobility of heavy metals.

An example of acid mine drainage and following remediation practices is the Britannia Mine in Vancouver, which is one of the more significant mines of North America in terms of pollution sources. Howe Sound, the fjord network to which the Britannia Mine drains is located north of Vancouver and has been exposed for over seventy years to metal-contaminated water. The main source of the problem are the naturally occurring metal sulphide ores which have been exposed to air and rain (Ministry of Forests, Lands and Natural Resource Operations, BC). The resulting sulphuric acid primarily discharges via two tunnels into Howe sound (figure 2.4): an upper and a lower tunnel. Remediation measures in 2001 resulted in the blocking of the upper tunnel causing all acid drainage to collect in the lower tunnel where it is treated. Other techniques reducing and preventing acid mine drainage from the Britannia Mine include covering sulphide mineralization with soils and rerouting uncontaminated surface waters away from underground mine workings (Ministry of Forests, Lands and Natural Resource Operations, BC).

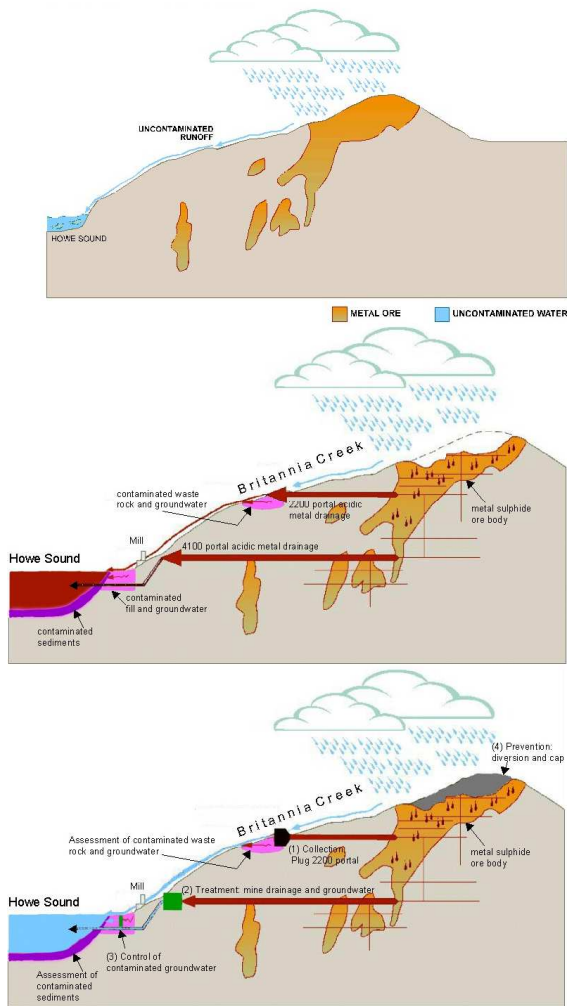


Figure 2.4: Pre- and post-mining conditions of the Britannia mine and necessary pollution prevention measures (Source: Ministry of Forests, Lands, and Natural Resource Operations [online image]).

2.1.3 The use of mercury in gold mining and associated environmental contamination

Amalgamation with mercury has been used as a method of gold and silver beneficiation since Roman times (Appleton et al., 1999). Nowadays it is used in more than 50 developing countries where it is named a toxic third-world-threat: traditional miners typically pan for gold and dump and mix mercury with their hands in a bucket filled with ores. Mercury is highly environmentally toxic and induces a severe health risk. Therefore it is not used anymore in gold mining in most western countries. Significant releases of mercury are associated with inefficient amalgamation techniques and releases are estimated to range from 800 to 1000 tonnes per year (Veiga et al., 2006). The total global release of mercury into the environment through this process prior to 1930 has been estimated at over 260,000 tonnes, after which emissions declined with the introduction of cyanidation processing technology (Lacerda and Salomans, 1998).

2.1.4 The use of cyanide in gold mining and associated environmental contamination

Cyanide in gold mining is a cheap gold production method and allows companies to reopen and expand mines which were previously assumed to be unprofitable mineral reserves. The process is as followed (Environmental mining council of British Columbia): (1) cyanide solution is sprayed on crushed ore or gold mine tailing which are piled up on top of a synthetic liner, (2) the cyanide solution trickles through the ore, binds to gold and other metals and sinks to the bottom of the heap from where it flows into collection ponds, (3) the gold is recovered from the solution by adsorption to carbon/charcoal. However, the presence of copper minerals reduces the gold production as it consumes large amounts of cyanide and oxygen and reduces the gold loading capacity of activated carbon (Coderre and Dixon, 1999).

Cyanide in biota binds to iron, copper and sulphur-containing enzymes and proteins required for oxygen transportation to cells (Donato et al., 2007) and therefore is toxic for animals, plants and humans. The formation of copper-cyanide complexes occurs preferentially to gold cyanide complexes indicating the relative importance of economic versus environmental considerations in the tailings water (Donato et al., 2007). An example of how cyanide in mining can impact the environment is the cyanide tailings spill in Romania in 2000. Cyanide tailings drained into the Tisza River and eventually the Danube, killing aquatic wildlife and polluted water supplies for more than 250 miles downstream.

In a large number of countries and territories the use of cyanide in gold mining is prohibited due to its severe environmental toxic nature. In other countries, The International Cyanide Management Code is established to provide guidelines for cyanide use in gold mining and to improve cyanide management practices. The use of cyanide in mining in Canada follows this Cyanide Code. The Musselwhite underground mine of Vancouver's Goldcorp was the first one certified by the International Cyanide Management Institute in 2010.

2.2 Dispersion of heavy metals in the environment

Rivers are perhaps the most common type of receiving waters for metal contaminated wastes from mining operations (Luoma and Rainbow, 2008). The contamination pattern in a hydrological system depends not only on anthropogenic inputs, but also on dilution processes driven by the hydrodynamics of the water system and the partitioning of heavy metals between dissolved and particulate forms (Luoma and Rainbow, 2008). Most metals have a high tendency to attach to particulates (explained in more detail in section 2.3.1), especially when moving away from the source where pH reaches neutral. The particulate concentrations are diluted by uncontaminated sediment from other parts of the catchment (Zwolsman et al., 1993). From this point on, the problem primarily becomes one of sediment transport rather than aqueous geochemistry (Helgen and Moore, 1996).

Figure 2.5 shows how concentrations decline further away from the source. Particulate concentrations of associated heavy metals decline more distinctly than concentrations of dissolved metals do and complete mixing usually occurs within 12 channel widths downstream of the tributary. Between sediment contamination and sediment input there is often a time lag, which is smaller when sediment transport is highly dynamic (Luoma and Rainbow, 2008).

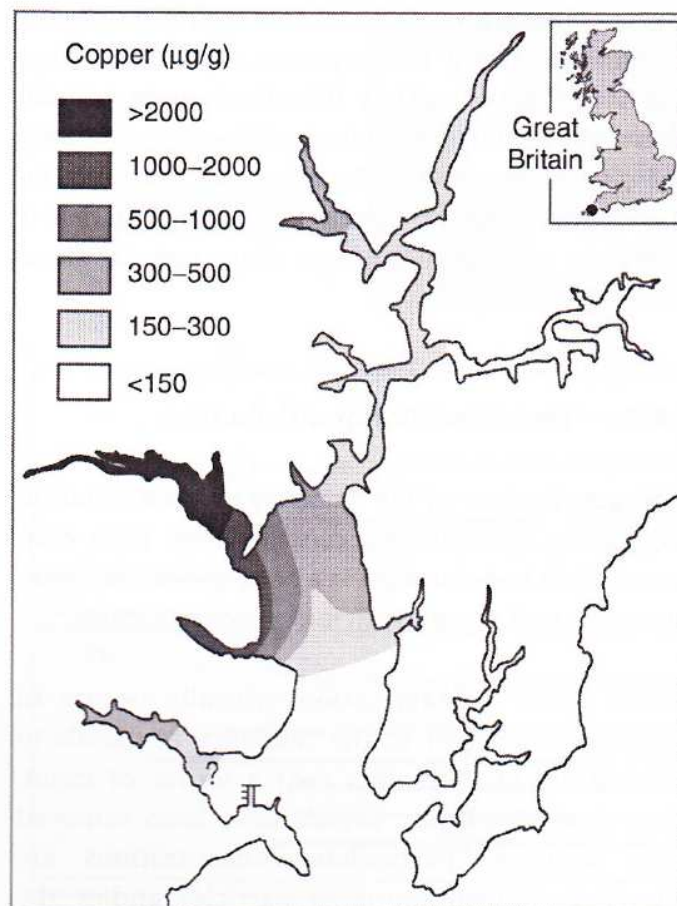


Figure 2.5: Cu concentrations in fine-grained sediments in the Fal estuary system in southwest England decline progressively from the river, through the estuary and toward the sea, due to the process of mixing with uncontaminated sediment (Source: Luoma and Rainbow, 2008, page 108).

The greatest transport is likely to occur during large floods and the minimum transport of contaminants during low discharge, because the sediment concentration depends in general on discharge a power-law:

$$C = aQ^b$$

Where C is the concentration in mg L^{-1} , Q the discharge in $\text{m}^3 \text{s}^{-1}$, and a and b are positive, empirical regression coefficients. Usually there is a high degree of scatter when relating concentrations to the discharge, especially during flood events. This is due to hysteresis effects, which are not included in the rating curve. Hysteresis holds the replenishment and depletion of stock during a hydrological year i.e. the availability of sediment. In the Horsefly River especially the annual freshet will be an important control in transporting the largest amounts of sediment. Also climate change affects the dispersion of contaminants, as already studied by Knox (1993): the modest climate change already has an impact on the magnitude and frequency of stream flow and alters the associated response of the sediment.

It is difficult to determine the effect of metal enrichment to be anthropogenic or natural. Since mines are located near ore bodies rich in heavy metals, natural processes such as weathering will increase the metal content and deliver metal-rich sediment to the drainage system next to anthropogenic enrichment. Weathering and processes that erode or expose the deposit eventually reach an equilibrium state with processes such as dilution by un-enriched tributaries, or reactions with rock adjacent to the ore body (Luoma and Rainbow, 2008). The result is mixing and the signal of a mine or ore body decreases significantly over a short distance downstream. The result of weathering is also a reduction in the metal concentrations of soils covering an unexploited ore body (Luoma and Rainbow, 2008). Helgen and Moore (1996) developed a model to predict the downstream dilution of contaminated sediment, which is usually a quick process due to the input of other un-enriched sediments even for the largest ore deposits (10-20 km). Their model resulted in acceptable fits in a variety of drainage systems, from which they concluded that dilution mixing and the size of the ore body are primary variables determining dispersion (Figure 2.6).

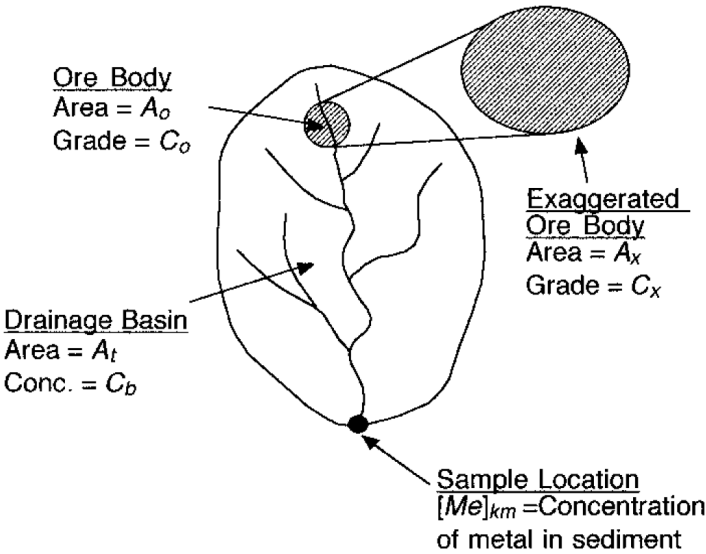


Figure 2.6: Basin diagram showing the visual terms used in the model to predict downstream dilution of contaminated sediment (Source: Helgen and Moore, 1996).

During floods the dispersion of contaminated sediment is immensely high and especially the finer fraction, associated with carrying heavy metals, will be deposited on floodplains where it can remain for centuries (Du Laing et al, 2009). The spatial variability of heavy metals on a floodplain is a matter of which particles settle where in the floodplain. Floodplain grain size distributions depend on flow velocity which in turn depends predominantly on (1) distance from the river, (2) flood strength, (3) heterogeneous roughness (e.g. vegetation) of the flood plain. It is known that low discharges transport the finest fraction, hence carry the largest amount of heavy metals. Therefore these fractions are deposited the furthest away from the river where low flow velocities prevail and even these fines can settle. The largest contamination therefore is likely to be found not directly over the river banks, which are usually sandy, but a distance away. However, flood magnitude is variable and not always the same area of the floodplain is inundated, which has consequences for the grain size- and contaminant distribution on the floodplain (Martin, 2000). Vertical trends of metals in the floodplain are thought to reflect the amount of metals carried by the river when deposition occurred (Knox, 1987). Temporal variability of heavy metals on a floodplain thus provides a history record of the catchment as layer after layer is deposited under different environmental conditions. For example a mining signal (such as in this study) can be traced back, or other land use activities and natural activity in the catchment (e.g. forest fires). Depth profiles of trace metals are generally used to investigate the pollution history of a drainage system (Santschi, 1984).

The majority of eroded sediments is often stored in the drainage basin rather than an immediate removal and the sediment with associated contaminants will only be re-suspended or mobilized by local physical processes. Over time scales of years to centuries sediment moves episodically rather than directly through the basin to the river's mouth (Martin, 2000). The main mechanisms able to bring these deposits back into the water system are: (1) bank scouring when a river cuts its own floodplain, (2) re-suspension by local overland flow, (3) during a subsequent flood, (4) the local land use activities of humans. Sediment storage is usually brief in geomorphically active areas: close to the channel and at high stream power reaches (Leece and Pavlowsky, 1997), but sediments in a more stable area may be stored for hundreds of years (Miller, 1997).

2.3 Sediment composition in floodplain soils

2.3.1 Grain size distribution and cation exchange capacity

The capacity of sediment to collect and concentrate trace metals depends on several physical properties of the sediment. The sediment physical properties include grain size distribution, cation exchange capacity and the composition of the sediment itself. The effect of grain size is one of the most significant in retaining trace metals as the associated higher specific surface area provides numerous adsorption sites for the trace metals to adsorb on. Even though metals are also able to adsorb to a variety of larger grain sizes, they are commonly found in the finer fraction. Adsorption can also be the result of cation exchange, which is often related to compounds with a large surface area such as clay minerals and organic matter. Most of these fine-grained sediments are negatively charged, which attracts the positively charged cations, the form in which most trace metals exist. The cation exchange capacity has a strong positive relationship with surface area and hence with grain size.

The composition of the sediment affects the retention of trace metals, since trace metals are strongly correlated with certain constituents. The constituents are able to bind trace metals chemically to their structure by means of adsorption, surface complexation and (co-)precipitation. As already explained, the compounds most able to retain trace metals are characterized by large specific surface areas, high surface charges, and high cation exchange capacities, which are generally related to the smaller grain sizes. The most common materials meeting these criteria are clay minerals, organic matter, hydrous manganese oxides, and hydrous iron oxides (Horowitz, 1991). Their ability to concentrate heavy metals in descending order is: manganese (hydr)oxides, organic matter, iron (hydr)oxides and clay minerals (Forstner, 1982a). Clay minerals also act as substrates for the precipitation and flocculation of organic matter and secondary minerals, such as hydrous iron and manganese oxide (Zhang and Yu, 2002; Lion et al., 1982). Thus rather than the metal adsorbs on to the clay mineral it is carried by the clay mineral on its coating of secondary minerals and organic matter. Therefore grain size is by far the parameter to help interpreting the data as it integrates all the other parameters (Horowitz, 1991). As floodplains are characterized by a considerably finer fraction of sediment, this will have a natural effect on the trace metal concentrations for which has to be accounted for (section 2.4).

2.3.2 Redox potential and pH

Partitioning between the solid phase and the dissolved phase of heavy metals ultimately determines the magnitude of their mobility and hence their dispersal into the environment. This partitioning is mainly controlled by redox potential and pH. The redox potential and the pH are inversely correlated due to the formation of H^+ ions during oxidation processes (Yu et al., 2007). The redox potential in floodplain ecosystems can drastically change due to water table level fluctuations, which in turn affects pH (Frohne et al., 2011). Also temporal inundations establish a low redox potential in floodplain soils (Reddy and DeLaune, 2008; Du Laing et al., 2007). During periods of flood, oxygen is consumed and increasingly alternate electron acceptors, such as nitrate, iron and manganese (hydr)oxides, are used by microbial organisms to acquire energy for their growth. This results in a more reduced soil (Du Laing et al., 2007). The concentrations of heavy metals in the pore waters will increase during such conditions as they are related to the manganese and iron cycles. Desorption of metals related to the now unstable manganese and iron (hydr)oxides is mainly responsible for trace metal mobilization. These released metals are able to re-adsorb to clay minerals and organic matter,

which are not affected by a change in redox potential. This change in chemical speciation has influence on the bioavailability (Palumbo et al., 2001). Longer periods of emerged floodplain are expected to decrease the activity of the microbial organisms and hence iron and manganese oxides will be reduced at a smaller rate (Du Laing et al., 2007). The oxic-anoxic interface can also partly be influenced as a result of microbial activity without the presence of an inundated floodplain. In this study this effect, if present, will probably be seasonal (temperature) as the study area is located in a severe continental climate.

The capacity of the soil (and water) to retain heavy metals is large under oxidized conditions and is controlled by adsorption and precipitation processes due to the affinity of these metals with many solids. In the presence of highly oxic conditions is the precipitation of trace metals with manganese and iron (hydr)oxides the dominant process and high correlations of trace metals with these (hydr)oxides exist (Luoma and Rainbow, 2008). The pH is the controlling factor under oxidized conditions (Van der Perk, 2006) as it controls adsorption, complexation and precipitation. At pH near neutral (i.e. most natural water bodies), the metals have a much higher tendency to be in the solid phase as a result of their affinity with particulates and sediment concentrations exceed the concentrations in solution by orders of magnitude (Luoma and Rainbow, 2008). At higher pH values the metals have a tendency to (co-)precipitate with calcite or iron, aluminum and manganese oxyhydroxides (Van der Perk, 2006). Under reduced conditions, iron and manganese (hydr)oxides in the solid phase are reduced to Mn^{2+} and Fe^{2+} which has consequences for the adsorbed metals (Du Laing et al., 2009). The mobility of most metals under reducing conditions is further decreased due to the formation of barely soluble sulphide minerals (Van der Perk, 2006; Du Laing et al., 2009), which microorganisms are able to catalyze (Burkhardt et al., 2010). Van Griethuysen et al. (2005) already described that the dynamics of trace metals are mainly controlled by redox chemistry of sulphur, iron, and manganese. Low pH values enhance the mobility of the heavy metals as they prefer the dissolved phase. This often results in acid mine drainage. The presence of carbonates in calcareous floodplain soils or sediments constitutes an effective buffer against a pH decrease, but they are also able to directly precipitate metals (Du Laing et al., 2009). In addition, plants affect metal mobility by (1) taking up metals, (2) oxidizing their rootzone, (3) excreting plant fluids and (4) stimulating activity of microbial symbionts in the rootzone (Du Laing et al., 2009).

An example of how alternating hydrological conditions can influence the redox potential of a floodplain soil and hence the metal concentrations is investigated in a study of Du Laing et al. (2007). In this study flooding conditions and associated lower redox potential did lead to increased Fe, Mn, Ni and Cr concentrations and decreased Cd, Cu and Zn concentrations in pore waters of the upper part of the soil. Lower pore water concentrations of Fe, Mn and Ni were found keeping the soil at field capacity, but Cd, Cu, Cr and Zn concentrations increased.

2.3.3 Correlations between metals

Ba, Sr, Ni, Cd, Co, Cu and Zn are often associated with manganese (hydr)oxides rather than iron (hydr)oxides (Frohne et al., 2011; Palumbo et al., 2001; Liu 2002 et al., 2002). Pb was found to be correlated with iron and manganese oxides (Palumbo et al., 2001; Liu et al., 2002). Iron oxides are reduced at a lower potential than manganese oxides (Brümmer, 1974), which is reflected in a study of Du Laing et al. (2007) in which manganese did show a faster response than iron when lowering the redox potential. The formation and re-oxidations of sulphides appeared to be dominant in the mobility of Cd, Cu, and to a lesser extent, Zn (Du Laing et al., 2007). The Irving-Williams series shows

the stability of the organic-matter-metal compound, which in descending order is: Pb, Cu, Ni, Co, Zn, Cd, Fe, Mn, Mg (Irving and Williams, 1948). Clay minerals are related to certain heavy metals, which are in descending order: Pb, Ni, Cu, and Zn (Horowitz, 1991). Anthropogenic Cd and Hg have stronger affinity to organic matter than to clays (Herut and Sandler, 2006). Se is often enriched in some of the pyrite ores from which Au and Cu are mined. As (arsenic) is often a constituent of waste products of Cu and Au mining. They both are of great environmental concern as they belong to the most hazardous and toxic of trace metals (Luoma and Rainbow, 2008).

2.4 Quantification of the impact of mining

Background concentrations of heavy metals from pre-mining conditions are needed to assess the anthropogenic effects of mining. These are the concentrations of trace metals that solely stem from local geology (figure 2.7). Sediment cores, if deep and hence old enough, can provide a record of such concentrations. Also control sites from which is known they are undisturbed, can be used to establish background concentrations. However, such sites are hard to find and it is difficult to be sure those sites always have been shielded from human influence.

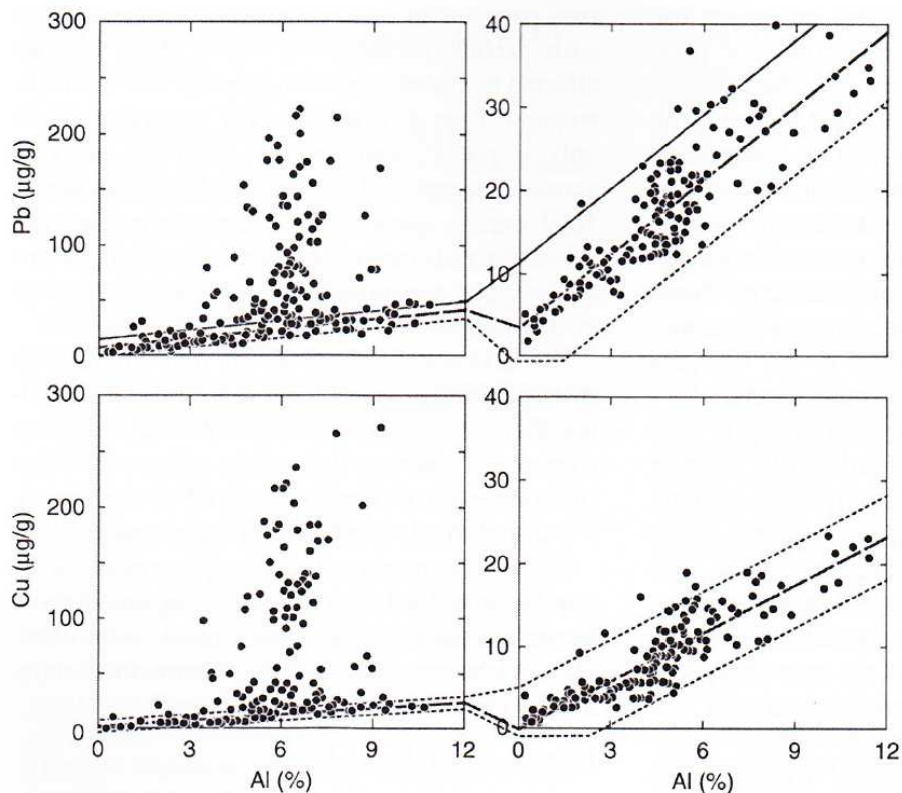


Figure 2.7: Concentrations of Cu and Pb in coastal zone sediments (USA) normalized by Al concentrations, which results in the baseline (local geology flux) (Source: Luoma and Rainbow, 2008, page 104).

A commonly used method to attain background concentrations and to evaluate the effect of the anthropogenic part of the concentration is global average geology. However, local geology can be very different compared to the global average, which biases the interpretation and has the possible consequence to over- or underestimate natural or anthropogenic contributions (Luoma and Rainbow, 2008).

Chemical extraction, physical separation of fine-grained materials, statistical techniques and normalization to particle size sensitive natural components of sediments, are a number of methods to improve comparability of metal concentrations in sediment. Separating the <63 μm is the most common practice (Luoma and Rainbow, 2008). As already discussed, heavy metals have a tendency to concentrate in the finer fraction of the sediment. Coarser material will result in a dilution of the heavy metal concentrations and hence will result in an interpretation which underestimates the anthropogenic input. Separation of the finer fraction will remove this bias.

Normalization procedures are common in heavy metal assessment studies as they improve the interpretability (figure 2.7). Aluminum, iron, grain size or organic carbon concentrations are used to remove the bias of the heterogeneity of the sediment. Percentage grain size normalizations are the most imprecise. Iron and organic carbon reflect both surface area and heterogeneous composition, which is harder to interpret (Luoma and Rainbow, 2008). Therefore aluminum is most commonly used in normalization procedures as it represents aluminosilicates, which is the main group of minerals generally found in the fine sediment fractions (Herut and Sandler, 2006). Clay is related to aluminum due to its high concentrations of aluminosilicates. Aluminum normalization removes the effect of grain size and composition on heavy metal concentrations.

3. Study area

The research in this thesis focuses on deposition of sediment and associated heavy metals on the Horsefly river floodplain, British Columbia in Canada. British Columbia has been one of the major mining areas throughout the world since the mid-1800s and historically, British Columbia's vast mineral resources have contributed extensively to the province's growth and development (Ministry of energy, mines and natural gas, BC). The first prospectors in the region were to arrive in 1860 in Quesnel Forks during the Fraser River gold rush and worked up to the Cariboo River towards Cariboo lake (Panteleyev et al., 1996). Underground mining became dominant after the Fraser River gold rush, but the feasibility of open-pit mining in the 1960s resulted in several huge copper mines to be opened (Ministry of energy, mines and natural gas, BC).

The Horsefly River watershed (appendix 4) is located south of Quesnel Lake, and east of Williams Lake on the eastern edge of the interior Fraser River plateau (figure 3.1). The elevation ranges between 2300 meters at the Horsefly's mountain headwaters to 739 meters at the Horsefly delta. The river mouths into Quesnel Lake forming a delta and is part of the Fraser River drainage basin.

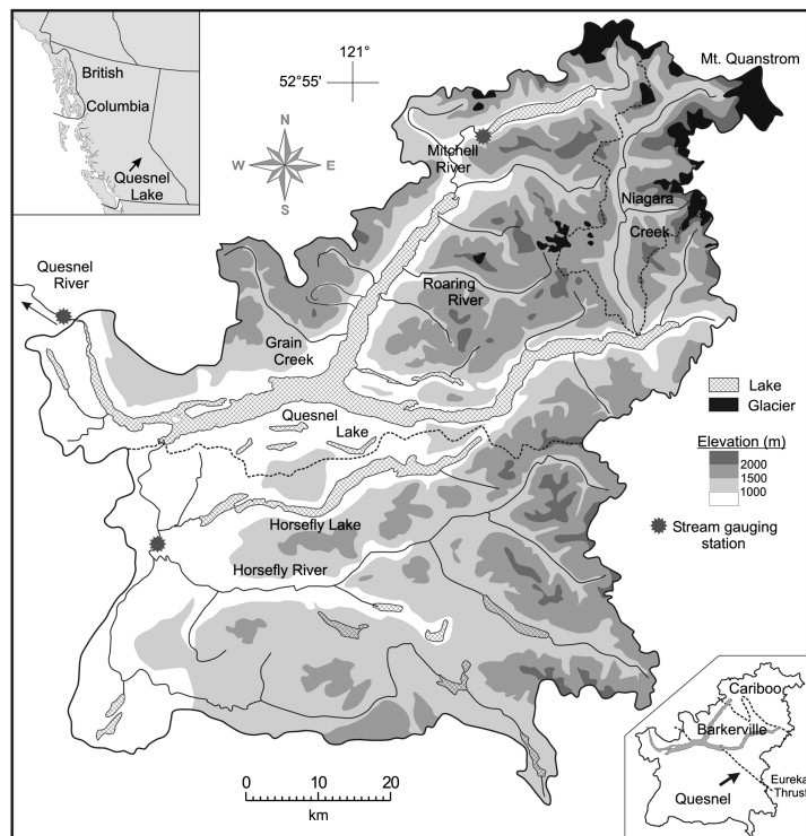


Figure 3.1: Drainage basin of Quesnel Lake from the National Topographic Survey 1:250.000 map 93A.

The Horsefly River (figure 3.2) is one of British Columbia's most significant salmon spawning rivers and provides one of the more important spawning habitats for Sockeye salmon and Rainbow trout throughout the Fraser River drainage basin. The annual salmon run on the Horsefly River supports the valley's ecosystem to a great extent as it provides a major food source for a substantial number of mammals and birds. About seven fish species including Rainbow trout, Dolly Varden char, Sockeye

salmon, Chinook salmon, Coho salmon, and mountain white fish, are part of the Horsefly valley ecosystem (British Columbia heritage rivers program).



Figure 3.2: Horsefly River near Horsefly Bridge just below the confluence with McKinley Creek.

3.1 Geology

3.1.1 Regional geology

The North American mountain range is the result of the accretion of far-traveled lithospheric blocks and slivers (terranes) to the western margin in the beginning of the Jurassic (Ricketts, 2008) (figure 3.3).

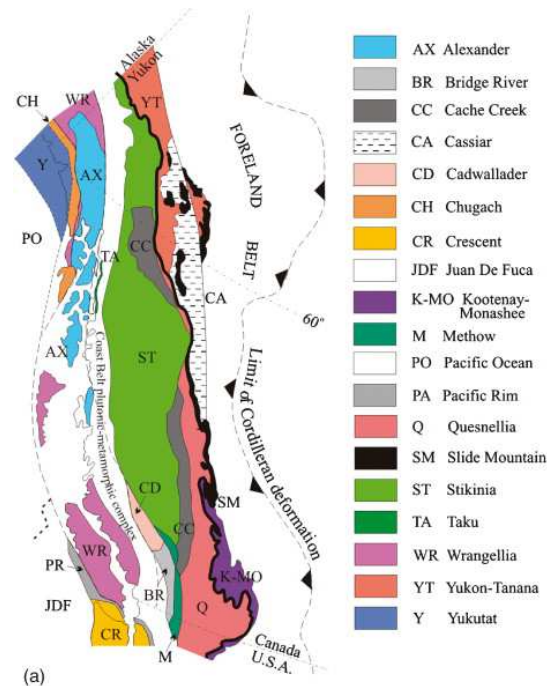


Figure 3.3: Map of the accreted terranes in British Columbia (Source: Ricketts, 2008).

The Quesnel and Horsefly rivers traverse the northwesterly trending axis of the central Quesnel belt, also known as the 'Quesnel Trough' (Panteleyev et al., 1996). The central Quesnel belt is positioned on the Quesnellia terrane (figure 3.3), a predominantly Mesozoic terrane which, during the Upper Triassic-Lower Jurassic, developed as a volcanic island arc to the west of Mesozoic North America (Bailey, 1990). The structures of the Central Quesnel belt can be separated into two groups: those formed during accretion of Quesnellia with North America and those which postdate this event (Bailey, 1990). The Quesnel area has a synclinal structure, which is formed within a Triassic continent-margin basin. Triassic sediments filled the basin first, followed by the infilling of Triassic-Jurassic volcanic rocks (Panteleyev et al., 1996). Together they constitute the Quesnel Trough.

3.1.2 Horsefly geology

The dominant rock types are mafic volcanic rocks of calcalkaline to alkaline affinity and the stratigraphic succession consists of mainly pyroxene-phyric basaltic flows, flow breccia, debris, flow or lahar deposits and locally derived epiclastic rocks (Panteleyev and Hancock, 1988). The Quesnel belt itself is comprised by the units in appendix 5.

The placers in the Cariboo are 14 million years older than the placers found around Horsefly and are related to pre- or post-Wisconsin gravels. Fluvial gravels under Miocene basalt flows contain the Horsefly placers and overlie either Eocene volcanic or sedimentary rocks or, less commonly, the Triassic-Jurassic Nicola rocks (Panteleyev et al., 1996). There are two of such fluvial (Miocene)

channels in the Horsefly area. The main Miocene channel follows the Horsefly River up to Horsefly village and then changes its direction going west through Antoine lake and into the Beaver Creek valley (figure 3.4). At some location the channel is found to be 150 meters deep and 610 meters wide (Lay, 1932). The second and smallest channel is located south from the main channel and has a southeast-northwest direction.

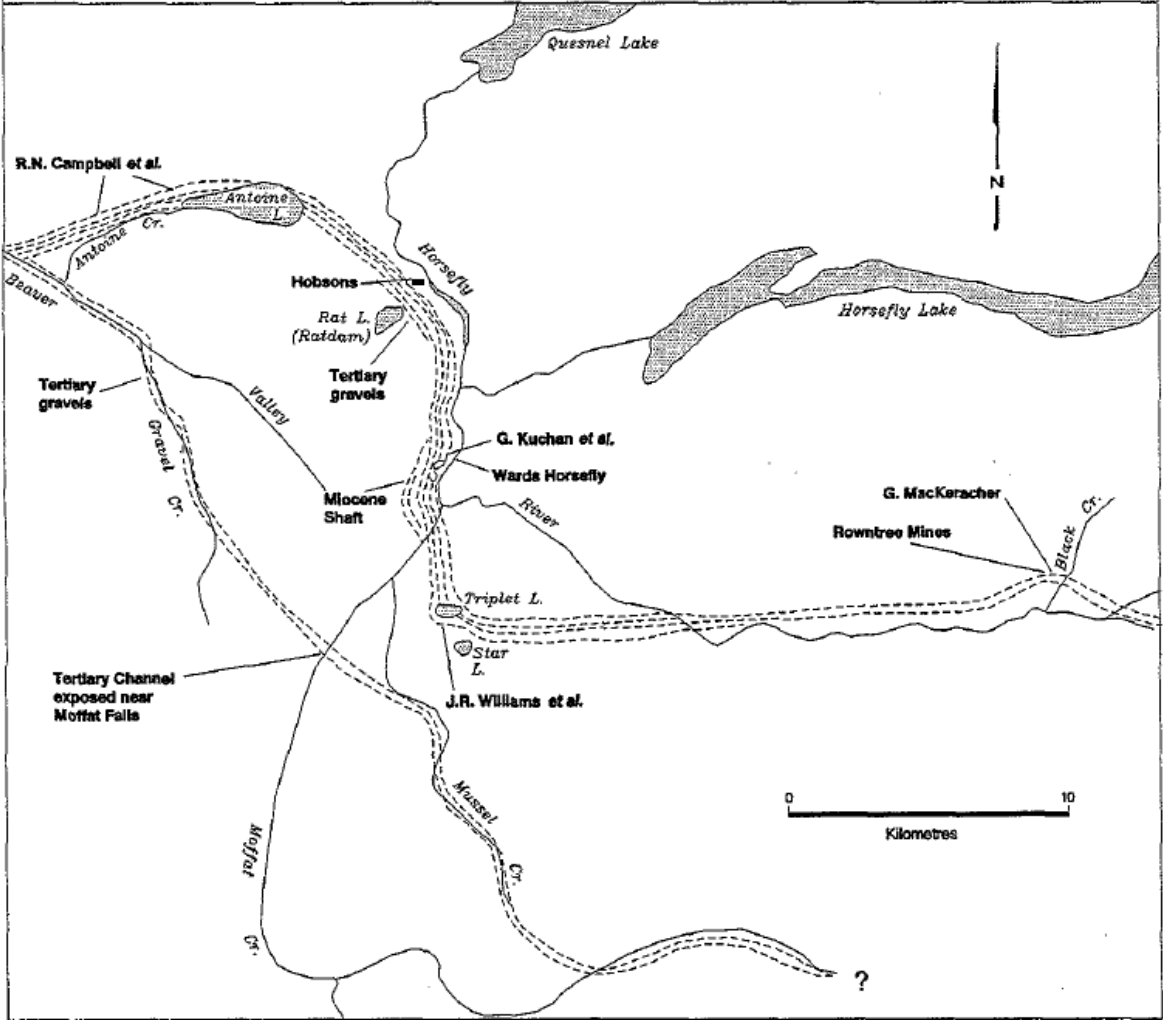


Figure 3.4: A sketch from Lay (1932) showing the Miocene channels and location of the mines: Miocene shaft (1897-1900), Wards Horsefly (1864-1913) and Hobsons Horsefly mine (1890-1899). The Black Creek is also visible following the Horsefly River in the eastern direction.

The mother lode of the placer gold is still unknown. According to Panteleyev and Hancock (1988) possibly all gold was originally transported within the Miocene white-quartz channel ways of unit 10A (appendix 5) and the source of these white quartz pebbles is speculated to be metamorphic terranes, possibly in the Eureka Peak – Crooked Lake – Horsefly River headwaters to the southeast or even further. However, glacial and postglacial re-concentration of the Miocene placer gold is generally not significant in the Horsefly area (Panteleyev et al., 1996).

3.2 Geomorphology of the Horsefly River area

The fossils found in Horsefly sediments have an age of 50 to 45 Ma (Wilson, 1977b), which indicates that the Horsefly River has been a basin for a long time already. The upper Horsefly River has its headwaters in the Cariboo mountain summits and five tributaries join the Horsefly River upstream of the Black Creek Mine. The floodplain arises downstream of the confluence with McKinley Creek and varies between 300 and 800 meters in this lower section of the Horsefly River.

The soils supporting lower and mid-elevation forests are derived from glaciations and modified by geomorphic processes, but at most locations the soils are gravelly sandy tills and colluviums, with some glacio-lacustrine sediments also present (R.L. Case and associates – Watershed consulting, 2000b). At higher elevations near the headwaters there is mainly bedrock present supporting treeless alpine tundra vegetation (R.L. Case and associates – Watershed consulting, 2000b). Glacial and fluvial-glacial sediments are deposited on all bedrock units. The Pleistocene melt water channel ways can be seen by the thick valley infill (appendix 5) in the upper reaches of the Horsefly River between Horsefly village and Antoine Creek and to the Northwest along Beaver Creek (Panteleyev, and Hancock, 1988). The riverbed alternates between gravel-dominated and sand-dominated. The sand-dominated areas show a high meander tendency and the channel way is narrower and deeper in these parts. An estimate from historic air photos and comments by local residents show that the annual lateral migration of the river varies between no movement along well-vegetated straight stretches and crossovers to a meter or more at some meander lobes (R.L. Case and associates – Watershed consulting, 2000a).

3.3 Climate

Cold winters and warm summers are representative for the continental climate in this region. The precipitation ranges between 400 and 2200 mm with maximum precipitation occurring in late spring and early summer (R.L. Case and associates, 2000b). River flow is dominated by the annual freshet usually resulting in overbank flow in the lower portions of the Horsefly catchment. These peak flows generally occur in late spring and overbank flooding can last for several weeks in May and June. The mean annual flow for the Horsefly River above McKinley Creek is about $20 \text{ m}^3 \text{ s}^{-1}$ (figure 3.5).

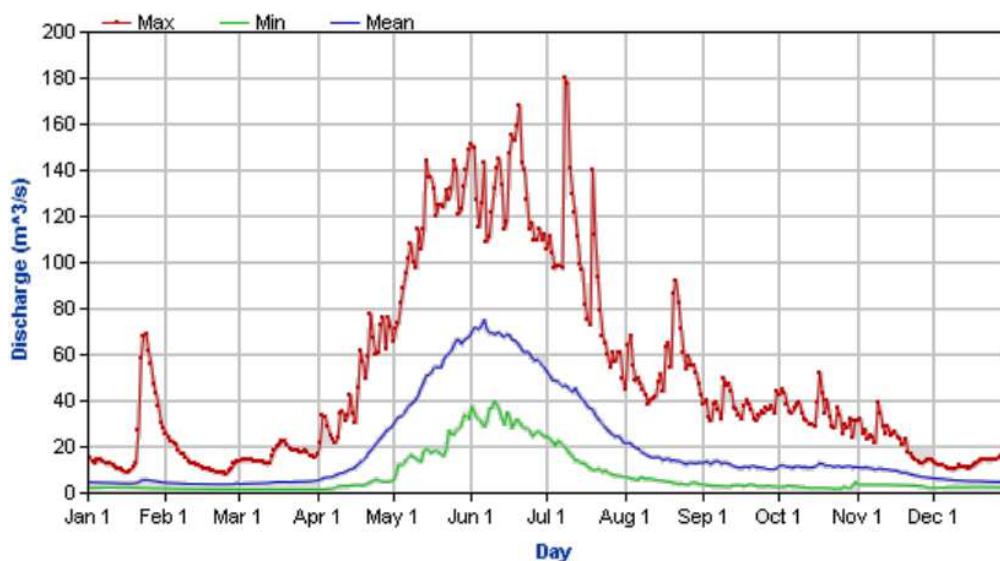


Figure 3.5: Mean, minimum and maximum daily discharge for the Horsefly River above McKinley Creek (08KH010). Statistics correspond to 47 years of data from January 1955 to December 2006.

The months December till March are marked with a constant low discharge due to low runoff in this cold season when water is mostly present in the form of ice and snow. In the summer the mean discharges decrease due to lack of precipitation, and hence runoff.

3.4 Mining history of the Horsefly River area

Placer mining in the region occurs since 1859 and includes some large-scale mining sites. Placers are glacial or alluvial deposits of relative coarse material containing valuable minerals. Attaining these minerals by placer mining is generally done by washing or dredging. Older Miocene fluvial systems in the area contain placer gold. Both pre-glacial and post-glacial rivers flowing out of the metamorphic highlands to the east have transported additional gold (Panteleyev et al., 1996). Fluvial sediments of the Quesnel River and its tributaries are mined since the 19th century. The largest deposit of this type is that of Bullion Pit, near Likely, where the gold was recovered from gravels within an early channel of the Quesnel River (Bailey, 1990).

Horsefly village was first known as Harpers Camp named after Thaddeus Harper who opened the first hydraulic mine in 1887. The first discovery of gold on the Horsefly River was by Peter Dunlevey in spring 1859 (Panteleyev et al., 1996). The first sites of placer mining were just outside town. The first mining practices were only some small-scale mining of placer deposits in the 1860s and large-scale development did not get under way until near the end of the century. At the end of the 19th century large mining companies exerted extensive large scale hydraulic mining along the Horsefly River. The most important mines were Hobson's Horsefly Mine, Ward's Horsefly mine and the Miocene Shaft, which was exploring ancient fluvial channels. Those mines were all located only a few miles south of the outlet of the Horsefly River in Quesnel Lake along Mitchell Bay Road (from Horsefly to Likely) (figure 3.4). Almost all mining activity ceased between 1902 and 1913. Mining shifted to the Bullion Pit mine near the town Likely. Placer mining is no longer allowed, since the Horsefly River is such an important salmon spawning area. Nowadays Horsefly is a community sustained by forestry, ranching and recreation.

3.4.1 The Black Creek gold mine

The mine in particular in this study is the Black Creek gold mine (figure 3.6) along the Black Creek which drains into the Horsefly River and is located 20 kilometers upstream of the village of Horsefly (figure 3.4). The Black Creek represents reworked placers in which gold is re-concentrated in Pleistocene glaciofluvial channelways which have cut into or through the Miocene gravels (Panteleyev and Hancock, 1988). The deposit is considered to be a paleogulch placer and consists of layered, unconsolidated, reworked glaciofluvial gravel and sand and the material contains abundant kyanite, schist fragments, garnet, quartz grains and only small quantities of magnetite (Ministry of Energy, BC). The glaciofluvial deposits rest on a bedrock of augite porphyry basalt flows, flow breccias and underlying bedded pyroxene-rich wackes and siltstones of the Upper Triassic Nicola Group (Ministry of Energy, BC). The Black Creek mine was a hydraulic mine i.e. the excavation of a gold-containing-bank by a jet stream of water. The resulting slurry is directed through sluices where the gold is separated by a series of sieves and riffles (figure 3.6: left). The remaining portion is discharged into the natural streams downstream. Unstable soils in the headwaters of Black Creek and Patenaude Creek have been a major source of sediment to the river floodplain of which placer mining may have contributed to this delivery (R.L. Case and associates – Watershed consulting, 2000a).

Following is a summary of the history of the Black Creek mine as recorded in a study of Panteleyev et al. (1996): active mining took place for over a hundred years until ten years ago. It was discovered in the late 1890s by Mr. Campbell. The claim was purchased by Phil Fraser and he did some keystone drilling in 1918 about 3.2 kilometer upstream of Black Creek, but little gold was discovered from this test. It appears that no mining was done until 1930, when James Armes optioned the leases of the mine. A ground sluice was developed with a length of approximately 300 meters, 3 kilometers upstream of the Black Creek mouth. Another 300 meters upstream of this 'lower' pit (figure 3.6: right) another pit was run for tests to discover gold from the gravels. This hydraulic operation was active until 1935 and after closure the Armes family worked the grounds intermittently till 1986. Mr. L. Shunter acquired the property in 1986 and worked it through steadily till about 10 years ago. Nowadays it is an abandoned open pit mine prone to enhanced weathering processes.

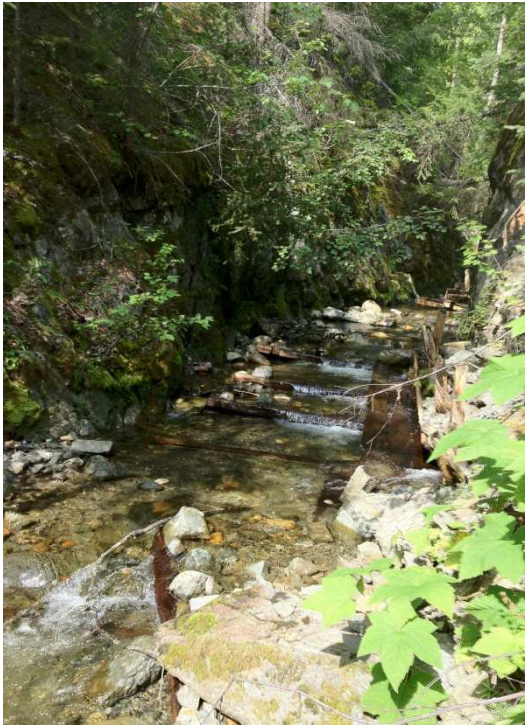


Figure 3.6: Left: Black Creek canyon with remnants of old sluice boxes. Right: Wall of the lower pit of the Black Creek mine.

4. Methods

4.1 Sample collection and analysis

4.1.1 Sample collection

The sampling method involved sediment coring. These cores were collected at several sites on the floodplain, upstream and downstream of the Black Creek alluvial fan and at different distances from the Horsefly River (figure 4.1). This was executed in September 2012. It is likely that the impact from the mine is concentrated in the part of the floodplain just below the Black Creek. This part of the floodplain has a strong meander tendency and acts as a sink for sediment during high discharge periods. In this area six cores were taken (A1, A2, A3, B1, B2, B3, figure 4.1). A core at the delta (D1, figure 4.2) of the Horsefly River at Quesnel Lake was taken to investigate whether the signal of the mine is strong enough to be traced further downstream of the meander-bend-area. The sediment cores collected ranged in length between 60 and 90 centimeters and were sealed before transport. The cores at transect B were the only ones collected on agricultural land. The cores E1, D1 and transect A were collected on barren land, from which transect 'A' was part of the land conservancy project. Coordinates of the cores can be found in table 4.1.

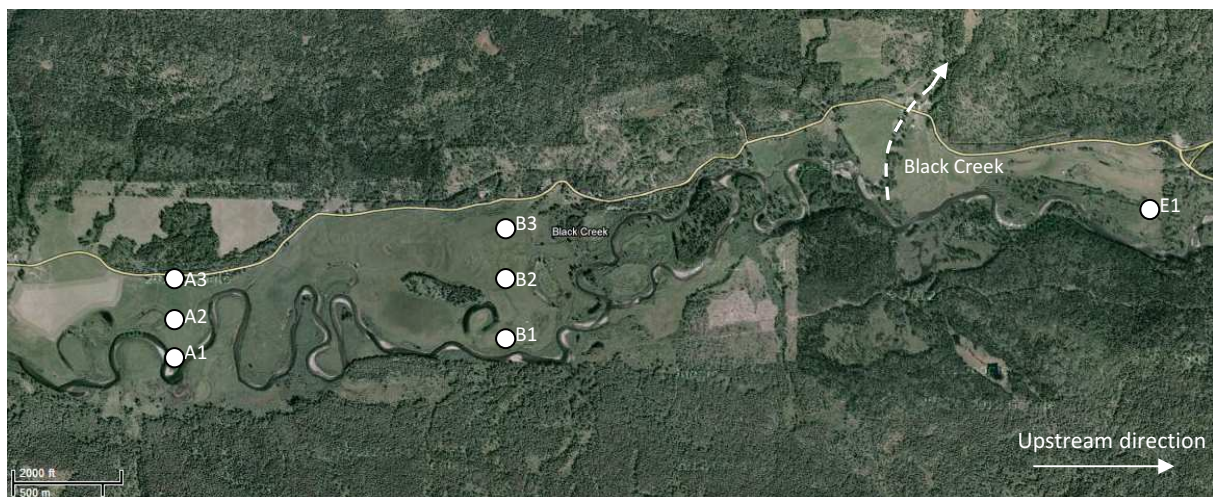


Figure 4.1: The image shows the cores upstream and downstream (meander-bend-area) of Black Creek.



Figure 4.2: The image shows the location of the delta core on the Horsefly delta at Quesnel Lake, about 55 kilometers further downstream of Black Creek.

Core	Coordinates	Date of collection
A1	52.283850° N, 121.154696° W	8th of September 2012
A2	52.285290° N, 121.154579° W	8th of September 2012
A3	52.286718° N, 121.154322° W	8th of September 2012
B1	52.458012° N, 121.411240° W	11th of September 2012
B2	52.287405° N, 121.127551° W	11th of September 2012
B3	52.290346° N, 121.127526° W	11th of September 2012
E1	52.291264° N, 121.073850° W	19th of September 2012
D1	52.458012° N, 121.411240° W	11th of September 2012

Table 4.1: Coordinates of the cores taken from the Horsefly River's floodplain.

4.1.2 Sample storage and preparation

After collection the cores were kept straight up, cool and dark before processing the samples. Each core was qualitatively described (appendix 3) and sliced in one-centimeter slices after which each slice was weighted and dried by air. The dry weight was determined for each slice for all the cores. Based on the research questions and the objective of this study, three cores were chosen for geochemical, particle size, organic matter and dating analysis: (1) the core upstream of Black Creek (E1), (2) a core just downstream of Black Creek (B1), (3) the core at the delta (D1). From now on these cores are referred to as: E1 is the upstream core, B1 is the downstream core and D1 is the delta core. For these cores a small amount of each dry sediment sample was sieved through a 63 µm sieve in order to retrieve enough fines for geochemical analysis, particle size analysis and organic matter determination. It also resulted in an estimation of the fine fraction distribution in the core and between different cores. Sieving was done from bottom to top of a core assuming mining impacts and associated contamination is more likely to be in the upper parts of the cores.

4.1.3 Sample analysis

Organic matter determination

The organic matter content of the <63 µm fraction was determined using the loss on ignition method for every slice of the three cores (E1, B1 and D1). A sample of about 1 gram (m_{air}) was put in the oven at 500° C for an hour and the weight of the sample is determined right after ($m_{oven-dry}$). It was prevented that vapor in the air adsorbed onto the sediment particles before weighing. The organic matter content (%) reads as:

$$Organic\ matter\ content\ (\%) = \frac{m_{oven-dry} - m_{air-dry}}{m_{air-dry}} * 100\%$$

Geochemical analysis of heavy metals

The geochemical analysis is conducted at the Australian Laboratory Services in Vancouver. This analysis was performed for every slice of the top 30 cm of each core, and for the lower centimeters every other slice. The geochemical procedure used is ME-MS41, which includes the analytical methods of ICP-AES (Inductively coupled plasma-atomic emission spectroscopy) and ICP-MS (Inductively coupled plasma-mass spectrometry). A sample of the <63 µm fraction is digested with aqua regia in a graphite heating block and (after cooling) the resulting solution is diluted with de-ionized water, mixed and analysed in the spectrometer (ALS group) to determine heavy metal concentrations.

Particle size analysis

About 1 gram of the <63 μm fraction of every slice of the top 30 cm, and the lower centimeters every other slice, was put in a beaker and treated with hydrogen peroxide to remove the organic matter from the sediment. 5 mL of de-ionized water was added to the beakers and the samples were soaked overnight. Then the samples were sonicated for 3 minutes at ~ 8 watt rms and a sub-sample was directly taken from the beakers into a pipette (~ 2 -3 mL) and put into the Malvern to determine particle size (conducted by the Quesnel River Research Centre).

Radiometric dating

The radiometric dating analysis is conducted at the University of Plymouth on the <2 mm fraction. The observed abundance of radionuclides of ^{210}Pb and ^{137}Cs in the sample is compared to its decay products. The samples were analysed at a 2 cm interval till a depth of 28.5 cm in each core.

4.2 Data analysis

As the most common heavy metals associated with (placer) gold mining are arsenic, cadmium, lead, zinc, selenium and copper (LaPierre et al., 1985), these will be the ones studied in this thesis. Pre-mining background concentrations of these metals are needed to assess the anthropogenic effect of the mine, which are the concentrations that solely stem from local geology. Sediment cores can provide a record of such concentrations, if deep and hence old enough. The metals are normalized to the reference element aluminum, which is a proxy for the variation in grain size of the aluminosilicate fraction (clay). However, it is necessary to verify the correlation between grain size and the aluminum content which is done by regression.

4.2.1 Lowest quantile regression

Establishing a baseline to calculate background concentrations is done by using the method of lowest quantile regression (Luoma and Rainbow, 2008; Cade and Noon, 2003). In this regression the lowest 25% (quartile) metal concentrations with associated aluminum values are used. These concentrations are assumed to represent background concentrations. To identify the lowest 25% of values without being high or low as a result of grain size effects, metal concentrations are divided by aluminum (the proxy). The corresponding metal concentrations of the lowest 25% of this ratio are chosen for the regression. Thus in order to establish the dataset for the regression and the following calculations of the baseline of a metal, a simple normalization procedure is already used. The output from the regression with background metal concentrations and aluminum represents the baseline i.e. the average metal concentration due to the local geology flux of the area.

A disadvantage when identifying the lowest quartile of all three cores together, is that possibly only one core is represented in the regression. However, separating each core and calculating three baselines reduces the comparability between cores. When relating to the research questions, it is concluded that the major importance is to be able to compare the upstream of Black Creek (E1) and the downstream of Black Creek (B1) core. Because the delta core (D1) is located in a different environment and receives sediment from the entire catchment, metal concentrations will be diluted as a result of mixing between the tributaries. When establishing a dataset using the lowest quartile of the combined dataset of all three cores, the only core that will be represented is the delta core (D1), as it likely contains the lowest 25% of metal concentrations per definition.

For these reasons two baselines are calculated: (1) from the regression of the lowest quartile of the delta core (D1) and (2) from the regression of the lowest quartile of the upstream of Black Creek (E1) and downstream of Black Creek(B1) core. The resulting baselines will be of the form:

$$\text{Baseline concentration (ppm)} = a * [Al] + b$$

4.2.2 Calculation of residual concentrations

The residual concentration represents that part of the total concentration that does not stem from local geology. They are calculated by subtracting the baseline concentrations from the total concentration of the metal:

$$\text{Residuals (ppm)} = \text{Total concentration} - \text{Baseline concentration}$$

These residuals represent the part of the concentration assumed not to stem from local geology, but from anthropogenic activities.

4.2.3 Establishing age-depth profiles

210-Pb

The ²¹⁰Pb dating method was first applied in the early seventies by Krishnaswamy et al. (1971), with the advantage to be able to date recent timescales. ²¹⁰Pb occurs in the decay chain of ²³⁸U (the radium series) and is formed after the decay of ²²⁶Ra to ²²²Rn, after which it turns into ²¹⁰Pb through a series of short-lived isotopes (Appleby and Oldfield, 1983). However, a fraction of the ²²²Rn atoms, after its formation by ²²⁶Ra decay, escapes to the atmosphere where it decays to ²¹⁰Pb. This fraction is named the excess ²¹⁰Pb or unsupported ²¹⁰Pb and is removed from the atmosphere followed by deposition on the surface soil. The unsupported ²¹⁰Pb concentration in each sediment layer declines with its age in accordance with the usual radioactive decay law (Appleby and Oldfield, 1983), which is an exponential function of the initial concentration of ²¹⁰Pb (A_0), the concentration at time 't' (A_t) and its decay constant (λ is 0.03114 y^{-1}):

$$A(t) = A(0) * e^{-\lambda t}$$

However, variations from this exponential function over depth may complicate calculations. ²¹⁰Pb dating is complicated by the fact that the concentration of ²¹⁰Pb found in sediments is a function of both the flux rate of the unsupported lead itself, as well as the background sedimentation rate (Cohen, 2003). At least one of these must be known, or assumed to determine the age of sediments. For this reason was the CRS (Constant Rate of Supply) model developed, which assumes that there is a constant rate of supply of ²¹⁰Pb to the sediments, but concentrations found might vary as they are susceptible to changes in sediment accumulation rates. Varying sedimentation accumulation rates are likely to result in a dilution or concentration of ²¹⁰Pb in the sediment (Appleby and Oldfield, 1983; Binford et al., 1993; Cohen, 2003).

Cs-137

¹³⁷Cs is a radioactive isotope related to anthropogenic activities, primarily to nuclear reactors or weapons and is also characterized by fallout from the atmosphere and subsequent deposition on the surface soil. Bomb testing of nuclear weapons in the USA reached a peak in 1963, which is followed by an associated peak in the concentrations of ¹³⁷Cs in sediment profiles (Cohen, 2003). Those peaks can be identified to have an age of 49 years and can be useful in fine-tuning the ²¹⁰Pb dating model. Another peak can be related to the Chernobyl accident of 1986. However, it is not really

distinguishable in the study area of this research (British Columbia, Canada), as concentrations didn't reach this distance.

This study

This study adopts the CRS model to calculate the ages of the sediment layers in the three cores (B1, E1, and D1). Generally the ^{210}Pb is not measured directly, since the decay of these low-energy beta particles are difficult to measure (Cohen, 2003). To determine the amount of unsupported ^{210}Pb , the activity of ^{214}Pb is measured resulting in estimates of the supported and unsupported ^{210}Pb activities. Therefore the excess amount of ^{210}Pb is calculated by subtracting the supported ^{210}Pb from the ^{214}Pb concentrations. As the samples are analysed for ^{210}Pb at a 2 cm depth interval, the concentrations were first interpolated to a 1 cm interval using an exponential function for the upper part and a linear function for the lower part of the column. However, the amount of excess ^{210}Pb below the deepest sample analysed was estimated to be considerable, which means that the interpolation techniques can result in deviations in estimating the total excess ^{210}Pb and associated age calculations. The distinct peak of ^{137}Cs in the delta core at a depth of 18.5 cm was used to fine tune the model and to minimize the effect of an error possibly introduced by the interpolation techniques. This peak corresponds to an age of 49 years. The considerable amount of excess ^{210}Pb below the deepest sample analysed applies to cores D1 and E1. This amount was extrapolated over depth by means of the same linear function of the lower parts of each column till it reached zero. Also for these depths the corresponding age is calculated. However, as an amount of uncertainty is added with this extrapolation, it provides only a very rough estimate.

4.2.4 Manganese and iron cycles

Manganese- and iron (hydr)oxides are the prime substrates metals are likely to adsorb on (Horowitz, 1991). The metals related to mining are compared to the iron- and manganese depth profiles for the reason that the iron- and manganese substances are very sensitive to redox processes, hence will influence the associated adsorbed metals. The hypothesis is that manganese and iron are not enriched in this area as a result of anthropogenic activity. Manganese alone already has a natural range in variability of 7 – 9000 ppm (Emsley, 2003). Peaks in the manganese and iron concentrations are likely to reflect local geology. Manganese and iron are often associated with each other in the local geology and their depth profiles will probably show strong correlations. However, for this reason they are also correlated with aluminum. Peaks and troughs in iron and manganese may well correlate with aluminum, but on the other hand they might very well be inconsistent with aluminum as a result of redox processes. For this reason also a regression analyses has been conducted on the lowest quartile of manganese and iron to identify correlations with aluminum. This regression analysis has been conducted in the same way as for the other metals: (1) over the dataset of the upstream (E1) and downstream (B1) core together, and, (2) over the dataset of the delta core (D1).

5. Results and discussion

5.1 Regression analysis

5.1.1 Assessment of the baseline concentrations

Assessment of a valid baseline using the quantile regression is based on R^2 (squared Pearson's cross correlation) and the p-value. R^2 is a standardized covariance and measures the relative strength of the linear relationship between two variables. It has values between 0 and 1, with 1 meaning a perfect correlation. The p-value is used as a measure of significance of the coefficient in the regression. Small p-values reflect small probabilities, and suggest that the coefficient is important in the regression. Since a 95% confidence interval is used in the regression, the p-value for a coefficient has to be smaller than 0.05 in order for the correlation to be significant. The closer the p-value is to 0.05, the less significant. Table 5.1 and 5.2 show the established baselines for cores B1, E1 and D1 and associated R^2 and p-values. The graphs of the regression analyses can be found in appendix 2.

Core B1 and E1	Baseline (ppm) (x=Al)	R^2	P-value
Cu	$y = 19.045x + 7.7191$	0.92	1.04E-13
Zn	$y = 28.94x + 32.983$	0.29	0.006993
Se	$y = 0.198x + 0.5129$	0.22	0.022407
Cd	$y = 0.0926x + 0.084$	0.19	0.035128
Pb	$y = 4.606x - 0.4312$	0.92	1.15E-13
As	$y = 4.2799x + 0.0108$	0.89	3.18E-12

Table 5.1: Regression coefficients and baselines for the upstream (E1) and downstream (B1) core.

Core D1	Baseline (ppm) (x=Al)	R^2	P-value
Cu	$y = 23.136x - 7.2548$	0.28	0.077316
Zn	$y = 44.526x + 12.758$	0.68	0.001
Se	$y = 0.5558x + 0.0071$	0.67	0.001121
Cd	$y = 0.0486x + 0.0988$	0.10	0.315285
Pb	$y = 4.61x + 0.5966$	0.95	1.24E-07
As	$y = 3.4737x - 0.354$	0.95	7.34E-08

Table 5.2: Regression coefficients and baselines for the delta core (D1). Note: Cd and Cu regressions are not statistically significant.

The regression for the upstream (E1) and downstream (B1) core resulted in especially high correlations of Cu, Pb and As with aluminum. Zn, Se and Cd regressions in these cores have much poorer results, with R^2 of 0.29, 0.22 and 0.19 respectively. The regressions of Cu and Cd for the delta core (D1) are not statistically significant (table 6.2). The p-value for these regressions is larger than 0.05. Pb and As show a remarkable high correlation with aluminum, which is shown by the high R^2 (0.95) and very low p-values. The regressions of Zn and Se have a slightly lower R^2 of 0.68 and 0.67 respectively, but are still considered to indicate a good correlation with aluminum.

5.1.2 Assessment of the regression dataset used (lowest quartile)

The Cu regression dataset (lowest quartile) for the upstream (E1) and downstream (B1) core, consists mainly of data from the upper part of the upstream core (E1). The upstream core (E1) is also dominantly represented in the Zn dataset and consists mainly of the lower part of core E1. About 70% of the dataset for the Se regression relates to the upstream core (E1) and 30% to the downstream core (B1). This dataset is concentrated in the lower part of both cores. Core B1 and E1 are about equally represented in the regression dataset for Cd and the lowest quartile mainly consists of the lowest part of each core. The lowest quartile that is used for the regression of Pb consists of the upper part of the column for core B1 and the lower part of the column for core E1. They are about equally represented in the regression dataset of Pb. The major part of data used for the regression of As represents the upper and lower part of the upstream core (E1).

The lowest quartile in the delta core (D1) is derived from the lower part of this core for all metals (Zn, Se, Pb, Cu and As). Appendix 2 contains the dataset (lowest quartile) used for the regressions.

5.2 Sediment characteristics

Note: One sediment layer from 1-2 cm depth has an average depth of 1.5 cm.

5.2.1 Organic matter and aluminum content

The measured organic matter content based on the loss on ignition method can be found in appendix 7. Figure 5.1 shows the organic matter content over depth for the upstream (E1), downstream (B1) and delta (D1) core. The organic matter content in core B1 in the lower part is on average 4% and remains approximately constant till a depth of about 18 cm. Further above this depth, the organic matter content increases to 12.5% in the top of the core. In E1 the average organic matter content is around 5.3% in the bottom part. It distinctly starts to increase at a depth of 20 cm to a value of 13.1% in the top layer. The delta core contains the highest organic matter content, which starts with 4.7% at the bottom, after which it distinctly starts to increase at around 30 cm depth to a value of 14.3% in the top layer. Table 5.3 shows the minimum, maximum and average organic matter content of each core.

	B1	E1	D1
Minimum OM (%)	2.95	3.80	3.39
Maximum OM (%)	12.62	13.08	15.22
Average OM (%)	5.70	7.11	9.52

Table 5.3: Minimum, maximum and average organic matter content for the upstream (E1), downstream (B1) and delta (D1) core.

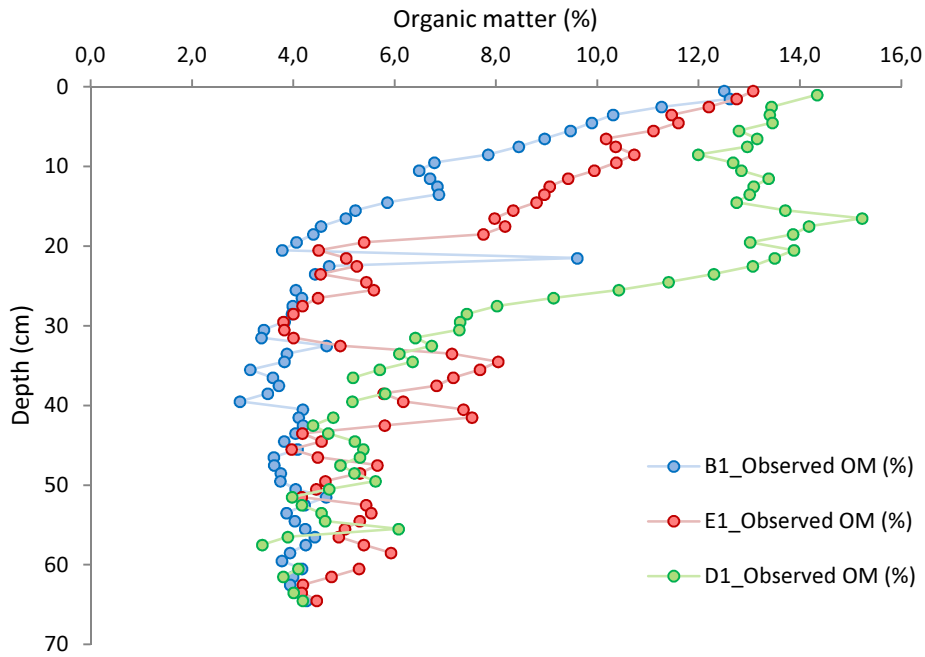


Figure 5.1: Organic matter content over depth for the upstream (E1), downstream (B1) and delta (D1) core.

The aluminum content has the smallest range of values in the delta core (D1) compared to the other cores (table 5.4, figure 5.2). The upstream core (E1) is marked by a gradual increase in aluminum content going deeper in the core. The downstream core (B1) has higher aluminum contents in the upper 13 cm. Further below, the aluminum content sharply declines and reaches a constant variability with an average of 1.6%.

	B1	E1	D1
Minimum Al (%)	1.31	1.35	1.11
Maximum Al (%)	2.11	2.59	1.65
Average Al (%)	1.70	1.79	1.37

Table 5.4: Minimum, maximum and average aluminum content for the cores B1, E1 and D1.

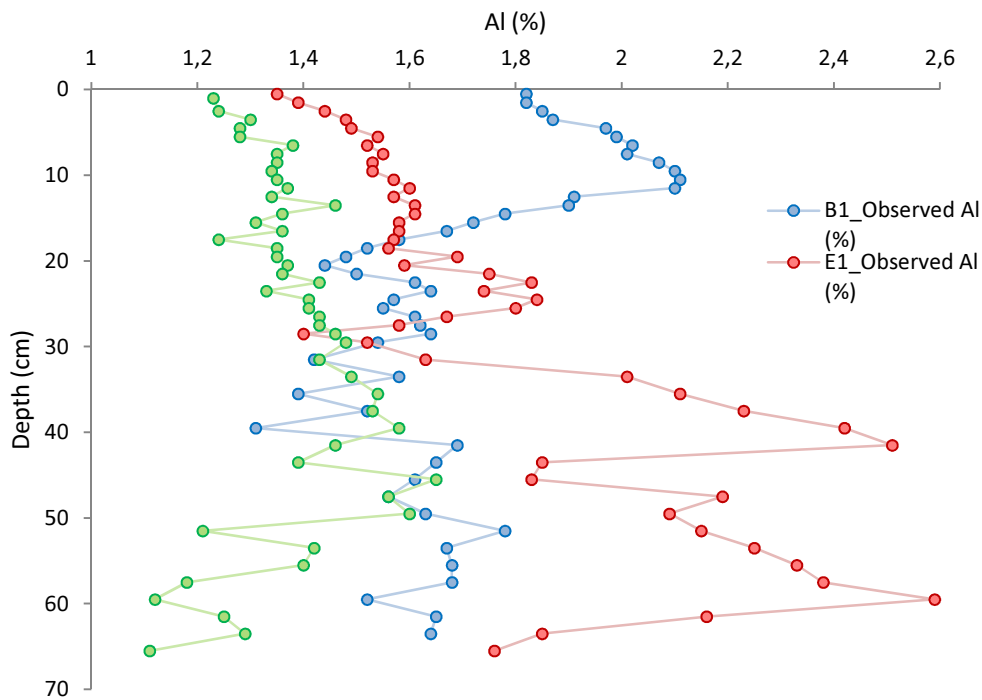


Figure 5.2: Aluminum content over depth for the upstream (E1), downstream (B1) and delta (D1) core.

It is expected that aluminum and organic matter will exert a positive correlation with one and another. Because they belong to the same size fraction, their deposition patterns will be similar during floods. However, this positive relationship was only valid for the lower parts of each core (figure 5.3).

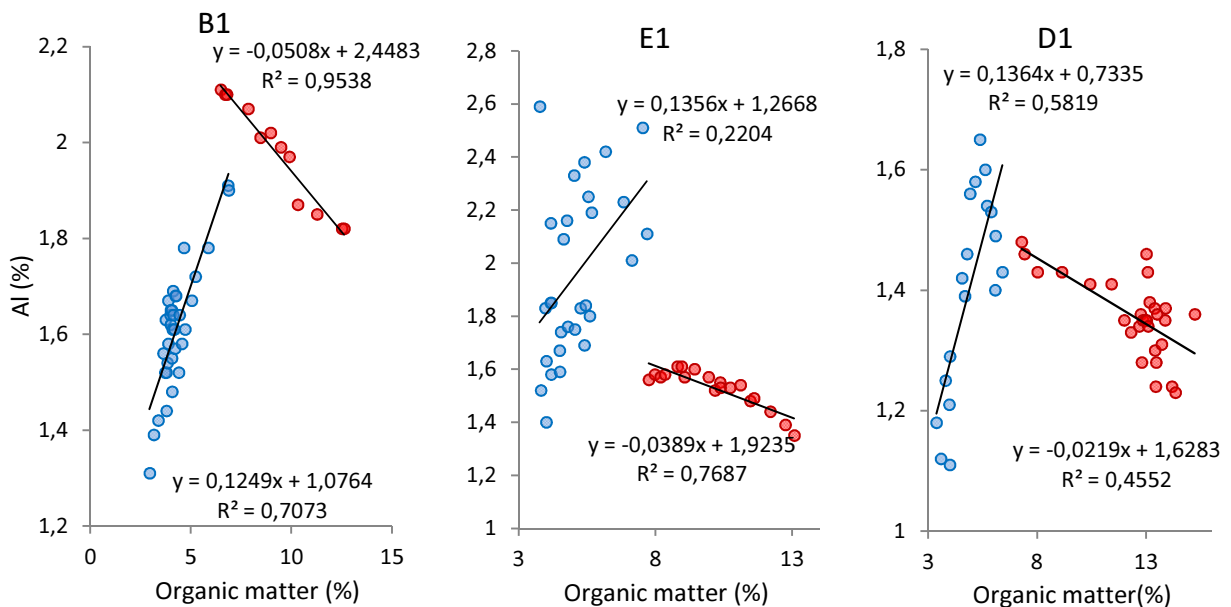


Figure 5.3: Correlation between aluminum and organic matter for the upstream (E1), downstream (B1) and delta (D1) core. The blue scatter plot represents the lower part of each core and the red scatter plot the upper part. The division between the upper and lower part of a core is based on sight i.e. where does the correlation between organic matter and aluminum change from positive to negative.

Figure 5.3 shows the relation between aluminum and organic matter. The division of the aluminum and organic matter data of the cores over the red and blue scatter plot is based on sight. It obviously shows that at higher organic matter concentrations the positive correlation is lost. This is most likely to be the result of terrestrial enrichment of organic matter due to the presence of vegetation. The aluminum content in the upstream (E1) and downstream (B1) core shows a small decrease in the upper 10 cm, which might add an extra effect to the negative relationship between organic matter and aluminum in the upper part of the cores. However, the organic matter increases with a factor of 2 to 3 in the upper part of all three cores compared to the lower part. The effect of the relatively small decrease in aluminum concentration in the upper 10 cm is therefore assumed to be negligibly small. During the qualitative assessment of the cores (appendix 3) it was observed that the largest part of organic matter (roots) was located in the top 20 cm of each core. The red scatter plots in figure 5.4 represent the upper 12 cm for the downstream core (B1), the upper 19 cm for the upstream core (E1) and the upper 30 cm for the delta core (D1).

5.2.2 Particle size and aluminum content

Regressions to validate the use of aluminum as a proxy for clay content result in positive correlations for the upstream (E1) and the downstream (B1) core (figure 5.4), although the degree of scatter is considerable. The delta core (D1) shows a high degree of scatter between aluminum and particle size (figure 5.4) and the regression trend line is not statistically significant. Probably the main reason for these poor results in correlation between aluminum and particle size, lies in the low range of aluminum concentrations present in each core, which is especially true for the delta core (D1) (figure 5.2 and table 5.4). Other reasons that might contribute to a lower correlation between particle size and aluminum are: (1) particle size analysis is often susceptible to errors partly due to the presence of air bubbles, (2) the removal of organic matter by hydrogen peroxide is not an exact science and possibly not all organic matter is removed, (3) the particle size is not measured in the same samples as the metals are (including aluminum). Particle size analysis is susceptible to more uncertainty compared to the aluminum analysis by ICP-MS. It is therefore a rather sensitive method and it is likely to have difficulties to detect small variations in clay content, which is the case in these cores. The strong correlation of aluminum with iron (section 5.2.4) and organic matter in all three cores already validates the use of aluminum as a normalizing constituent, as they are all three considered to be a proxy for clay (section 2.4). The <2 μ m fraction (clay) can be found in appendix 6.

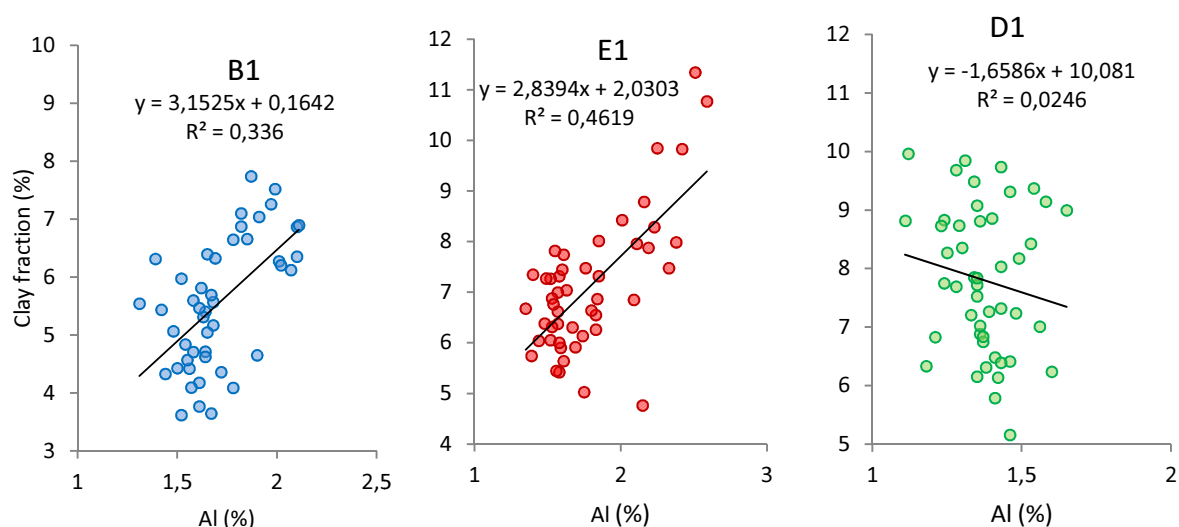


Figure 5.4: Aluminum and clay fraction for the downstream (B1), upstream (E1) and delta (D1) core.

5.2.3 Age-depth profiles and sedimentation

The established decay equations for age calculations of the sediment are given below. The decay constant (λ) for ^{210}Pb decay is $0.03114 \text{ years}^{-1}$. $A(0)$, the cumulative initial concentration integrated over depth, is highest for the delta core (D1), followed are the upstream (E1) and downstream (B1) core respectively:

$$t(D1) = \frac{1}{0.03114} * \ln \frac{514.7}{A(x)}$$

$$t(E1) = \frac{1}{0.03114} * \ln \frac{441.9}{A(x)}$$

$$t(B1) = \frac{1}{0.03114} * \ln \frac{310.1}{A(x)}$$

Figure 5.5 shows the age-depth profiles of the three cores. The delta core (D1), as expected, shows the highest sedimentation rate, which is marked by its steep slopes. Followed in sedimentation rate are the upstream core (E1), which is only slightly less steep than the delta core (D1), and the downstream core (B1), which has remarkably low sedimentation rates. The age of the sediment is the late 1890s, the late 1920s and the early 1940s at 26.5 cm depth for the downstream (B1), upstream (E1) and delta (D1) core respectively. These are expressed as approximate ages as a consequence of the considerable excess in ^{210}Pb below the deepest sample analysed. The outlier at 28.5 cm depth for the downstream (B1) core is likely to be more inaccurate. The dashed lines of the upstream (E1) and delta (D1) core represent the extrapolation of the excess ^{210}Pb below the deepest sample analysed. The ages calculated for this part of the column are therefore a very rough estimate. Appendix 8 contains the ^{210}Pb and ^{137}Cs data.

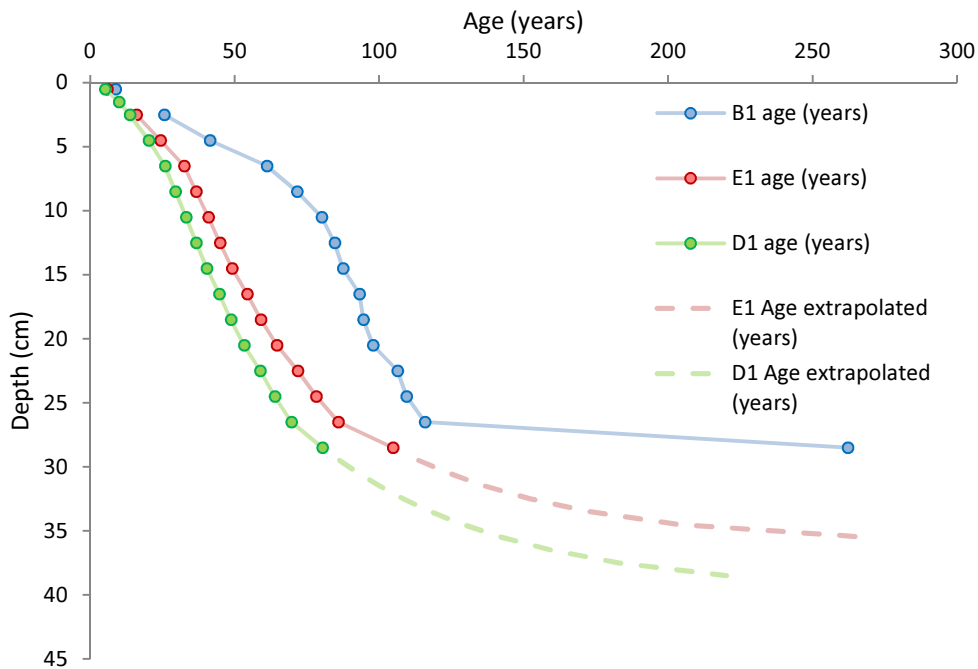


Figure 5.5: Established age-depth profiles for the upstream (E1), downstream (B1) and delta (D1) core.

The ^{137}Cs profiles in figure 5.6 again show the differences in sedimentation rate. Only the delta core (D1) is marked by a distinct peak that is related to the nuclear bomb tests in 1963 in North America.

The other cores show no such peak. From the age-depth profiles can be determined that those peaks should be at around 14.5 cm depth for the upstream core (E1) and 5.5 cm depth for the downstream core (B1). The ^{137}Cs peak was used as a time proxy to optimize the model parameters for the ^{210}Pb dating.

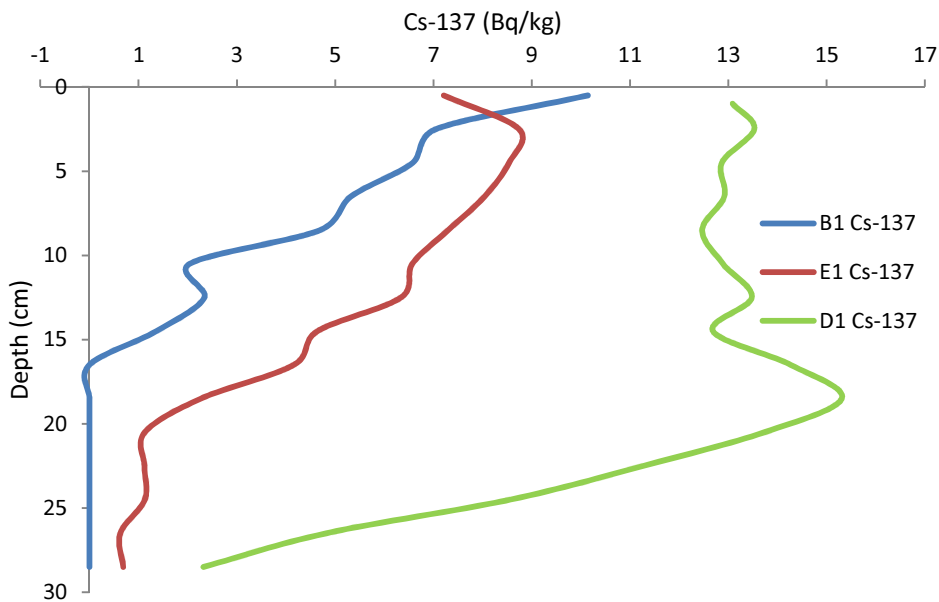


Figure 5.6: ^{137}Cs profiles for the upstream (E1), downstream (B1) and delta (D1) core. Note the significant peak in the delta core (D1) at 18.5 cm depth.

5.2.4 Manganese and iron depth profiles

The manganese- and iron depth profiles are correlated in all three cores, except for the distinct peak in iron content (6%) in the delta core (D1) at a depth of 17.5 cm (figure 5.7, 5.8 and 5.9). The patterns of both manganese and iron are irregular and spiky in all three cores. The manganese concentrations in the upstream (E1) and downstream (B1) core are considerably higher compared to the delta core (D1) (table 5.5).

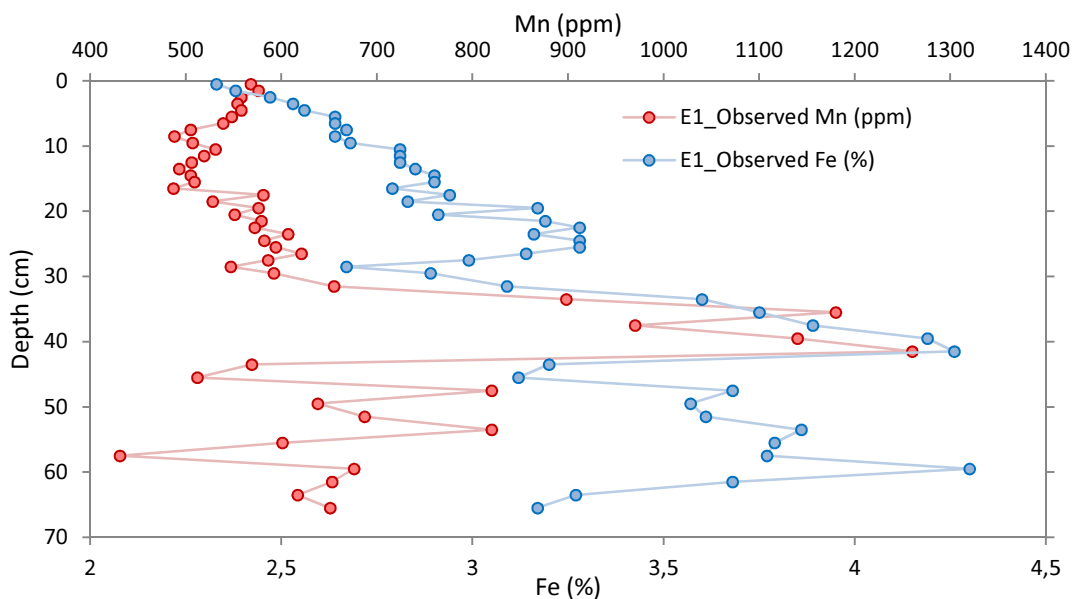


Figure 5.7: Observed manganese concentration and iron content in the upstream core (E1).

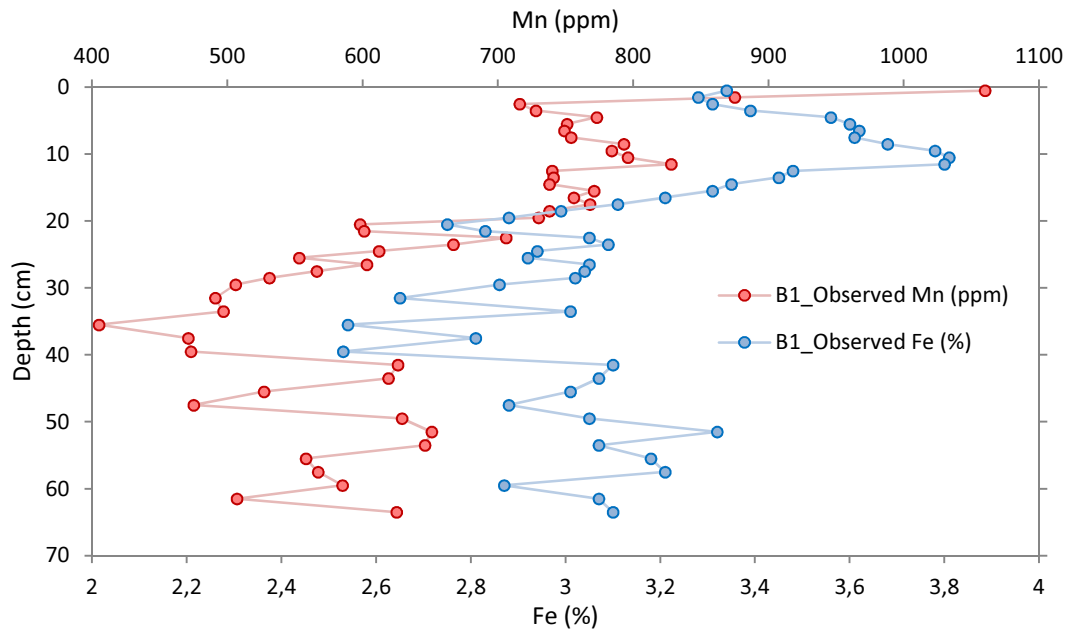


Figure 5.8: Observed manganese concentration and iron content in the downstream core (B1).

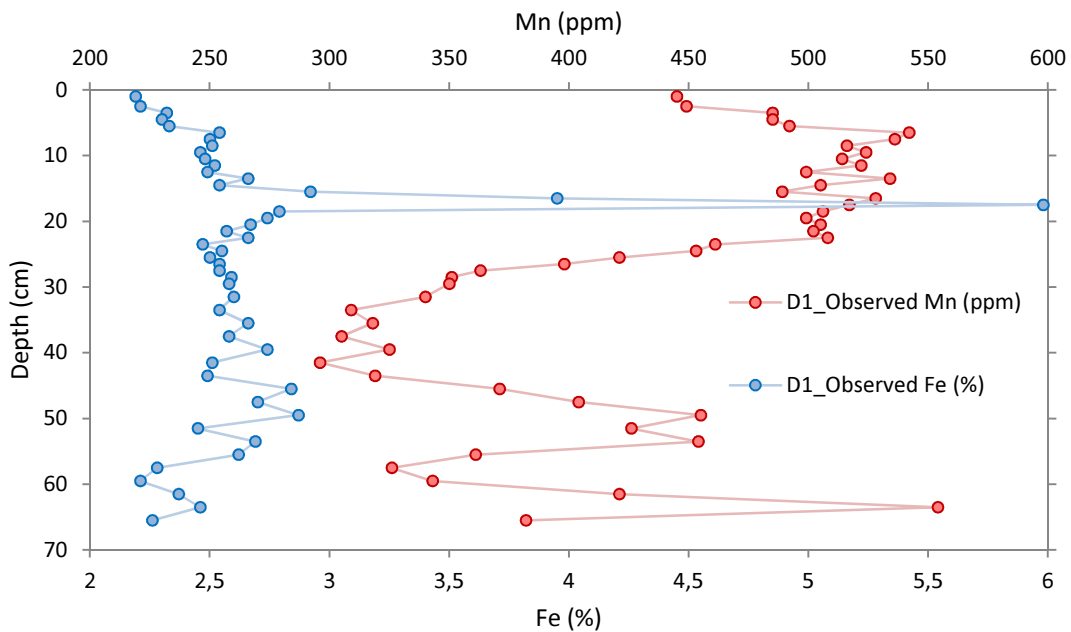


Figure 5.9: Observed manganese concentration and iron content in the delta core (D1).

	B1	E1	D1
Minimum Mn (ppm)	405	431	596
Maximum Mn (ppm)	1060	1260	554
Average Mn (ppm)	657	630	438
Minimum Fe (%)	3.16	2.33	2.19
Maximum Fe (%)	2.53	3.14	2.63
Average Fe (%)	3.81	4.3	5.98

Table 5.5: Minimum, maximum and average manganese concentration and iron content for the upstream (E1), downstream (B1) and delta (D1) core.

The baselines (figure 5.10) for iron show a good correlation with aluminum and iron in the upstream (E1) and downstream (B1) cores (R^2 is 0.99 and p-value is $1.79E-22$). Manganese shows less correlation with aluminum (R^2 is 0.47 and p-value is 0.0002), which is marked by the high degree of scatter around the baseline plot. The baseline of iron for the delta core (D1) (figure 5.11) also indicates a strong correlation with aluminum (R^2 is 0.88, p-value is $5.83E-06$). However, manganese is not correlated with aluminum.

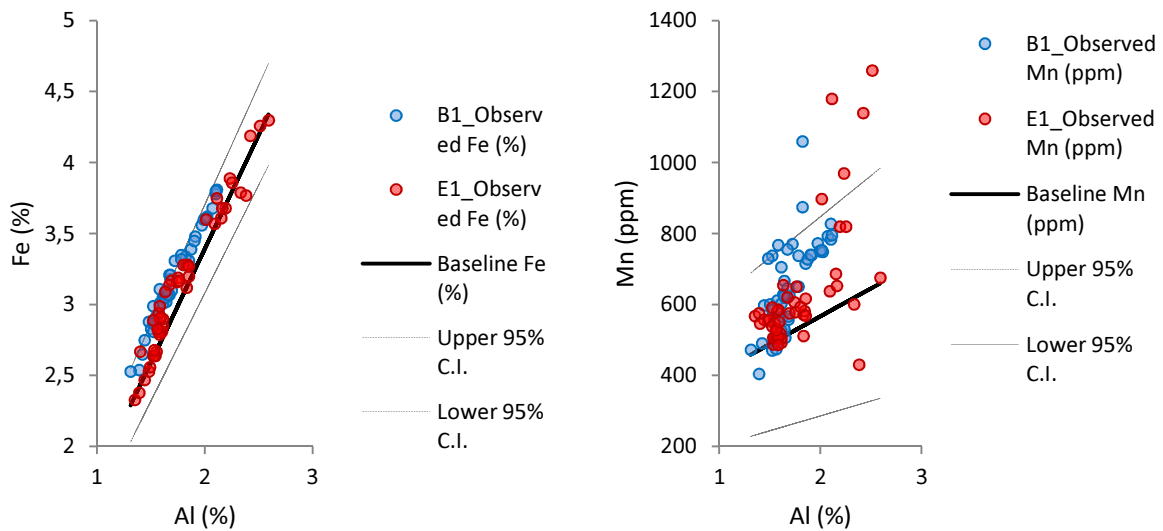


Figure 5.10: Iron and manganese baselines from regression analyses for the upstream (E1) and downstream (B1) cores.

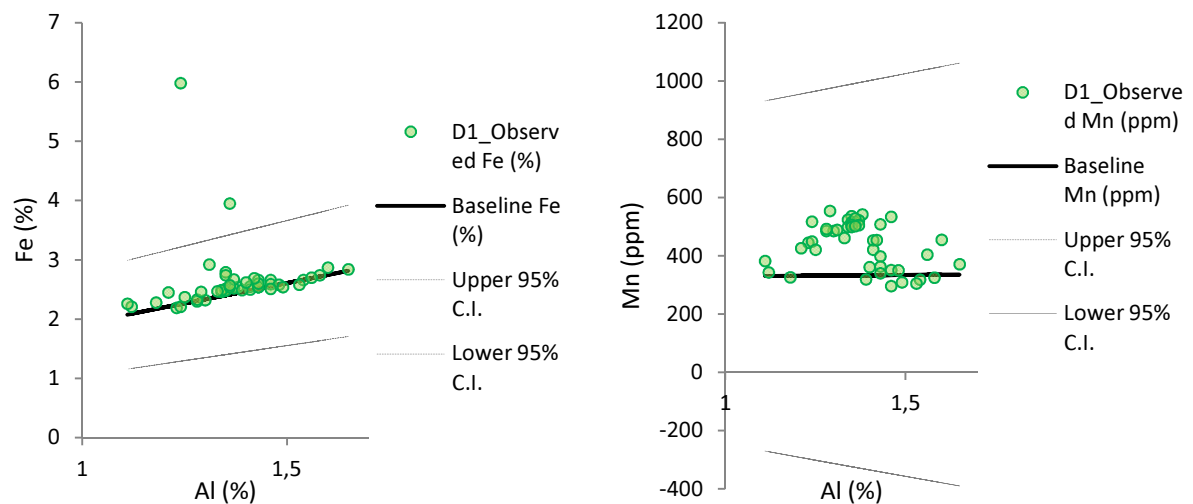


Figure 5.11: Iron and manganese baselines from regression analysis for the delta core (D1).

According to the study of Du Laing et al. (2007), as described in the literature study, the main mechanism responsible for trace metal mobilization is the desorption of metals related to the unstable manganese and iron (hydr)oxides due to a lowering of redox potential. However, the good correlation between iron and aluminum indicates no such mechanism (vertical migration) to take place substantially in these floodplain cores. Except one peak in iron concentration present in the delta core (D1) at 17.5 cm depth, which shows no correlation with aluminum, might indicate an effect of redox potential. The lower correlation between manganese and aluminum is likely the result of the large range in natural variability (7 – 9000 ppm) of manganese (Emsly, 2003) and not redox potential as manganese follows the same pattern over depth as iron.

5.3 Metal depth profiles

This section describes the metal depth-profiles of the residual concentrations and the distribution of the total concentrations around the calculated baseline for the metals Cu, Zn, Pb, Cd, Se and As. *Note: Appendix 1 shows the total concentrations against depth as measured by ICP-MS.*

5.3.1 The upstream (E1) and downstream (B1) core

Copper (figure 5.12)

The concentrations in the upstream core (E1) are more concentrated around the baseline of Cu compared to the concentrations in the downstream core (B1). The concentrations of the upstream core (E1) show a more scattered pattern. Even though concentrations in the downstream core (B1) on average lie about 15.9 ppm above the baseline, it shows a more linear relationship with aluminum. The residual plot shows almost no residual concentration for the upper 19.5 cm in the upstream core (E1) and has an average residual concentration of 0.055 ppm compared to 16.3 ppm in the downstream core (B1) in this part. There is a sudden increase in residual concentration below 19.5 cm depth in the upstream core (E1) till a depth of 21.5 cm (11.1 ppm). Below this depth the residual concentration remains approximately constant till a depth of 29.5 cm. The downstream core (B1) mirrors this pattern in the upper 29.5 cm. Whereas the upstream core (E1) residual concentrations fluctuate heavily below 29.5 cm depth, the downstream core (B1) residual concentrations remain relatively constant below 29.5 cm with an average of 15.6 ppm. At 33.5, 47.5 and 59.5 cm depth peaks in the upstream core (E1) occur, but on average (15.8 ppm) the residual concentration below 29.5 cm is similar to that of the downstream core (B1). It is therefore not attributed to anthropogenic activity.

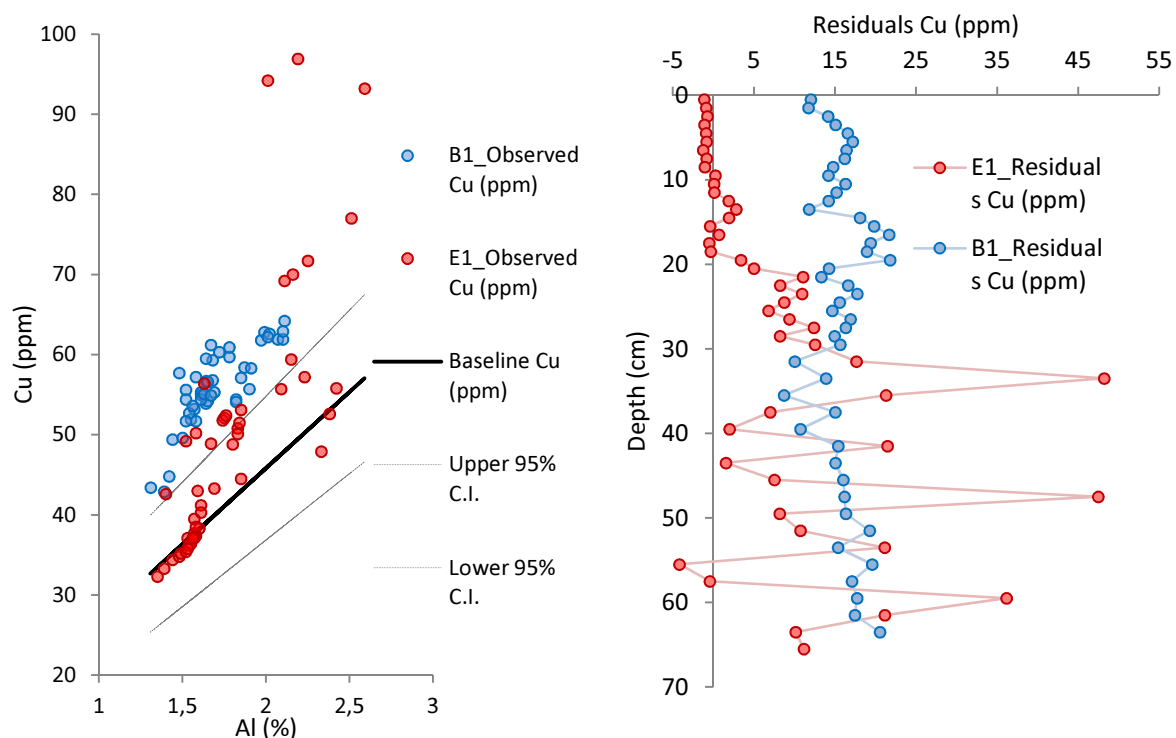


Figure 5.12: Left: Copper baseline and confidence levels in a scatter plot with total concentrations of the upstream (E1) and downstream (B1) core. Right: depth profile of the copper residual concentrations in the upstream (E1) and downstream (B1) core.

Zinc (figure 5.13)

The upstream core (E1) concentrations give a more scattered pattern, but on average are closer to the baseline than the downstream core (B1) concentrations. The downstream core (B1) concentrations are less scattered and therefore show a better linear correlation with aluminum. Just as for Cu, this linear correlation in the downstream core (B1) concentrations lies consistently above the baseline with on average 16.8 ppm. The upper 12.5 cm is marked by a higher residual concentration in the downstream core (B1) with on average 17.2 ppm compared to 9.9 ppm for the upstream core (E1). At 12.5 cm depth the residual concentrations are approximately the same, after which the downstream core (B1) is again marked by much higher residual concentrations. This difference becomes larger below 37.5 cm depth. No distinct peaks or patterns relating to anthropogenic activity can be seen. The pattern of Zn in the deeper part of both the upstream (E1) and the downstream (B1) core shows a higher variability in residual concentration.

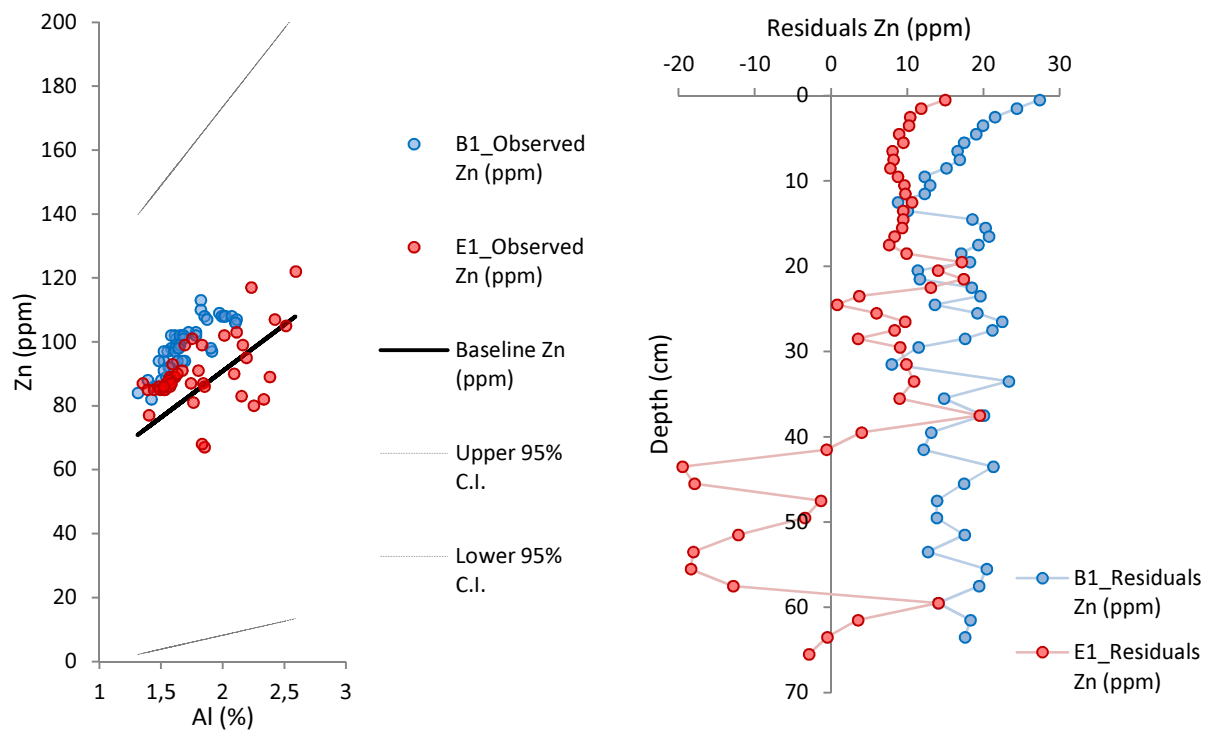


Figure 5.13: Left: Zinc baseline and confidence levels in a scatter plot with total concentrations of the upstream (E1) and downstream (B1) core. Right: depth profile of the zinc residual concentrations in the upstream (E1) and downstream (B1) core.

Selenium (figure 5.14)

The majority of the concentrations of both the upstream (E1) and downstream (B1) core are positioned above the baseline. This is reflected in the depth profile of the Se residual concentrations. The lowest part of the column was represented in the regression, while the upper part of both cores are marked by relatively high residual concentrations. In the upper 6.5 cm, the downstream core (B1) has higher residual concentrations. Below 6.5 cm depth the upstream core (E1) has higher residual concentrations till about 49.5 cm depth. The downstream core (B1) again prevails below 49.5 cm depth. The Se profile in both cores has no real distinct peaks, but is marked by a more or less constant lower part below 29.5 cm, after which it gradually increases in the upper part of the column till a residual concentration of 1.33 ppm (B1) and 0.62 ppm (E1). This gradual increase in selenium concentrations in both cores reflects anthropogenic activity.

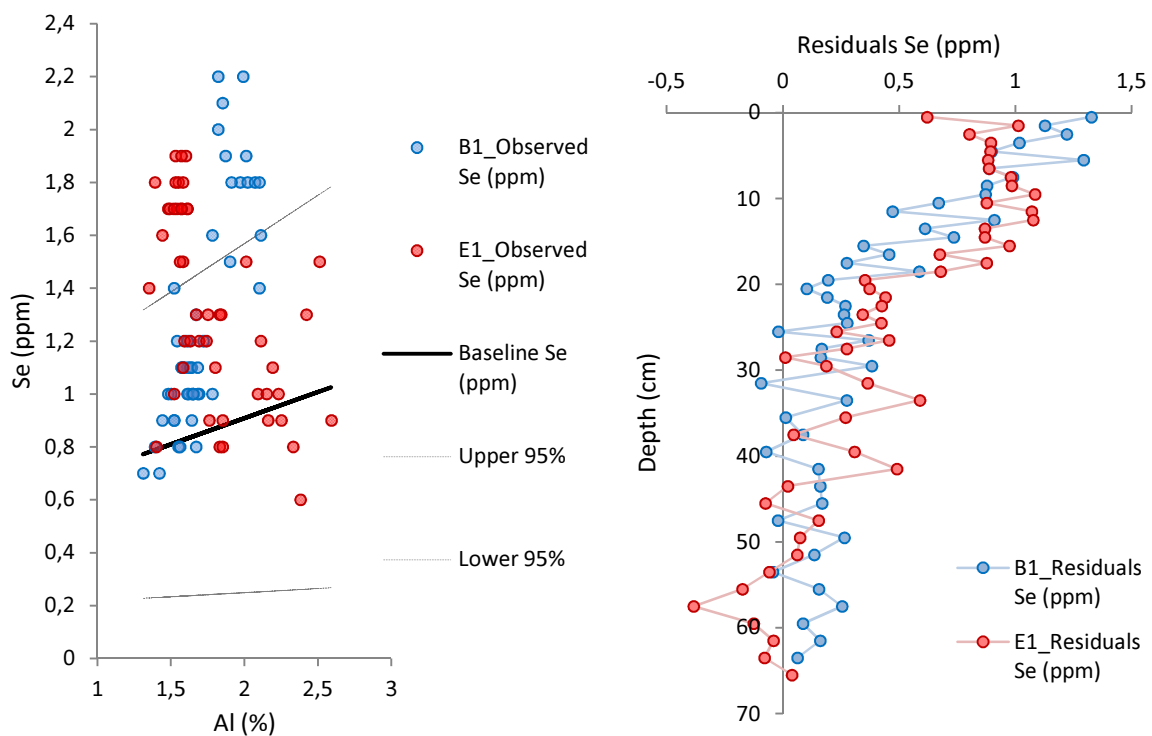


Figure 5.14: Left: Selenium baseline and confidence levels in a scatter plot with total concentrations of the upstream (E1) and downstream (B1) core. Right: depth profile of the selenium residual concentrations in the upstream (E1) and downstream (B1) core.

Cadmium (figure 5.15)

Both cores show a poor correlation with aluminum and the majority of the observed total concentrations are positioned well above the baseline. A large part of the upstream core (E1) is even positioned above the upper confidence interval. The upper 24.5 cm is marked by a mirrored behavior with the upstream residual concentrations being on average 0.24 ppm higher. The residual concentrations between 24.5 and 31.5 cm are approximately the same for both cores, but below 31.5 cm, the concentrations in the upstream core (E1) exceed again. The depth profile of the upstream core (E1) shows a higher degree of variation in residual concentrations compared to the downstream core (B1). In both cores no indication of anthropogenic activity can be distinguished.

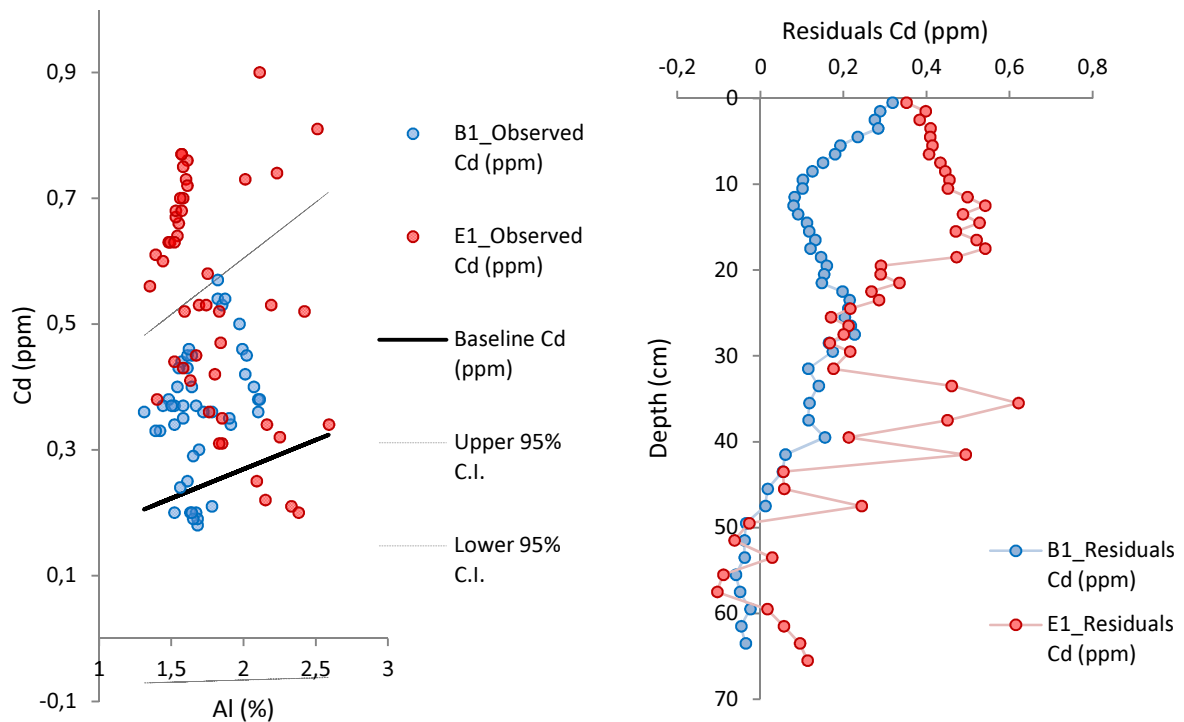


Figure 5.15: Left: Cadmium baseline and confidence levels in a scatter plot with total concentrations of the upstream (E1) and downstream (B1) core. Right: depth profile of the cadmium residual concentrations in the upstream (E1) and downstream (B1) core.

Lead (figure 5.16)

The majority of the concentrations for both cores are close to baseline concentrations. The upstream core (E1) is more concentrated along the whole length of the baseline, showing a linear correlation, while the concentrations of the downstream core (B1) are more distributed in a cluster. In the upper 11.5 cm of the cores, residual concentrations in the upstream core (E1) exceed residual concentrations in the downstream core (B1) with an average of 0.98 ppm and -0.069 ppm respectively. The behavior of the residual concentration in both cores is similar in this section. Below 11.5 cm, the downstream core (B1) exceeds the upstream core (E1) for the rest of the column depth. The residual concentrations steadily increase in the upstream core (E1), but the downstream core (B1) shows the opposite pattern. Also here, no pattern or peak indicating anthropogenic activity can be seen.

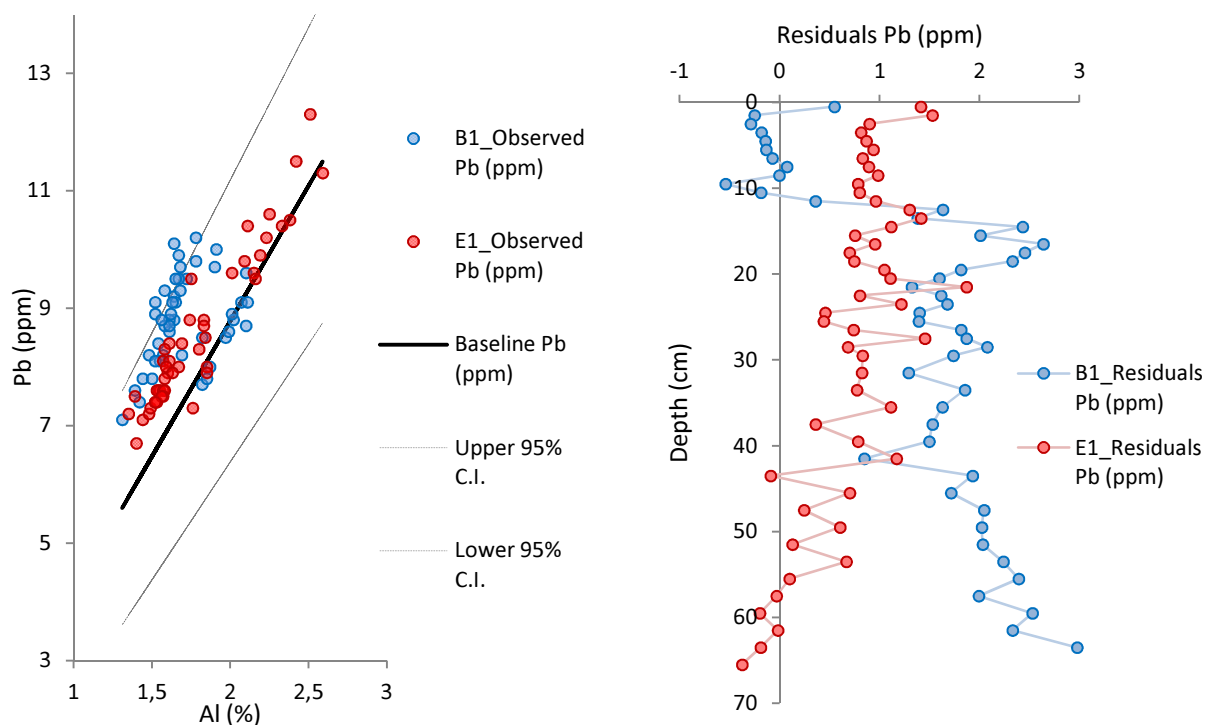


Figure 5.16: Left: Lead baseline and confidence levels in a scatter plot with total concentrations of the upstream (E1) and downstream (B1) core. Right: depth profile of the lead residual concentrations in the upstream (E1) and downstream (B1) core.

Arsenic (figure 5.17)

The baseline plot shows a scattered behavior for both cores, with concentrations of the downstream core (B1) clearly exceeding concentrations of the upstream core (E1) on average. Also a good quantity of concentrations is located above the upper confidence level of the baseline. The upper 19.5 cm of the cores is marked by higher residual concentrations in the downstream core (B1) compared to the upstream core (E1) with average residual concentrations of 3.66 ppm and 0.34 ppm respectively. A distinct peak occurs at 17.5 cm depth in the downstream core (B1) with a residual concentration of 10.4 ppm. The absence of this peak in the upstream core (E1) indicates that this peak reflects past activity of the Black Creek mine. Below a depth of 20.5 cm the residual concentrations stay approximately constant over the rest of the column depth with an average of 2.55 ppm. The upstream core (E1) shows not much variation in residual concentration over depth.

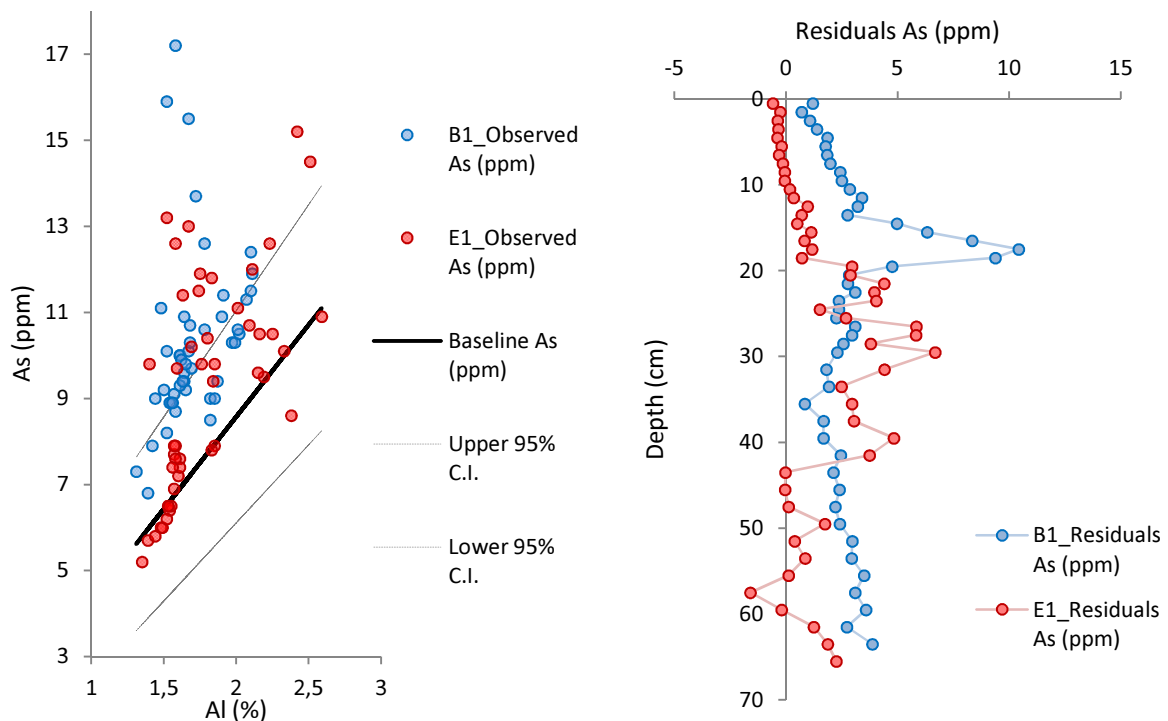


Figure 5.17: Left: Arsenic baseline and confidence levels in a scatter plot with total concentrations of the upstream (E1) and downstream (B1) core. Right: depth profile of the arsenic residual concentrations in the upstream (E1) and downstream (B1) core.

5.3.2 The delta core

Copper (figure 5.18)

Except for one data point on the baseline plot, the majority of the total concentrations are well distributed around the baseline. A distinct peak occurs at a depth of 17.5 cm with a residual concentration of 38.2 ppm. The rest of the column shows not much variation in residual concentration and therefore represents the local geology flux of Cu.

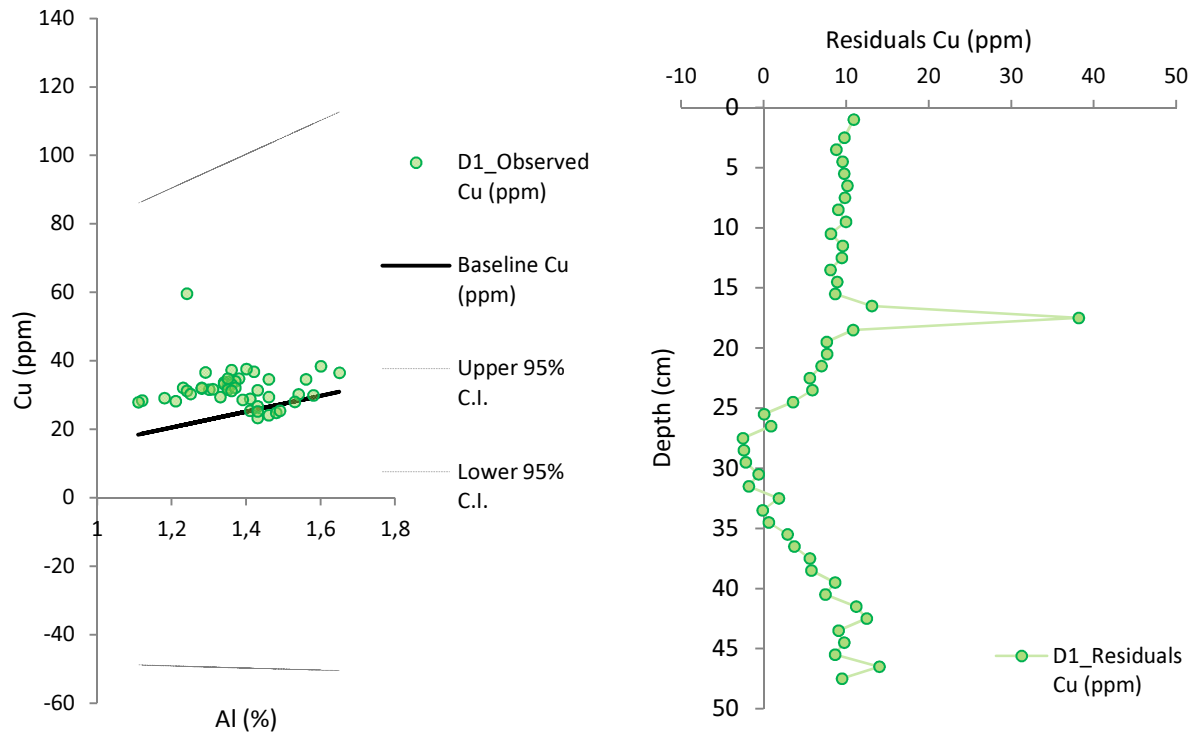


Figure 5.18: Left: Copper baseline and confidence levels in a scatter plot with total concentrations of the delta core (D1). Right: depth profile of the copper residual concentrations in the delta core (D1).

Zinc (figure 5.19)

There is a high degree of scatter around the baseline indicating a low correlation with aluminum. The scatter plot of Zn is marked by: (1) a group concentrated around the baseline and correlated with aluminum, (2) a cluster positioned well above the baseline and upper confidence level, and (3) a few data points in between. The upper 20.5 cm is marked by a constant high residual concentration with an average value of 274.6 ppm, which is followed by a sharp decline. Below 35.5 cm depth the residual concentrations reach an asymptote with an average of -0.63 ppm till a depth of 56 cm. Below 56 cm depth the residual concentrations increase slightly.

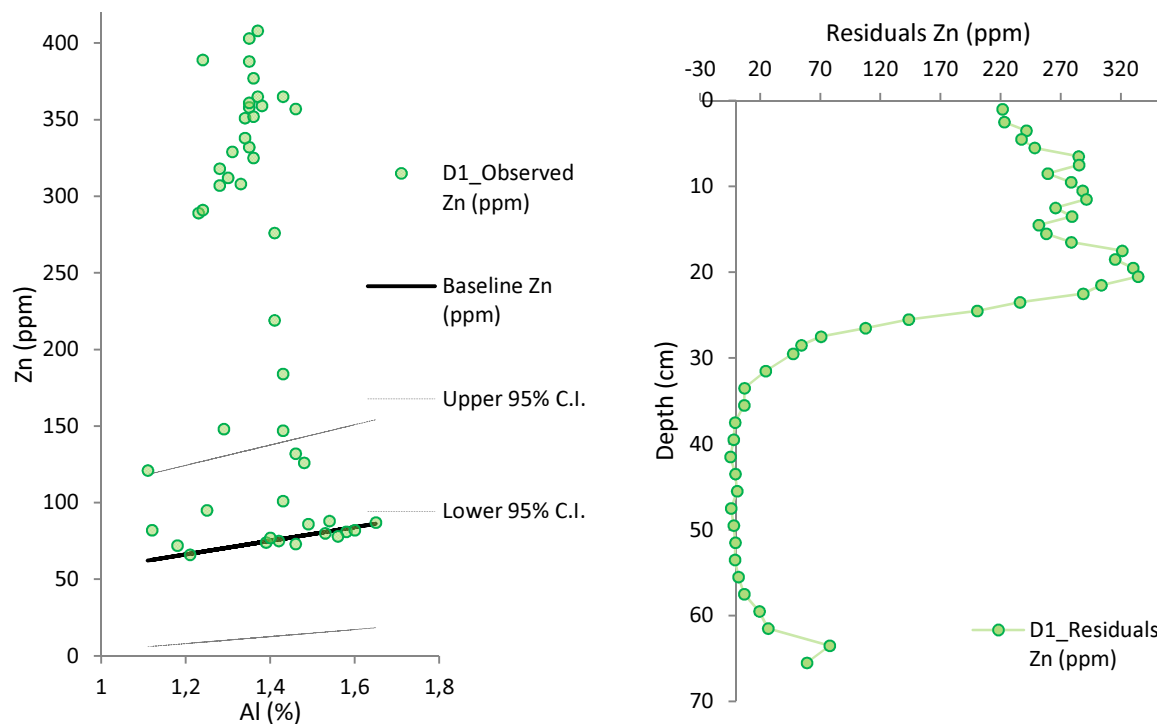


Figure 5.19: Left: Zinc baseline and confidence levels in a scatter plot with total concentrations of the delta core (D1). Right: depth profile of the zinc residual concentrations in the delta core (D1).

Selenium (figure 5.20)

The majority of the concentrations is located on or well above the baseline and upper confidence level. Selenium shows the same pattern over depth as Zn. The top 20.5 cm is marked by a high residual concentration with an average value of 0.79 ppm and is followed by a sharp decline. The residual concentration below 35.5 cm depth varies around an average of 0.05 ppm.

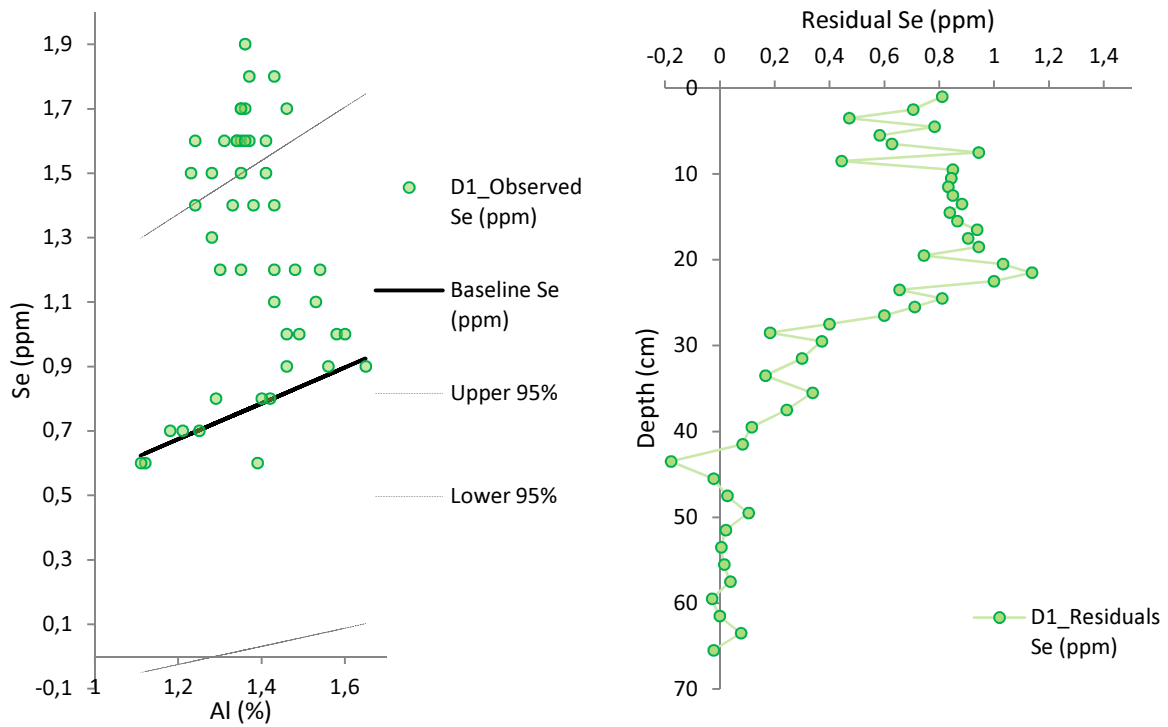


Figure 5.20: Left: Selenium baseline and confidence levels in a scatter plot with total concentrations of the delta core (D1). Right: depth profile of the selenium residual concentrations in the delta core (D1).

Cadmium (figure 5.21)

The majority of the total concentrations are positioned well above the baseline and a large part even above the upper confidence level. The scatter plot of Cd shows a similar pattern as for Zn. The distribution of the residual concentrations shows the same pattern as for Zn and Se, with an average high residual concentration of 0.76 ppm in the upper 20.5 cm, which decreases sharply to an average of -0.0067 ppm below 35.5 cm depth.

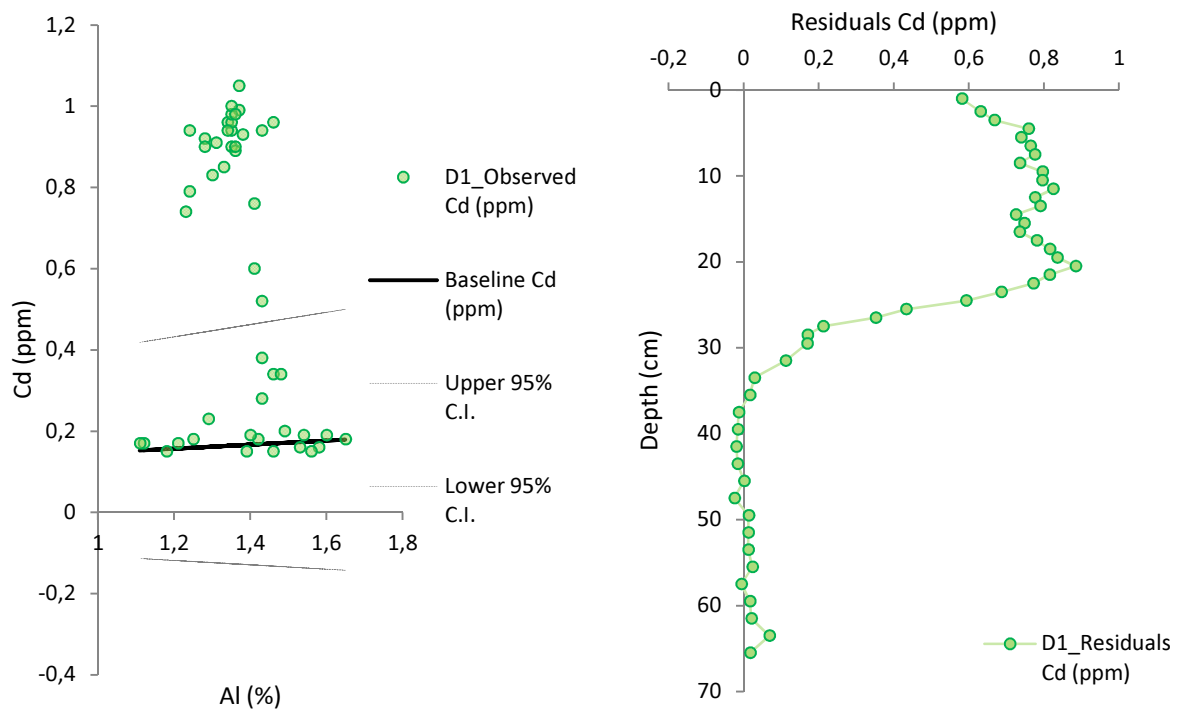


Figure 5.21: Left: Cadmium baseline and confidence levels in a scatter plot with total concentrations of the delta core (D1). Right: depth profile of the cadmium residual concentrations in the delta core (D1).

Lead (figure 5.22)

A part of the Pb total concentrations is concentrated around the baseline and correlates well with aluminum, while a cluster appears far above the baseline and upper confidence level similar in pattern as Zn and Cd. Pb also shows the same pattern in metal distribution as Zn, Se, and Cd with an average residual concentration of 24.2 ppm in the upper 20.5 cm. Below 35.5 cm depth the residual concentration reaches an asymptote with an average value of 0.19 ppm.

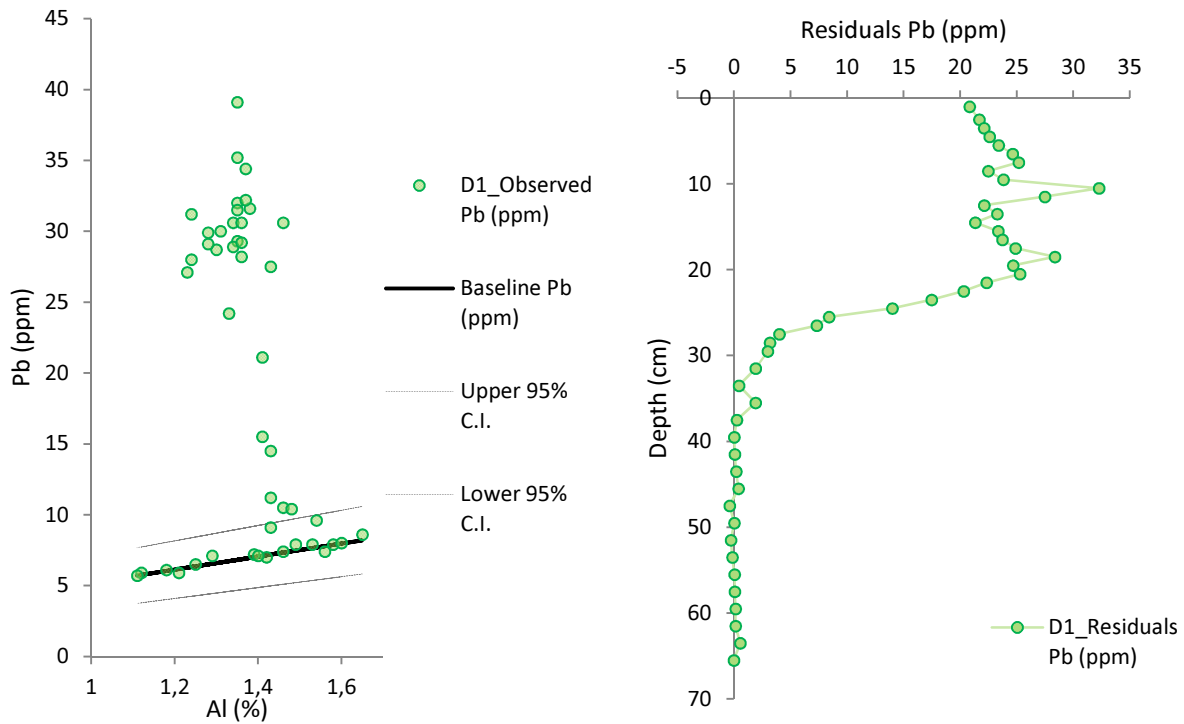


Figure 5.22: Left: Lead baseline and confidence levels in a scatter plot with total concentrations of the delta core (D1). Right: depth profile of the lead residual concentrations in the delta core (D1).

Arsenic (figure 5.23)

As (arsenic) shows a linear correlation with aluminum, however, a large part of the concentrations are consistently between 0.5 and 1 ppm higher than baseline concentrations. The depth profile of the residual concentrations is remarkably similar as for Cu, with a distinct peak at 17.5 cm depth (4.0 ppm). The peaks in As and Cu are probably related.

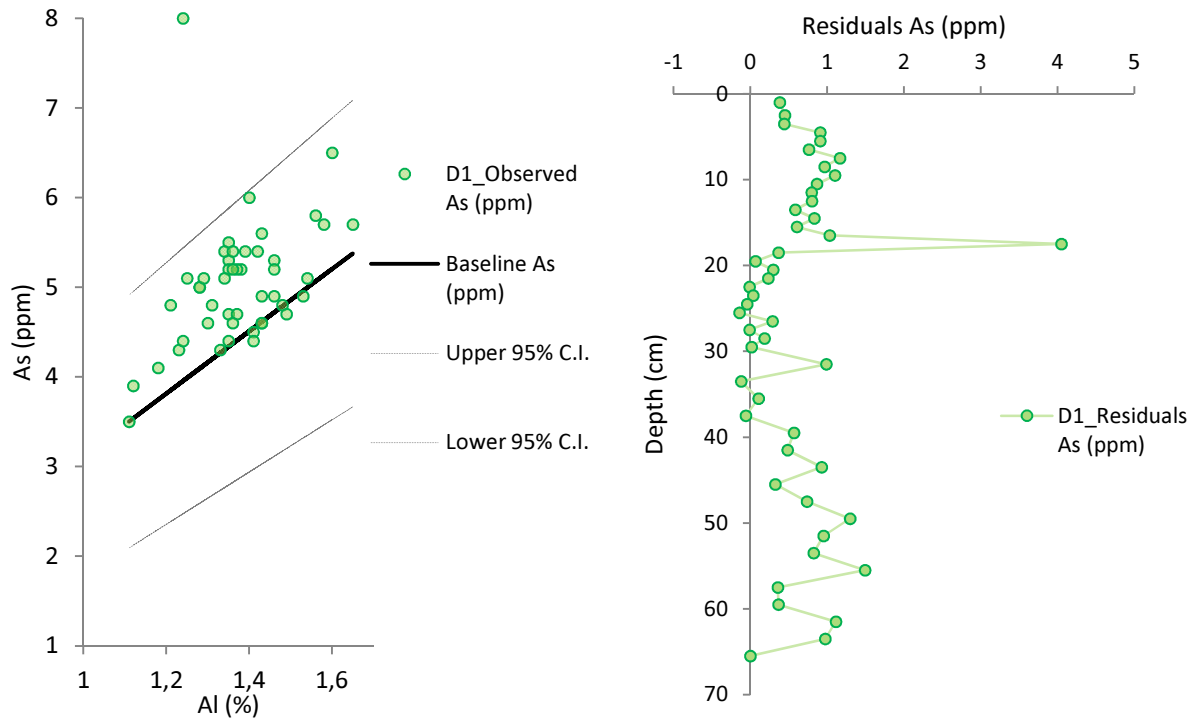


Figure 5.23: Left: Arsenic baseline and confidence levels in a scatter plot with total concentrations of the delta core (D1). Right: depth profile of the arsenic residual concentrations in the delta core (D1).

5.4 Interpretation and discussion

The majority of the variability in residual concentrations described for the upstream (E1) and downstream (B1) core are relatively small and reflect natural variability. Natural variability can result from, for example, the different subsequent responses of sediment mobilization in different parts of the catchment with associated different chemical compositions (section 2.2). Especially the lower parts of these columns (below 30 cm) show a higher degree of variation in residual concentrations over depth. However, as this part is already over a hundred years old and represent pre-Black Creek mine times, this variation is insignificant to assess the impact of the Black Creek mine. Although, it of course reflects natural activities of the Horsefly River itself. The delta core (D1) has more consistent residual concentrations in the lower part of its column, which is probably due to the high degree of mixing when the sediment reaches the delta. The chemical footprint of a particular area in the upstream catchment during storm is diluted by other sediment while transported downstream. For this reason the natural variability of metals in the delta core (D1) is not as pronounced compared to the upstream (E1) and downstream (B1) core.

The main results of the depth profiles of all three cores, which possibly do indicate mining or another anthropogenic activity, are:

1. The peak in arsenic in the downstream (B1) core at 17.5 cm depth, which is absent in the upstream (E1) core, reflects activity of the Black Creek mine.
2. The selenium profiles of the upstream (E1) and downstream core (B1), which show a gradual increase going from 20-30 cm depth till present day, indicate a further upstream located source.
3. The arsenic and copper residual metal distribution in the delta core (D1) in which they both distinctly peak at 17.5 cm depth.
4. The profiles of zinc, cadmium, selenium and lead in the delta core, which show remarkably high residual concentrations in the upper 20.5 cm of the core compared to the lower part of the core.

These profiles are compared to the age-depth profiles and the relative contribution of residual concentration compared to the total concentration is calculated. The residual part of the total concentration is assumed to be that part in concentration originating from anthropogenic activities, but small deviations from the calculated baseline or low regression results also attribute a small value (residual concentration) to the natural variability in the core. This natural variability must be subtracted from the total residual concentration to achieve a more accurate residual concentration related to anthropogenic activity.

5.4.1 Response of metal contamination to mining activities in the Horsefly floodplain

Mining activities in the Horsefly River floodplain manifest mainly in clearly elevated concentrations (above the baseline) of arsenic and selenium. The downstream core (B1) shows a peak in arsenic concentration at a depth of 17.5 cm, which marks a high concentration on the onset of an anthropogenic activity and decreases after. Selenium concentrations are marked by a gradual increase in residual concentrations going upwards in both the upstream (E1) and downstream (B1) core and remain high after the onset of anthropogenic activities. Other metals have little to no impact on the fine sediment geochemistry upstream of Horsefly in the Horsefly catchment.

The impact of the Black Creek mine on fine sediment geochemistry

The absence of this arsenic peak in the upstream core (E1) reflects the impact of the Black Creek mine at this depth (age). The peak comprises 60.6% - 26.4% (23.5 cm and below) is 34.2% of the total concentration (17.2 ppm) that does not stem from local geology (figure 5.24). The average concentration below the peak in arsenic is subtracted, because it is a part that does not stem from anthropogenic activities and reflects an asymptote of natural variability. The peak corresponds in age to the early 1920s, which was in the time of gold drilling tests in the Black Creek mine by Phil Fraser (Panteleyev et al., 1996). It seems odd this test would give a signal in contrast to the hydraulic operation, which was developed in 1930 by James Armes and was in production for 5 years. The peak also corresponds to the general response of arsenic to mining: high productivity will result in a peak concentration, but after mine closure the concentrations will go back to pre-mining conditions. This is because arsenic is usually not easily released by weathering. This arsenic peak at 17.5 cm depth in the downstream core (B1) therefore indicates a high mining productivity period. Thus, if there would be a peak present in the downstream core (B1) related to the Black Creek mine, it has the highest probability to be present around the early 1930s in the time the hydraulic mine was in operation. As the excess ^{210}Pb in the downstream core (B1) decreased considerably fast over depth, this may result in a larger deviation from accurate age determination. With this in mind, maybe the age determination did even give a reasonable estimate to indicate the period of the early part of the 20th century to correspond to a peak relating to mining activities in the Black Creek mine.

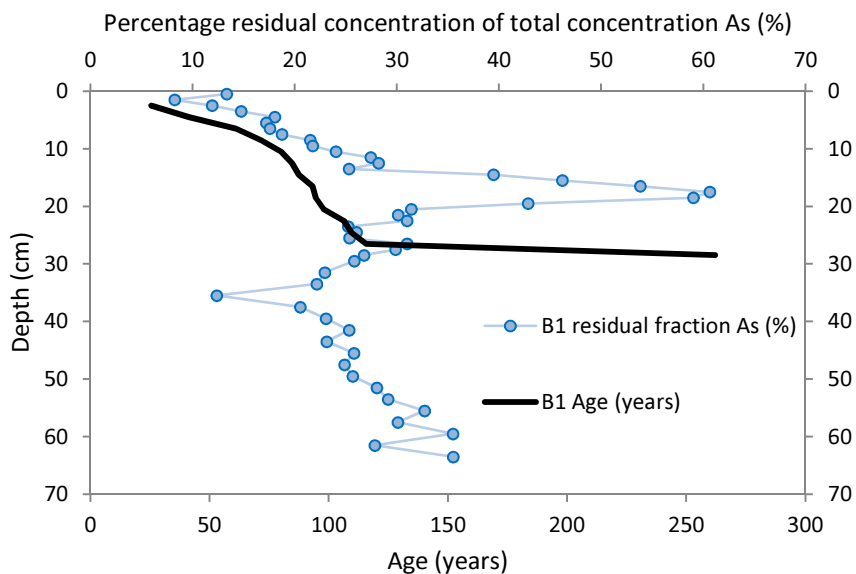


Figure 5.24: The percentage residual concentration of the total concentration for the downstream (B1) core for arsenic to compare the peak occurring at 17.5 cm depth to its age.

Source concentrations of arsenic in the Black Creek mine are still elevated at present with an average concentration of 45.0 ppm (Clark, 2013) (figure 5.28). Even in the lower part of Black Creek, although already partly diluted, the concentrations are still elevated (22.0 ppm). The fraction residual concentrations of arsenic in the downstream core (B1) diminish rapidly over time after the occurrence of the peak at 17.5 cm depth (figure 5.24). Apparently, although still elevated in the lower part of the Black Creek, this signal is not strong enough to be traced back on the Horsefly floodplain (or delta). This already reveals the magnitude of the Horsefly River compared to the Black Creek. Only a strong pulse, such as the hydraulic operation in the Black Creek mine in the early 1930s is able to give a signal on the Horsefly floodplain and to overcome the dilution by, the in comparison, enormous amount of uncontaminated sediment from the Horsefly River itself.

An uninvestigated source of selenium upstream of the Black Creek

The onset of selenium coincides somewhere below the deepest sample analysed for ^{210}Pb and therefore the approximate year of this onset is determined using the extrapolation of excess ^{210}Pb . This is shown in figure 5.25 together with the moving average of the percentage residual concentrations as a guide to identify this onset. The onset of the selenium increase can be more clearly seen in the downstream core (B1) and lies around 23.5 cm depth corresponding to an age of the early 1900s. The upstream core (E1) shows an increase in selenium concentrations deeper in the core, but this rise is not clearly marked. Comparing the age of early 1900 of the downstream core (B1) to a corresponding depth in the upstream core (E1) results in a depth of approximately 28.5 cm. Below the depths of 23.5 cm (B1) and 28.5 cm (E1), the average percentage residual concentration are 12.1% and 4.0% respectively. The fraction of the total concentration that is not related to the local geology (residual concentration) is at present 48.2% (60.3%-12.0%) and 40.3% (44.3%-4.0%) for the downstream (B1) and upstream (E1) core respectively. The pattern of selenium concentrations in the downstream core (B1) shows an increase in concentrations since the early 1900s till present day, but in the upstream core (E1) the increase seems to stagnate at 17.5 cm depth (approximate age is 55 years). However, it is inaccurate to estimate patterns in the upper part of the downstream core (B1), since the sedimentation rate is even lower than the upstream core (E1) at present day. The associated depth in the downstream core (B1) with an approximate age of 55 years lies in the upper 5 cm of the core. It is difficult to identify a pattern in a cluster of only 5 metal concentrations. As the source of input of selenium in both cores is the same, the signals in both cores are assumed to be similar, but influenced by the deposition pattern. Therefore recent information about the behaviour (release rates) of the selenium source is best to be read from the profile of the upstream core (E1), because the same range of data (1900 till present day) is stretched over more measurement points.

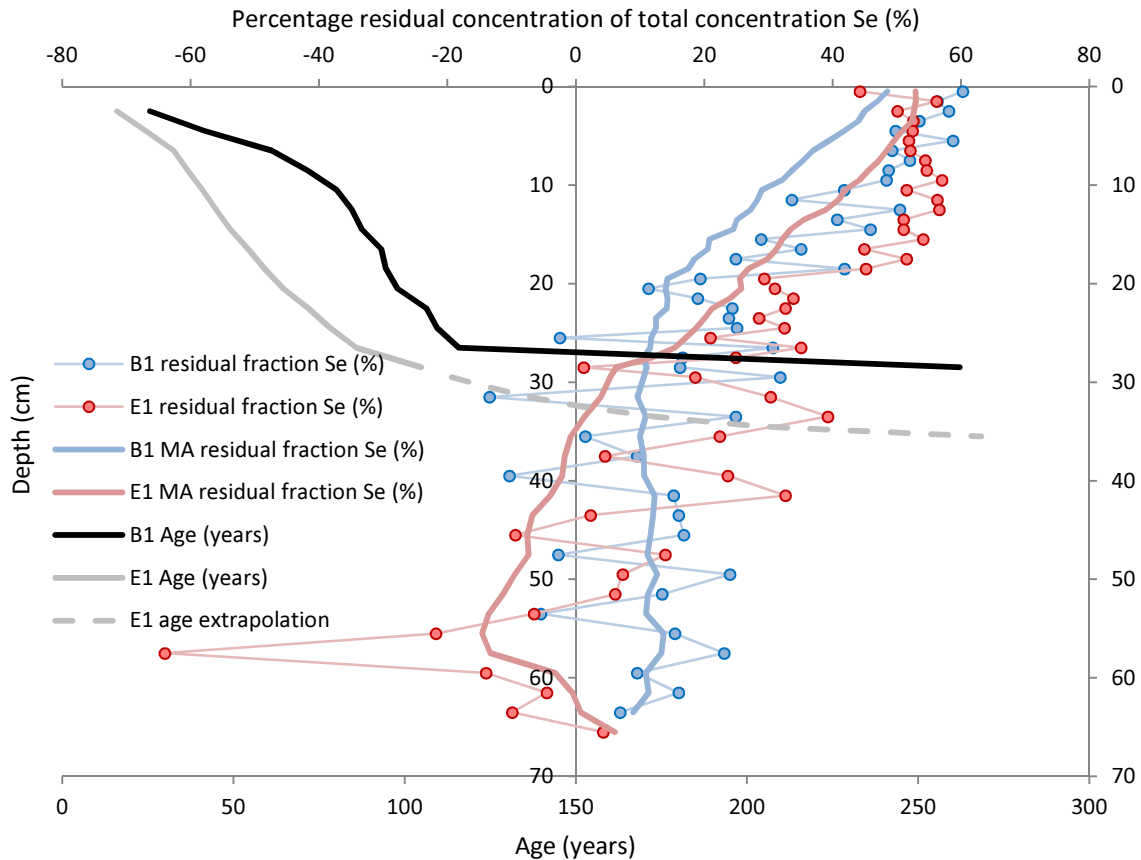


Figure 5.25: The percentage residual concentration of the total concentration for the downstream (B1) and upstream (E1) core for selenium. Included is a moving average of 15 and the age-depth profile.

The selenium profiles in these cores indicate an, in this study, uninvestigated mining source further upstream at the Horsefly River and are not a result of any processes related to the Black Creek mine. The study of Clark (2013) shows present elevated selenium concentrations in the lower part of the Black Creek (1.04 ppm, figure 5.28), which are absent in the source concentrations (0.42 ppm, figure 5.28). It is likely that these elevated concentrations stem from the same source upstream of the Horsefly River as the location of these samples in the Black Creek is susceptible to annual flooding of the Horsefly River itself. Mining districts are characterized by naturally occurring metals in soil, sediment, rock, and water at concentrations that could result in their classification as contaminated sites (Painter et al. 1994). However, such a sudden increase in selenium concentrations of this magnitude reflects anthropogenic activities. It is interesting to see that the onset of this increase is related to the early 1900s. The first records about mining of the two gold occurrences upstream of the Black Creek, Fraser gold and the Dor showing, come from the seventies (Ministry of Forests, Lands and Natural Resource Operations, BC: Minfiles 093A-150 and 093A-117). According to Luoma and Rainbow (2008), selenium contamination issues might be expected if a region is semi-arid or arid, rich in energy sources, mined, and/or usage of fossil fuels, particularly coals. Thus the selenium contamination in the upstream Horsefly catchment still seems to originate from gold mining (no coal ores are present in the watershed).

5.4.2 Response of metal contamination to mining activities in the Horsefly delta

A past mining response or a natural process of arsenic and copper

The peaks in arsenic and copper in the delta core (D1) occur at a depth of 17.5 cm and correspond in age to the late 1960s. The copper peak represents 64% minus an average of about 21.3% (average concentration far below peak: 35.5 cm depth) is 42.7% of the total concentration, which does not stem from local geology. For the arsenic peak this is 38.5% of the total concentration (50.6% - 12.1%). Copper pollution may arise from copper mining and smelting and the corrosion of these metal products (van der Perk, 2006). The prime source of arsenic in the environment originates from natural or enhanced processes, such as weathering and mining (van der Perk, 2006; Garelick et al., 2008). Thus the simultaneous occurrence of a copper and arsenic peak in this area rich in pyrite ores, strongly implies to be related to mining activity. However, mines located downstream of the Black Creek were all closed before 1915 (section 3.1.2). Weathering of abandoned pits are not able to give pulses in fine sediment geochemistry of this magnitude, as this effect should be still ongoing today and affect the fine sediment geochemistry in the delta core still. Probably the iron peak at this depth (17.5 cm) is related to the occurrence of this arsenic and copper peak and indicate vertical migration as a consequence of redox potential. Precipitation of iron with arsenic and copper is able to give enhanced sediment concentrations due to the transformation into the particulate form. From the above can be concluded that these peaks are more likely to reflect a natural process, rather than past mining.

Present day anthropogenic activity reflected in cadmium, zinc, lead and selenium

The similar patterns of cadmium, zinc and lead show a different response (figure 5.26). Each of these metals show a constant variability in the lower part of the delta core (below 35.5 cm), which is followed by a sharp increase between about 20.5 to 35.5 cm depth and ends with a constant high concentration going upwards in the upper 20.5 cm. The upper 20.5 cm is chosen to calculate average fraction of residual concentrations, because that is the point the concentrations reach an asymptote of constant variability. Cadmium has the highest fraction of total concentrations with an average excess (average upper 20.5 cm – average 35.5 cm and below) of 79.6% in the upper 20.5 cm. Followed are zinc (69.6%) and lead (76%). Selenium has a different signal in the delta core. Fraction residual concentrations of selenium are initially going up at about the same rate as for cadmium, lead and zinc, but this rise stagnates earlier reaching a value of on average 47.1% in the upper 20.5 cm (figure 5.26).

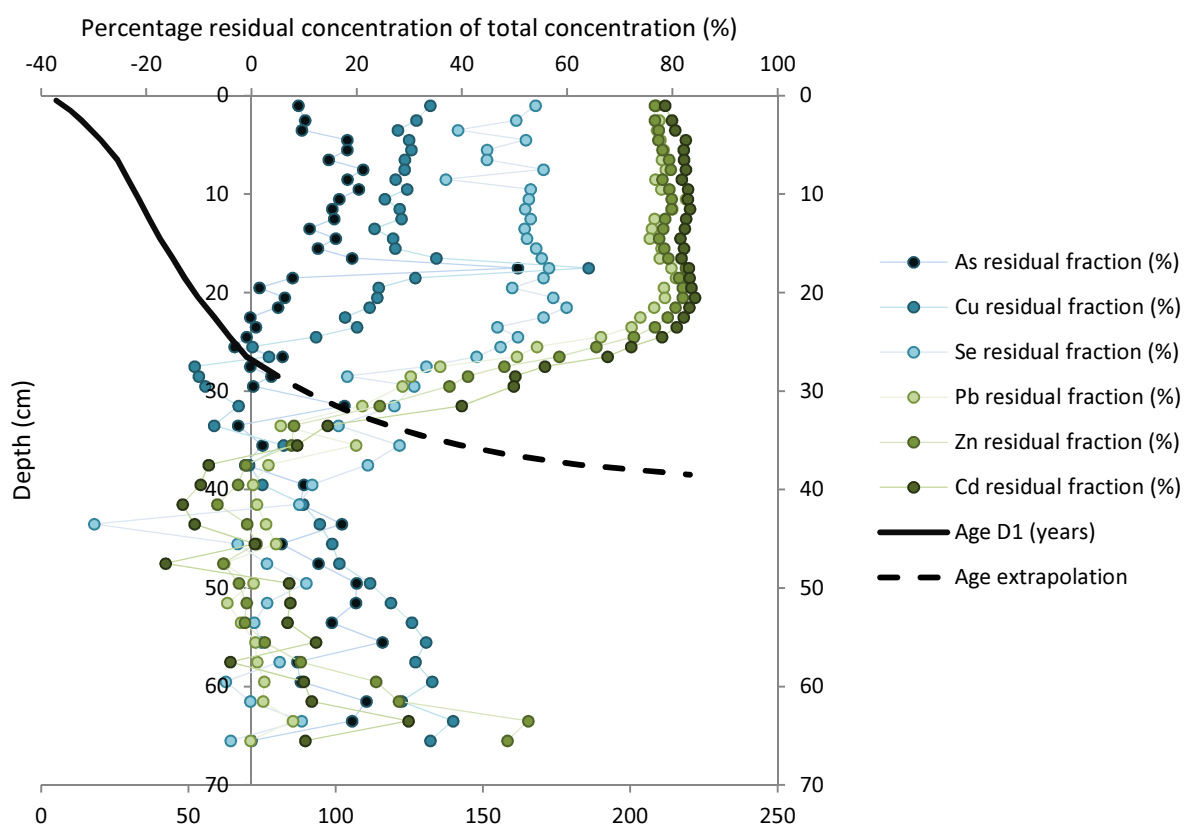


Figure 5.26: The percentage residual concentration of the total concentration for the delta core (D1) including the age-depth profile.

The onset of these increasing concentrations is just below the deepest sample analysed for the ^{210}Pb excess, hence the extrapolated excess ^{210}Pb is used to approximate the age. The moving average of the profiles of figure 5.26 is plotted in figure 5.27 to estimate this onset of rising residual concentrations. The onset of the selenium increase seems to start earlier between 30.5 and 35.5 cm depth, however the range in years is rather large between these depths (1870-1920) due to low sedimentation rates in these times. Lead, zinc and cadmium concentrations start rising at about 30.5 cm depth and correspond in age with the early 1920s.

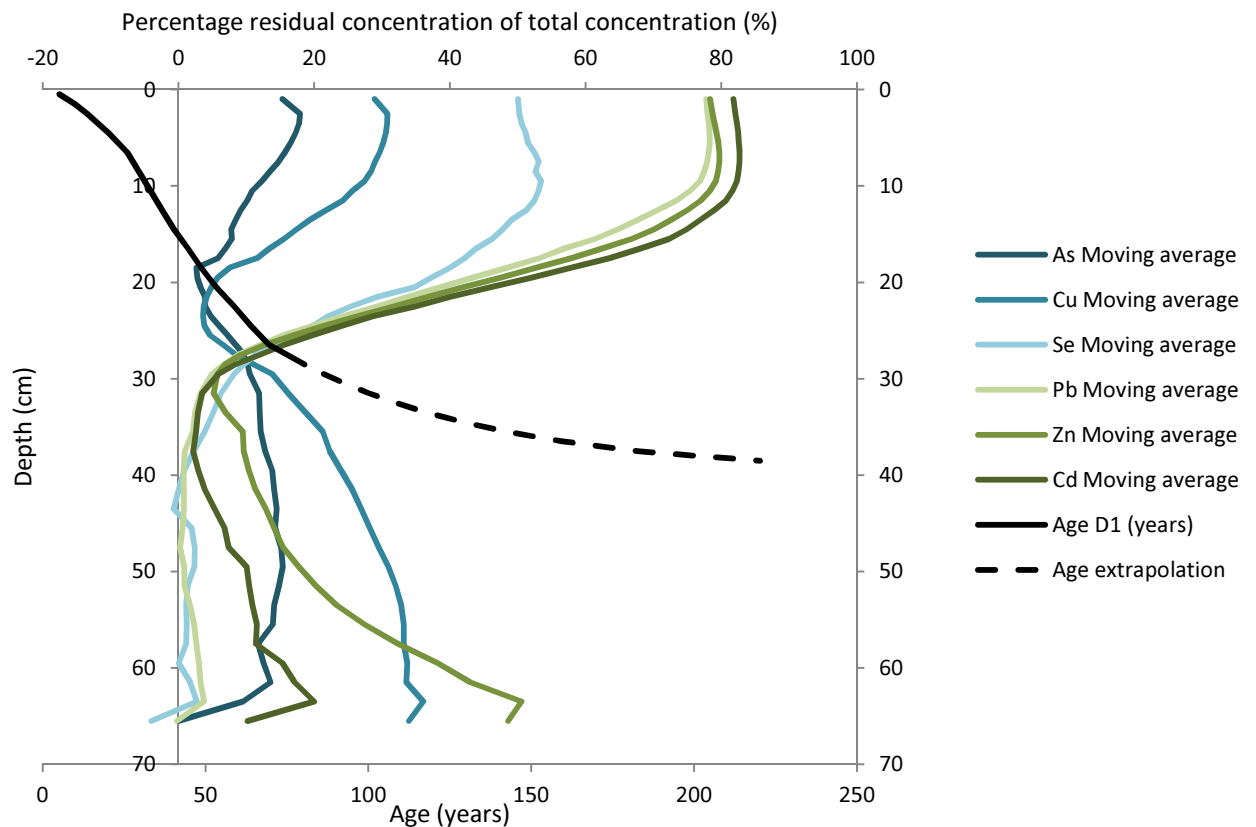


Figure 5.27: Moving average of 15 of the percentage residual concentration of total concentration in the delta core.

The similar signals of cadmium, zinc and lead over depth imply that they stem from the same source of input. Also, the values of average fraction residual concentrations in the upper 20.5 cm for cadmium (79.6%), zinc (69.6%) and lead (76%) indicate similar release rates. The village of Horsefly is excluded to be the source of elevated cadmium, lead and zinc, as concentrations downstream of the village near Rat Creek (9.5 kilometers upstream of the delta) in present day Horsefly sediments are not yet elevated (Clark, 2003) (figure 5.28). However, the present day selenium concentrations near Rat Creek are 1.9 ppm and 1.3 ppm (Clark, 2013) (figure 5.28). These are in the same order of magnitude as the selenium concentrations found at present in the delta (1.5 ppm), the upstream core (1.4 ppm) and the downstream core (2.2 ppm) (figure 5.28). The onset in selenium increase in the upstream (E1) and downstream (B1) core was related to the early 1900s. Selenium seems to have an earlier onset in the delta core (D1) compared to zinc, cadmium and lead, as mentioned earlier (1870-1920). The pattern of selenium is similar as for the cores upstream of Horsefly: the approximate year at which the selenium concentrations stagnate in the upstream (E1) core (and downstream core) is around 1957 and relating the depth of 20.5 cm in the delta core (D1) to an age results in approximately 53 years (around 1959). From the above can be stated that the elevated selenium concentrations originate from the same uninvestigated source upstream of the Black Creek inlet, while the source of elevated concentrations of lead, zinc and cadmium is located somewhere between Rat Creek and the delta in a 9.5 kilometers long river transect. The origin of these high concentrations in cadmium, lead and zinc is not mining-related as the Horsefly River catchment contains no lead or zinc ores and associated mining. The major part of such mines in the area is located at Spanish Mountain North of Quesnel Lake, which is far outside the Horsefly River's watershed.

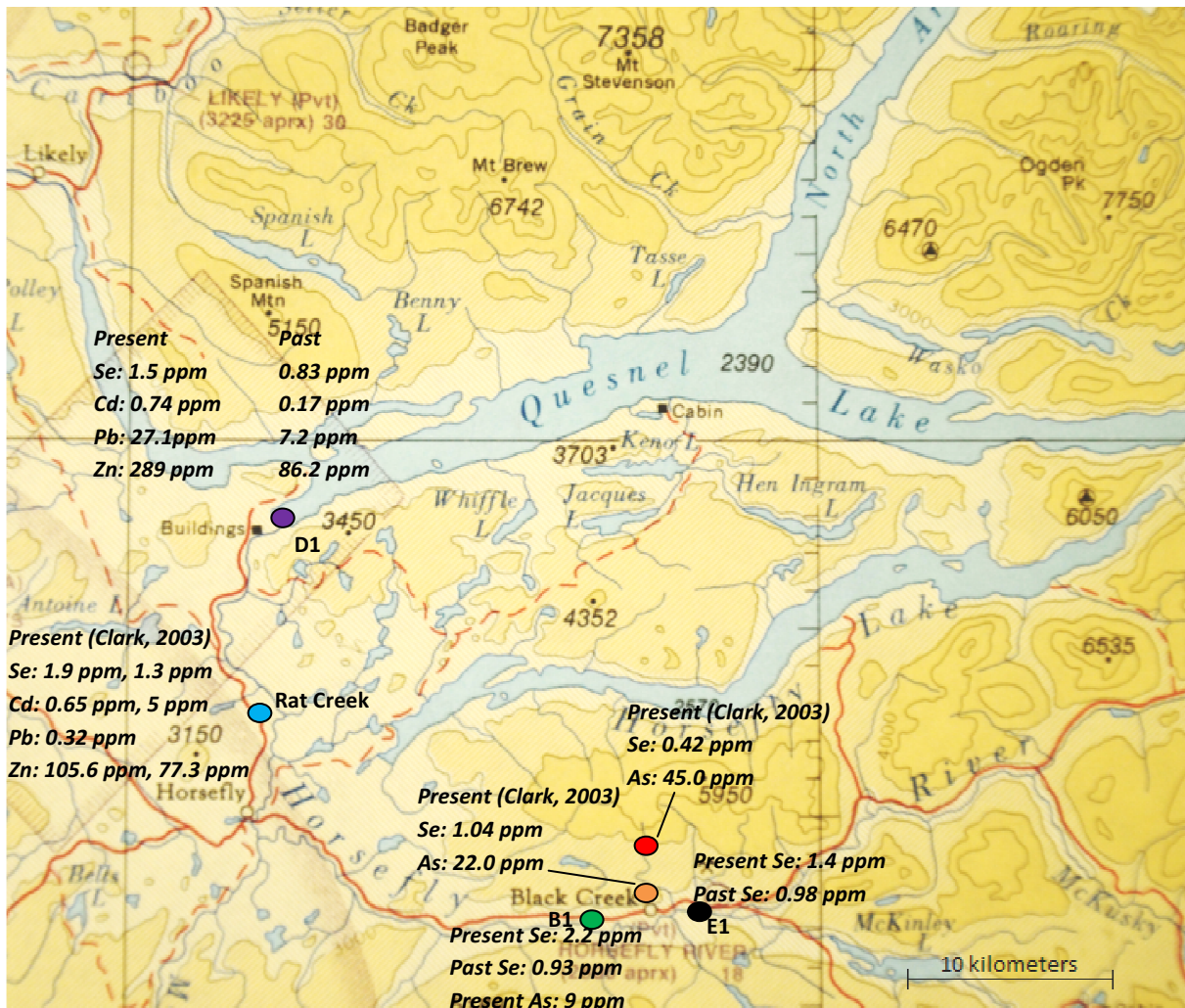


Figure 5.28: Present (and past) concentrations along the Horsefly for the main results. Past concentrations are derived from the cores and represent the average concentrations of 35.5 cm and below for cores E1, B1 and D1. Present concentrations are either derived from the study of Clark (2013) or the concentration in the upper slice of the core at that location. The red circle is located in the pit of the hydraulic mine and therefore represent source concentrations nowadays coming from the abandoned mine. The orange circle is the part of the Black Creek, which is likely to be flooded by the Horsefly during high discharge. Rat Creek is located at the blue circle downstream of the village of Horsefly.

Present day sediment quality and comparison with other studies

The delta core depth profiles of zinc, cadmium, lead and the profiles of selenium in the upstream (E1), downstream (B1) and delta core (D1) are of concern as they reflect a massive increase in anthropogenic activity. Zinc and cadmium are above Canadian sediment quality levels (table 5.6) and concentrations of zinc even exceed the probable effect level. However, these guidelines are not normalized to aluminum and should be used with caution. Active mining in the Quesnel watershed was found to result in lower concentrations in zinc and cadmium and little higher concentrations of selenium in a pilot study of Smith and Owens (2010) compared to the delta core (D1). In a study of Karimlou (2012), concentrations of cadmium, lead and zinc were substantially lower in a mine drainage site compared to this study. In contrast to the concentrations of selenium, which were remarkably high. This again emphasizes the statement that concentrations of lead, cadmium and zinc in the delta core (D1) are not mining related.

	Average total concentration in the upper part (20.5 cm) (ppm). RP=residual part	Interem SQG (ppm)	Probable effect level (PEL) (ppm)	Luoma and Rainbow, 2008 freshwater ambient criteria (ppm)	Clark (2013) Observed present day concentrations at Rat Creek	Mining land use (Smith and Owens, 2010)	Hazeltine Creek (Karimlou, 2011)
Cadmium	0.92 (RP=0.75)	0.6	3.5	-	0.65, 0.5	0.5	0.49
Lead	30.9 (RP=23.9)	35	91.3	-	0.32	-	7
Zinc	347 (RP =277)	123	315	-	105.6, 77.3	235	100
Selenium	1.54 (RP=0.82)	-	-	2-4	1.9, 1.3	1.8	9.1

Table 5.6: Average total concentrations of Cd, Pb, Zn and Se are compared to literature and other research. Canadian sediment quality guidelines (CCME) are given for Cd, Pb and Zn. Included is a criteria for Se from Luoma and Rainbow, 2008. The comparison with other research in the area includes Clark (2013), Smith and Owens (2010) and Karimlou (2011). The average concentration in the upper 20.5 cm is chosen, since the concentration stagnates above this depth.

6. Conclusions

Present weathering and past mining activities from such small-scale mines as the Black Creek mine do not affect the fine sediment geochemistry of the Horsefly floodplain soils to a large extent. Only one peak in arsenic represents an active period of the mine, while the abandoned years do not influence the fine sediment geochemistry at all. The peak in arsenic in the downstream core at a depth of 17.5 cm reflects an active mining period of the hydraulic operation in the Black Creek mine and is related to the early 1930s. This signal of arsenic is not detectable in the delta core as expected. The meander-bend-area just downstream of the Black Creek acts as a sink for all the sediment. Also the dilution with other sediment sources would minimize any mining signal originating from the Black Creek mine in the delta core, which is reflected by the dilution of the presently elevated source concentrations in the Black Creek mine. A mine similar in size as the Black Creek mine does not affect fine sediment geochemistry to a large extent as concluded in this study. However, British Columbia is characterized by many small-scale abandoned (or active) mines. This raises the question, if the added effects of numerous of such small-scale mines, are able to affect fine sediment geochemistry in floodplain soils.

The upstream core, as well as the downstream and the delta core is enriched in selenium. This source is not investigated in this study and is located in the upstream watershed of the Horsefly River, upstream of the Black Creek inlet. The onset of this selenium release is related to the early 1900s. Although there are mineral deposits and associated mining activities present in the upstream part of the Horsefly River, earliest reports of activities stem from the seventies. It is therefore not clear what the potential source could be, as this pattern is not seen for the other metals investigated in this study. However, it is likely to be mining related in this gold mining area. Selenium is one of the most hazardous of the trace metals, following mercury (Luoma and Rainbow, 2008). Although the release rate of selenium is presently constant and lies within Canadian sediment quality criteria, it might be useful to identify the source in future investigations, since the sediment profile history of these cores marks almost a doubling in selenium release in the Horsefly watershed.

Alongside the elevated selenium concentrations, also zinc, lead and cadmium are elevated compared to the local geology flux of the Horsefly area. However, these metals are not mining related in this area. The village of Horsefly is excluded to be the source of these elevated concentrations. Future research should especially focus on identifying the source of elevated cadmium, zinc and lead along the river transect between Rat Creek and the delta. The concentrations of zinc and cadmium are above Canadian sediment quality guidelines. Zinc can be classified with certainty to indicate severe pollution with concentrations exceeding the probable effect level by far. To locate the source of lead, zinc and cadmium, bed sediments along the transect between Rat Creek and the delta and some additional cores at the delta, would give valuable information. Identification of this source of input between Rat Creek and the delta is of major concern to maintain a healthy ecosystem in the delta as it is the pathway of several salmon species to upstream gravel beds in the Horsefly River.

7. References

- Akcil, A., Koldas, S., 2006, Acid mine drainage (AMD): causes, treatment and case studies. *Journal of Cleaner Production*, Vol. 14, pp. 1139 – 1145.
- Appleton, J.D., Williams, T.M., Breward, N., Apostol, A., Miguel, J., Miranda, C., 1999, Mercury contamination associated with artisanal gold mining on the island of Mindanao, the Philippines. *Science of The Total Environment*, Vol. 228, pp. 95 – 109.
- Appleby, P.G., Oldfield, F., The assessment of ^{210}Pb data from sites with varying sediment accumulation rates, 1983. *Hydrobiologica*, Vol. 103, pp. 29 – 35.
- Bailey, D.G., 1990, *Geology of the Central Quesnel belt*. Issued by the Geological Survey Branch, ISBN 0-7718-8981-X.
- Binford, M.W., Kahl, J.S., Norton, S.A., Interpretation of ^{210}Pb profiles and verification of the CRS model in PIRLA project lake sediment cores, 1993, *Journal of Paleolimnology*, Vol. 9, pp. 275 – 29.
- British Columbia heritage rivers program, Conservation of B.C. rivers, Horsefly River. Available online at: http://www.env.gov.bc.ca/bcparks/heritage_rivers_program/bc_rivers/horsefly_river.html.
- British Columbia State of the Environment Report, 1993, pp. 29 – 31.
- Brümmer, G., 1974, Redox potentials and redox processes of manganese, iron and sulfur-compounds in hydromorphic soils and sediments. *Geoderma*, Vol. 12, pp. 207 – 222.
- Burkhardt, E., Akob, D.M., Bischoff, S., Sitte, J., Kostka, J.E., Banerjee, D., Scheinost, A.C., Küsel, K., 2010, Impact of biostimulated redox processes on metal dynamics in an iron – rich creek soil of a former uranium mining area. *Environmental Science Technology*, Vol. 44, pp. 177 – 183.
- Cade, B.S., Noon, B.R., 2003, A gentle introduction to quantile regression for ecologists. *Ecological Environment*, Vol. 1, pp. 412 – 420.
- Coderre, F., Dixon, D.G., 1999, Modeling the cyanide heap leaching of cupriferous gold ores: Part 1: Introduction and interpretation of laboratory column leaching data. *Hydrometallurgy*, Vol 52, pp. 151 – 175.
- CCME, Canadian sediment quality guidelines for the protection of aquatic life: Summary tables, 2002. Updated. In: *Canadian Environmental Quality Guidelines*, 1999. Canadian Council of Ministers of the Environment, Ottawa, Canada. Canadian
- Clark, D.E., 2013, Effect of mining on fine sediment geochemistry in the Horsefly catchment, British Columbia, Canada . Utrecht University, Faculty of Geosciences, Dep. Physical Geography.
- Cohen, A.S., 2003, *Paleolimnology: The history and evolution of lake systems*. Oxford University Press.
- Donato, D.B., Nichols, O., Possingham, H., Moore, M., Ricci, P.F., Noller, B.N., 2007, A critical review of the effects of gold cyanide-bearing tailings solutions on wildlife. *Environment International*, Vol. 33, pp. 974 – 984.

Dubé, M.G., MacLatchy, D.L., Kieffer, J.D., Glozier, N.E., Culp, J.M., Cash, K.J., 2005, Effects of metal mining effluent on Atlantic salmon (*Salmo salar*) and slimy sculpin (*Cottus cognatus*): using artificial streams to assess existing effects and predict future consequences. *Science of the Total Environment*, Vol. 343, pp. 135 – 154.

Du Laing, G., Vanthuyne, D.R.J., Vandecasteele, B., Tack, F.M.G., Verloo, M.G., 2007, Influence of hydrological regime on pore water metal concentrations in a contaminated sediment-derived soil. *Environmental Pollution*, Vol. 147, pp. 615 – 625.

Du Laing, G., Rinklebe, J., Vandecasteele, B., Meers, E., Tack, F.M.G., 2009, Trace metal behaviour in estuarine and riverine floodplain soils and sediments: A review. *Science Of The Total Environment*, Vol. 407, pp. 3972 – 3985.

Environmental Mining Council of British Columbia. Available online at:

http://dwb4.unl.edu/Chem/CHEM869R/CHEM869RLinks/emcbc.miningwatch.org/emcbc/library/amd_water.htm#Heap

Emsley J., 2001, *Nature's building blocks: an A-Z guide to the elements*, Oxford University Press.

Forstner, U., 1982a, Chemical forms of metal enrichment in recent sediments. *Ore Genesis*, Special Publication of the Society for Geology Applied to Mineral Deposits, Vol. 2, pp. 191 – 199.

Frohne, T., Rinklebe, J., Diaz-Bone, R.A., Du Laing, G., 2011, Controlled variation of redox conditions in a floodplain soil: Impact on metal mobilization and biomethylation of arsenic and antimony. *Geoderma*, Vol. 160, pp. 414 – 424.

Garelick, H., Jones, H., Dybowska, A., Valsami-Jones, E., 2008, Arsenic pollution sources. *Reviews of Environmental Contamination and Toxicology*, Vol. 197, pp. 17 – 60.

Grice, T., 1998, *Underground mining with Backfill*. The 2nd Annual Summit – Mine Tailings Disposal Systems, Brisbane.

Grybos, M., Davranche, M., Gruau, G., Petitjean, P., 2007, Is trace metal release in wetland soils controlled by organic matter mobility or Fe-oxyhydroxides reduction? *Journal Of Colloid and Interface Science*, Vol. 314, pp. 490 – 501.

Hammack, R.W., Watzlaf, G.R., 1990, The effect of oxygen on pyrite oxidation. *Proceedings of the Annual Meeting of the American Society for Surface Mining and Reclamation*, Vol. 1, pp. 33 – 41.

Helgen, S.O., Moore, J.N., 1996, Natural background determination and impact quantification in trace metal-contaminated river sediments, *Environmental Science & Technology*, Vol. 30, pp. 129 – 135.

Herut, B., Sandler, A., 2006, Normalization methods for pollutants in marine sediments: review and recommendations for the Mediaterranean. *Israel Oceanographic & Limnological Research*, Submitted to UNEP/MAP.

Hogsden, K.L., Harding, J.S., 2012, Consequences of acid mine drainage for the structure and function of benthic stream communities: A review. *Freshwater Science*, Vol. 31, pp. 108 – 120.

Horowitz, A.J., 1985, *A primer on trace metal-sediment chemistry*. Lewis: Chelsea, USA

- Irving, H., Williams, R., 1948, Order of stability of metal complexes. *Nature*, Vol. 162, pp. 746 – 747.
- Jennings, S.R., Neuman, D.R. and Blicher, P.S., 2008, Acid Mine Drainage and Effects on Fish Health and Ecology: A Review. Reclamation Research Group Publication, Bozeman, MT.
- Karimlou, G., 2011, Effects of mining on fine sediment quality; a comparison with regional metal background concentrations. Master thesis, Utrecht University, Faculty of Geosciences, Dep. Physical Geography.
- Kleinmann, R. L. P., Crerar, D.A., Pacelli, R.R., 1980, Biogeochemistry of acid mine drainage and a method to control acid formation. *Mining Engineering*, Vol. 33, pp. 300 – 306.
- Knox, J.C., 1987, Historical valley floor sedimentation in the Upper Mississippi valley. *Annals of the Association of American Geographers*, Vol. 77, pp. 224 – 244.
- Knox, J.C., 1993, Large increases in flood magnitude in response to modes changes in climate. *Nature*, Vol. 361, pp. 430 – 432.
- Krishnaswamy, S., Lal, D., Martin, J.M., Meybeck, M., Geochronology of lake sediments, 1971. *Earth Planet Science Letters*, Vol. 11, pp. 407 – 414.
- Lacerda, L.D., Salomons, W., 1998, Mercury from gold and silver mining: a chemical time bomb? Berlin, Springer, 1998.
- LaPerriere, J.D., Wagener, S.M., Bjerklie, D.M., 1985, Gold-mining effects on heavy metals in streams, Circle Quadrangle, Alaska. *Journal of the American Water Resources Association*, Vol. 21, pp. 245 – 252.
- Lay, D., 1932, North-eastern mineral survey district (no. 2), Horsefly section. B.C. Ministry of energy, mines and petroleum resources, minister of mines annual report 1931, pp. A96 – A101.
- Leece, S.A., Pavlowsky, R.T., 1997, Storage of mining-related zinc in floodplain sediments, Blue River, Wisconsin. *Physical Geography*, Vol. 18, pp. 424 – 439.
- Liu, F., Colombo, C., Adamo, P., He, J.Z., Violante, A., 2002. Trace elements in manganese–iron nodules from a Chinese alfisol. *Soil Science Society America Journal*, Vol. 66, pp. 661 – 670.
- Lin, C., Tong, X., Lu, W., Yan, L., Wu, Y., Nie, C., Chu, C., Long, J., 2005, Environmental impacts of surface mining on mined lands, affected streams and agricultural lands in the Dabaoshan mine region, Southern China. *Land Degradation and Development*, Vol. 16, pp. 463 – 474.
- Lion, L., Altmann, R., Leckie, J., 1982, Trace metal adsorption characteristics of estuarine particulate matter: evaluation of contributions of Fe/Mn oxide and organic surface coatings: *Environmental Science and Technology*, Vol. 16, pp. 660 – 666.
- Loring, D.H., 1991, Normalization of heavy-metal data from estuarine and coastal sediments. *Marine Science*, Vol 48., pp. 101 – 115.
- Luoma, S.N., Rainbow, P.S., 2008, Metal contamination in aquatic environments. Cambridge press, Cambridge, UK.

Martin, C., 2000, Heavy metal trends in floodplain sediments and valley fill, River Lahn, Germany. *Catena*, Vol. 39, pp. 53 – 68.

Martins, M., Faleiro, M.L., Barros, R.J., Verissimo, A.R., Barreiros, M.A., Costa, M.C., 2009, Characterization and activity studies of highly heavy metal resistant sulphate-reducing bacteria to be used in acid mine drainage decontamination. *Journal of Hazardous Materials*, Vol. 166, pp. 706 – 713.

Miller, J.R., 1997, The role of fluvial geomorphic processes in the dispersal of heavy metals from mine sites. *Journal of Geochemical Exploration*, Vol. 58, pp. 101 – 118.

Ministry of Energy, Mines and Natural gas, BC Mining: A rich history and a promising future. Available online at: <http://www.empr.gov.bc.ca/Mining/Pages/History.aspx>.

Ministry of Forests, Lands and Natural Resource Operations, British Columbia. Britannia Mine Remediation Project. Available online at: <http://www.agf.gov.bc.ca/clad/britannia/background.html>

National Geographic, 2009. Available online at: <http://news.nationalgeographic.com/news/2009/12/photogalleries/091222-british-columbia-flathead-wildlife/#>).

Painter, S., Cameron, E.M., Allan, R., Rouse, J., 1994, Reconnaissance Geochemistry and Its Environmental Relevance. *Journal of Geochemical Exploration*, vol. 51, pp. 213 – 246.

Palumbo, B., Bellanca, A., Neri, R., Roe, M.J., 2001, Trace metal partitioning in Fe – Mn nodules from Sicilian soils, Italy. *Chemical Geology*, Vol. 173, pp. 257 – 269.

Panteleyev, A., Hancock, K.D., 1988, Quesnel mineral belt: Summary of the geology of the beaver creek – Horsefly river map area. British Columbia geological survey, *Geological fieldwork 1988*, pp. 159 – 166.

Panteleyev, A., Bailey, D.G., Bloodgood, M.A., Hancock, K.D., 1996, Geology and mineral deposits of the Quesnel River – Horsefly map area, Central Quesnel trough, British Columbia. NTS map sheets 93A/5, 6, 7, 11, 12, 13; 93B/9, 16; 93G/1; 93H/4, (Bulletin; 97), Issued by the Geological Survey Branch, ISBN 0-7726-2973-0.

PhysOrg, 2012. Available online at: <http://phys.org/news/2012-10-indiana-coal-reclamation-years.html>.

Reddy, K.R., DeLaune, R.D., 2008, *Biogeochemistry of Wetlands: Science and Applications*. Taylor & Francis Group, LLC, Boca Raton, London, New York.

Ricketts, B.D., 2008, Chapter 10: Cordilleran sedimentary basins of western Canada record, 180 million years of terrane accretion. *Sedimentary basins of the world*, Vol. 5, pp. 363 – 394.

R.L. Case and associates – Watershed consulting, 2000a, Horsefly River Black Creek restoration project : Riparian assessments and prescriptions.

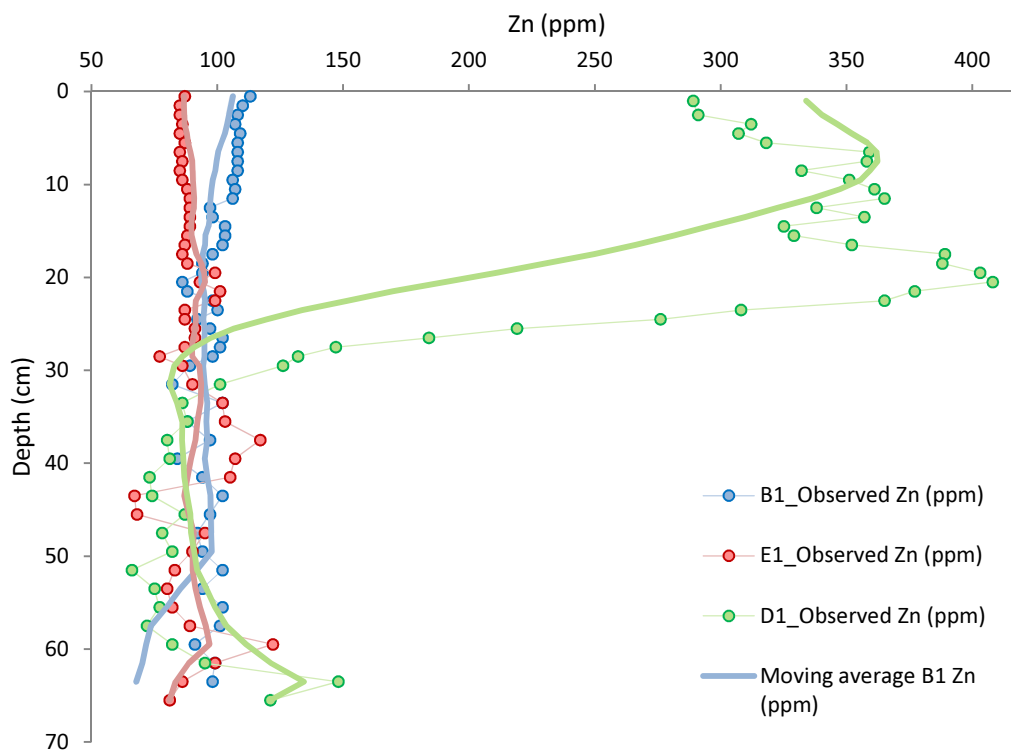
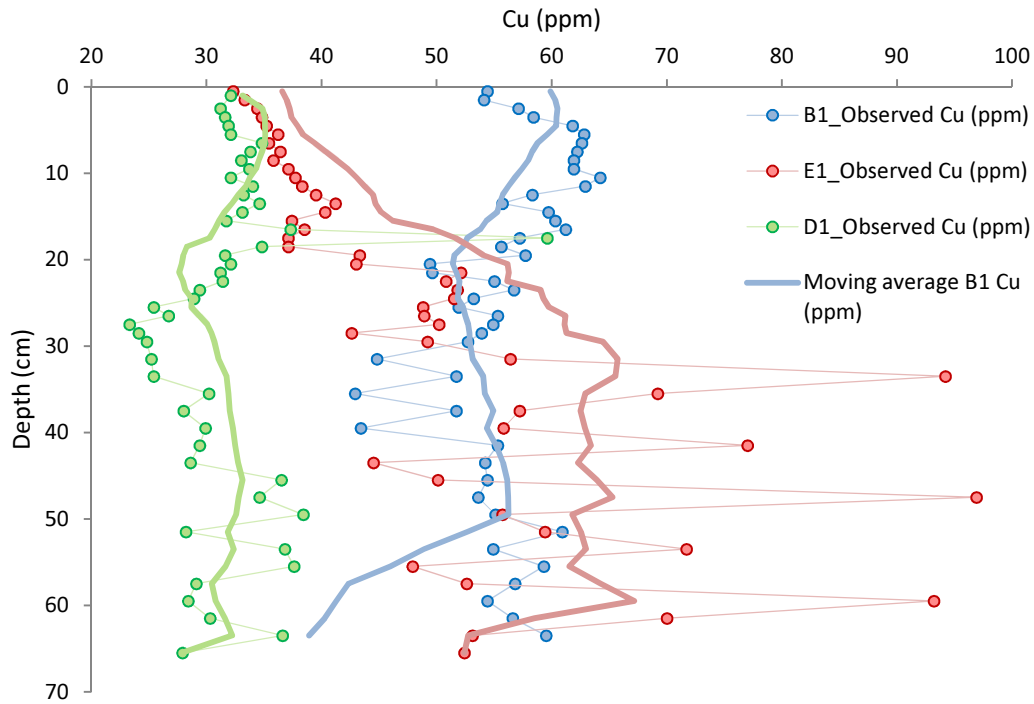
R.L. Case and associates – Watershed consulting, 2000b, Horsefly River watershed stewardship review: A synthesis of reports and stake holder initiatives.

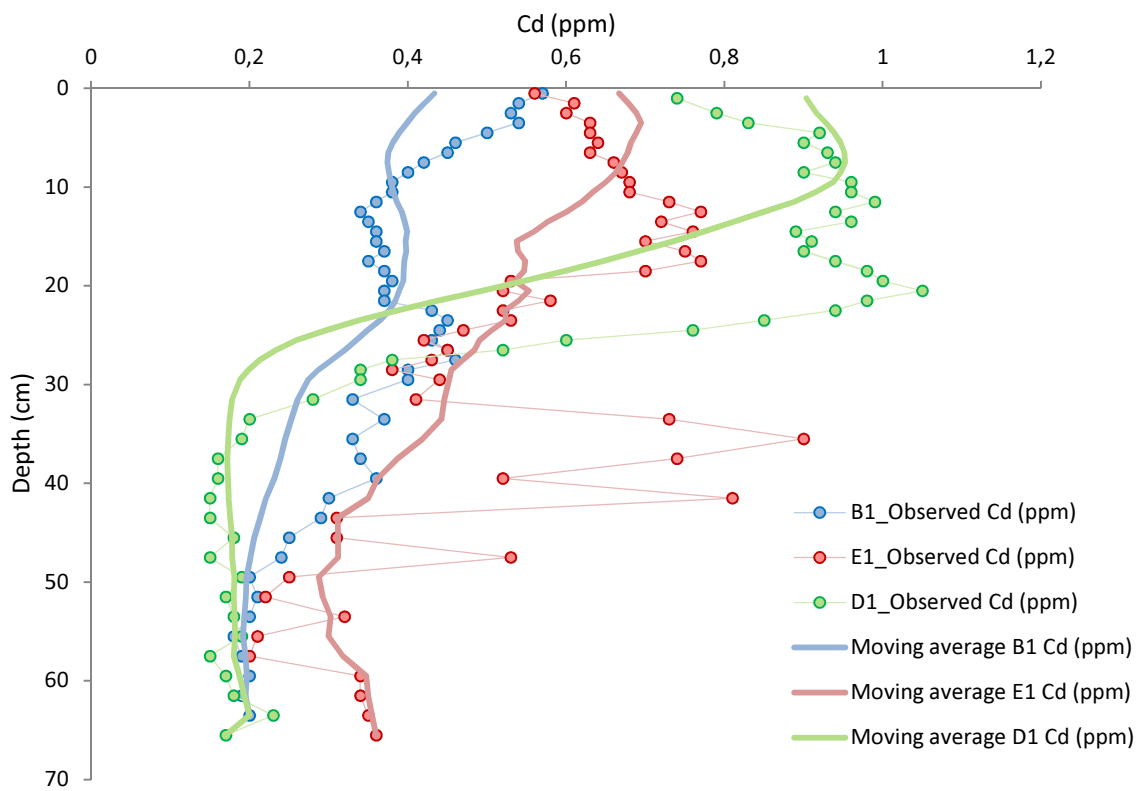
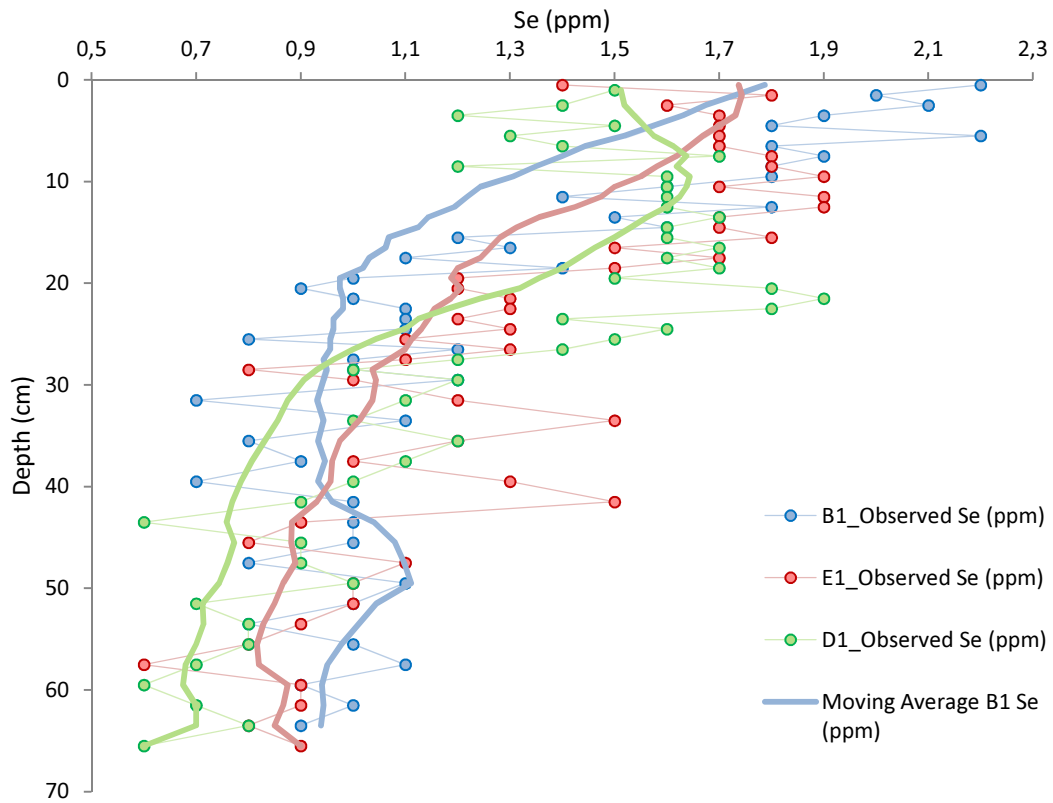
- Santschi, P.H., Nixon, S., Pilson, M., Hunt, C., 1984, Accumulation of sediments, trace metals (Pb, Cu) and total hydrocarbons in Narrangansett Bay, Rhode Island. *Estuarine, Coastal and Shelf Science*, Vol. 19, pp. 427 – 449.
- Smith, T.B., Owens, P.N., 2010, Impact of land use activities on fine sediment-associated contaminants, Quesnel River Basin, British Columbia, Canada. *Sediment Dynamics for a Changing Future (Proceedings of the ICCE symposium held at Warsaw University of Life Sciences – SGGW, Poland, 14 – 18 June 2010)*. IAHS Publ. 337.
- Vandecasteele, B., Quataert, P., Tack, F.M.G., 2005, The effect of hydrological regime on the bioavailability of Cd, Mn, and Zn for the wetland plant species *Salix Cinerea*. *Environmental Pollution*, Vol. 135, pp. 303 – 312.
- Van der Perk, M., 2006, *Soil and water contamination: From molecular to catchment scale*, Taylor and Francis group, Leiden.
- Van Griethuysen, C., Luiwieler, M., Joziase, J., Koelmans, A.A., 2005, Temporal variation of trace metal geochemistry in floodplain lake sediment subject to dynamic hydrological conditions. *Environmental Pollution*, Vol. 137, pp. 281 – 294.
- Veiga, M.M., Maxson, P.A., Hylander, L.D., 2006, Origin and consumption of mercury in small-scale gold mining. *Journal of Cleaner Production*, Vol. 14, pp. 436 – 447.
- Wilson, W.M.H., 1977b, Paleocology of Lacustrine Varves at Horsefly, British Columbia. *Canadian journal of Earth Sciences*, Vol. 14, pp. 953 – 962.
- Yu, K., Böhme, F., Rinklebe, J., Neue, H., DeLaune, R.D., 2007, Major biogeochemical processes in soils – A microcosm incubation from reducing to oxidizing conditions. *Soil Science Society of America Journal*, Vol. 71, pp. 1406 – 1417.
- Zhang, J., Yu, G.R., 2002, Effects of surface coatings on electrochemical properties and contaminant sorption of clay minerals. *Chemosphere*, Vol. 49, pp. 619 – 628.
- Zwolsman, J.J.G., Berger, G.W., Van Eck, G.T.M., 1993, Sediment accumulation rates, historical input, postdepositional mobility and retention of major elements and trace metals in salt marsh sediments of the Scheldt estuary, SW Netherlands. *Marine Chemistry*, Vol. 44, pp. 73 – 94.

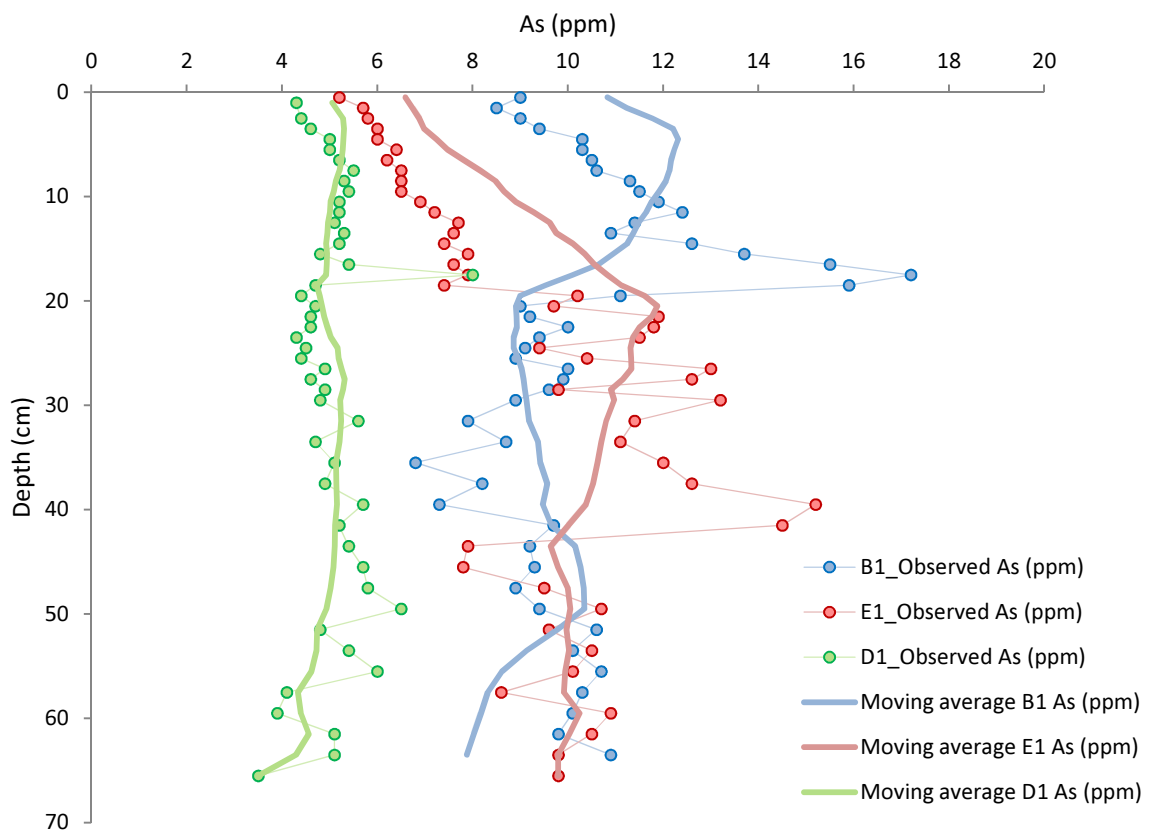
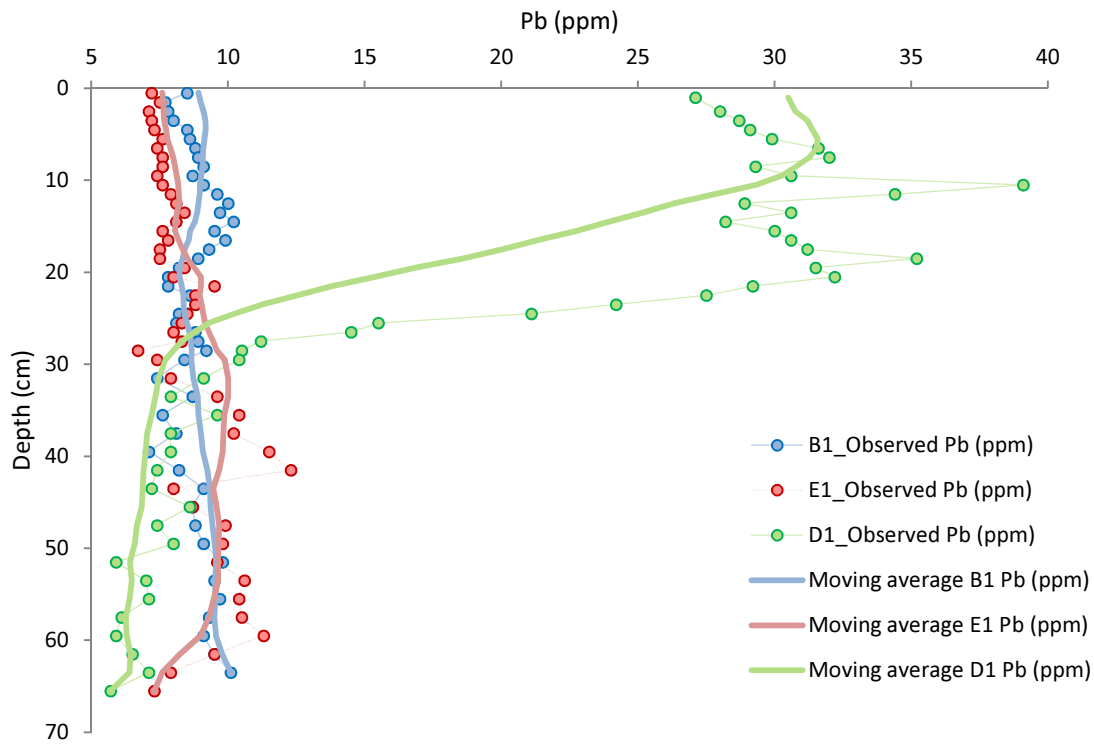
8. Appendices

A1 Metal depth-profiles

Metal profiles as measured by ICP-MS (ALS, Vancouver) over depth. A moving average of 15 is added to each graph.



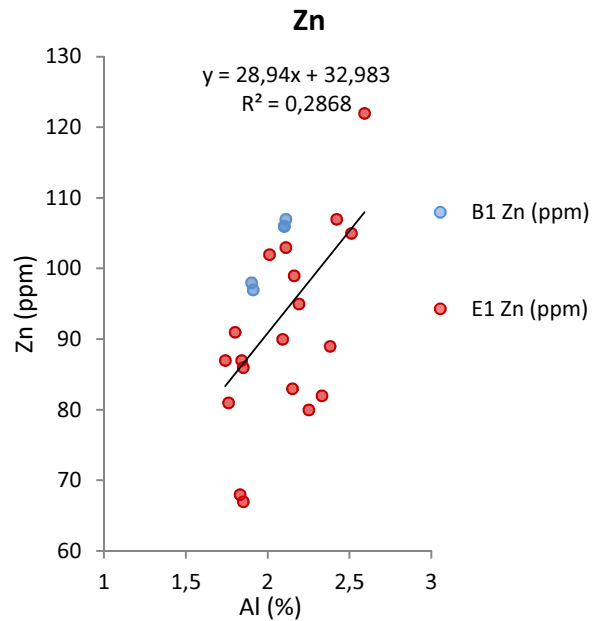
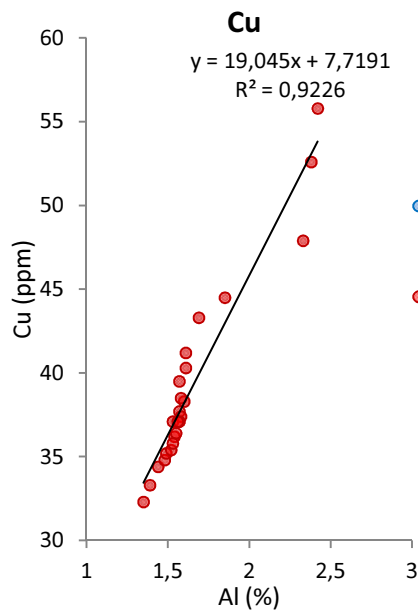




A2 Regression dataset

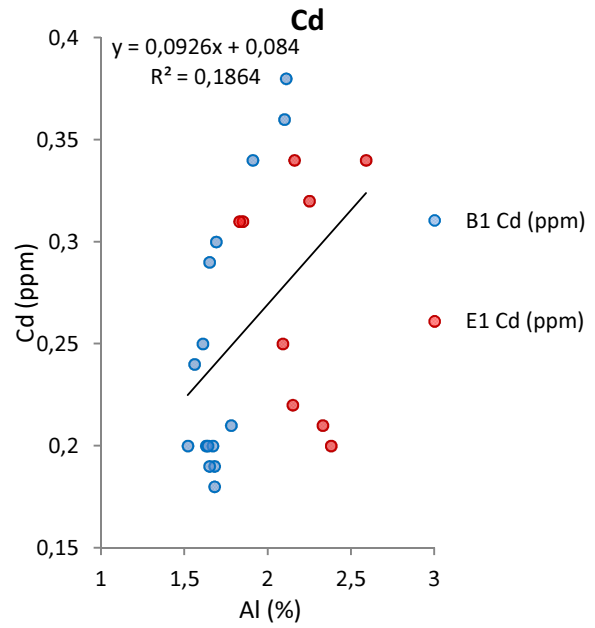
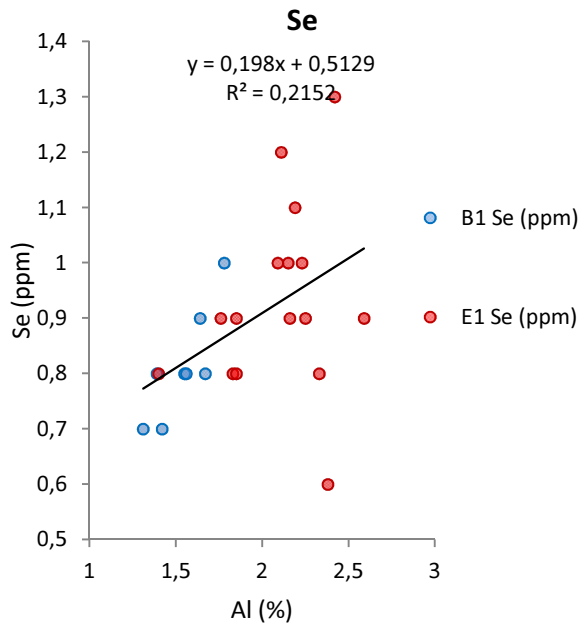
The graphs show the distribution of the regression dataset. The dataset used is given below each graph. Data of core E1 is indicated in red and data of core B1 is indicated in blue.

The upstream (E1) and the downstream core (B1)



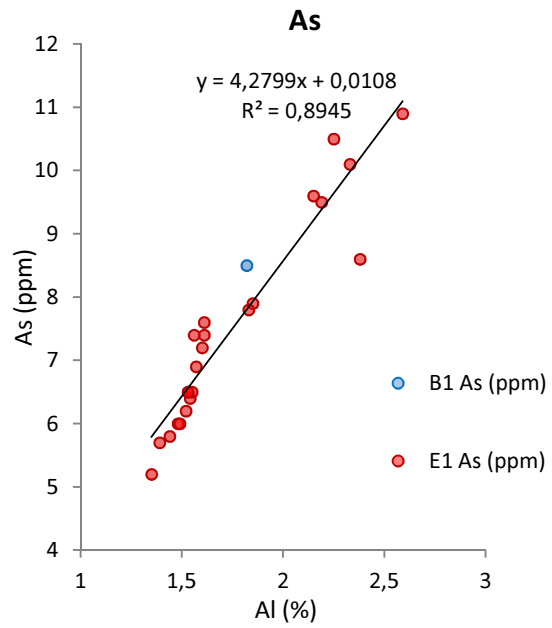
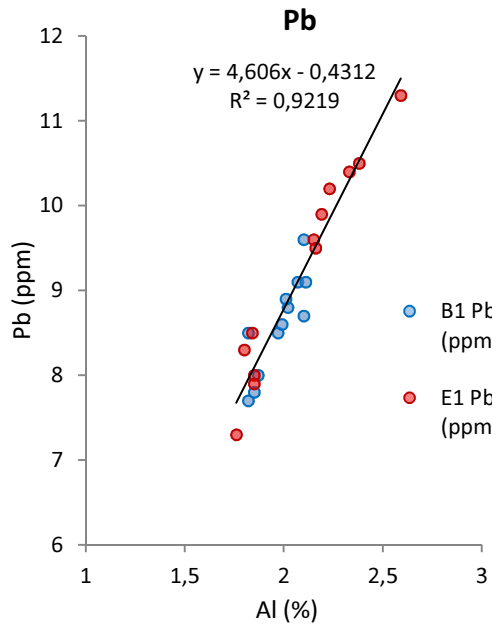
Depth (cm)	Cu (ppm)	Al (%)
1	32,3	1,35
2	33,3	1,39
3	34,4	1,44
4	34,8	1,48
5	35,2	1,49
6	36,2	1,54
7	35,4	1,52
8	36,4	1,55
9	35,8	1,53
10	37,1	1,53
11	37,7	1,57
12	38,3	1,6
13	39,5	1,57
14	41,2	1,61
15	40,3	1,61
16	37,4	1,58
17	38,5	1,58
18	37,1	1,57
19	37,1	1,56
20	43,3	1,69
40	55,8	2,42
44	44,5	1,85
56	47,9	2,33
58	52,6	2,38

Depth (cm)	Zn (ppm)	Al (%)
10	106	2,1
11	107	2,11
12	106	2,1
13	97	1,91
14	98	1,9
24	87	1,74
25	87	1,84
26	91	1,8
34	102	2,01
36	103	2,11
40	107	2,42
42	105	2,51
44	67	1,85
46	68	1,83
48	95	2,19
50	90	2,09
52	83	2,15
54	80	2,25
56	82	2,33
58	89	2,38
60	122	2,59
62	99	2,16
64	86	1,85
66	81	1,76



Depth (cm)	Se (ppm)	Al (%)
26	0,8	1,55
32	0,7	1,42
36	0,8	1,39
40	0,7	1,31
48	0,8	1,56
52	1	1,78
54	0,8	1,67
64	0,9	1,64
29	0,8	1,4
36	1,2	2,11
38	1	2,23
40	1,3	2,42
44	0,9	1,85
46	0,8	1,83
48	1,1	2,19
50	1	2,09
52	1	2,15
54	0,9	2,25
56	0,8	2,33
58	0,6	2,38
60	0,9	2,59
62	0,9	2,16
64	0,8	1,85
66	0,9	1,76

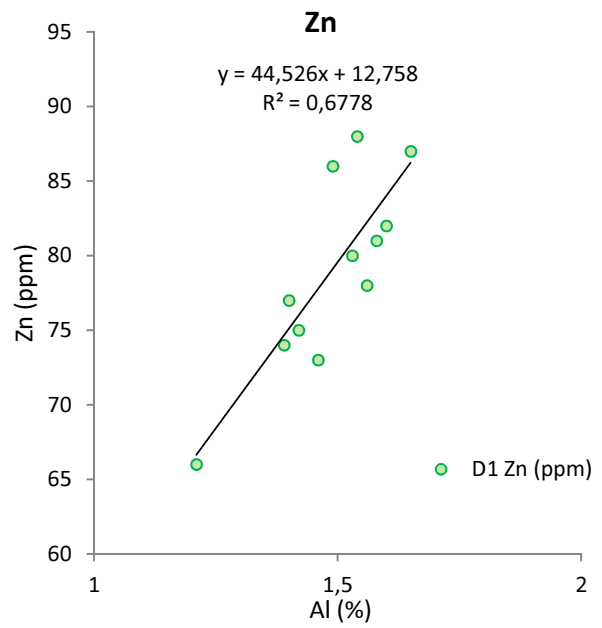
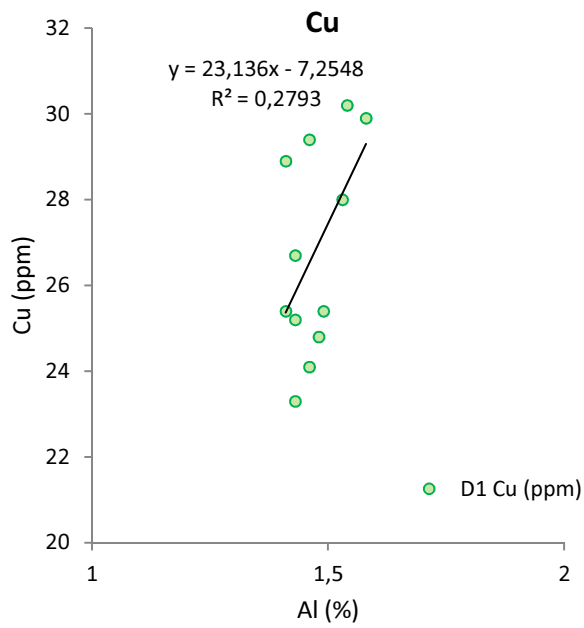
Depth (cm)	Cd (ppm)	Al (%)
11	0,38	2,11
12	0,36	2,1
13	0,34	1,91
42	0,3	1,69
44	0,29	1,65
46	0,25	1,61
48	0,24	1,56
50	0,2	1,63
52	0,21	1,78
54	0,2	1,67
56	0,18	1,68
58	0,19	1,68
60	0,2	1,52
62	0,19	1,65
64	0,2	1,64
44	0,31	1,85
46	0,31	1,83
50	0,25	2,09
52	0,22	2,15
54	0,32	2,25
56	0,21	2,33
58	0,2	2,38
60	0,34	2,59
62	0,34	2,16



Depth (cm)	Pb (ppm)	Al (%)
1	8,5	1,82
2	7,7	1,82
3	7,8	1,85
4	8	1,87
5	8,5	1,97
6	8,6	1,99
7	8,8	2,02
8	8,9	2,01
9	9,1	2,07
10	8,7	2,1
11	9,1	2,11
12	9,6	2,1
25	8,5	1,84
26	8,3	1,8
38	10,2	2,23
44	8	1,85
48	9,9	2,19
52	9,6	2,15
56	10,4	2,33
58	10,5	2,38
60	11,3	2,59
62	9,5	2,16
64	7,9	1,85
66	7,3	1,76

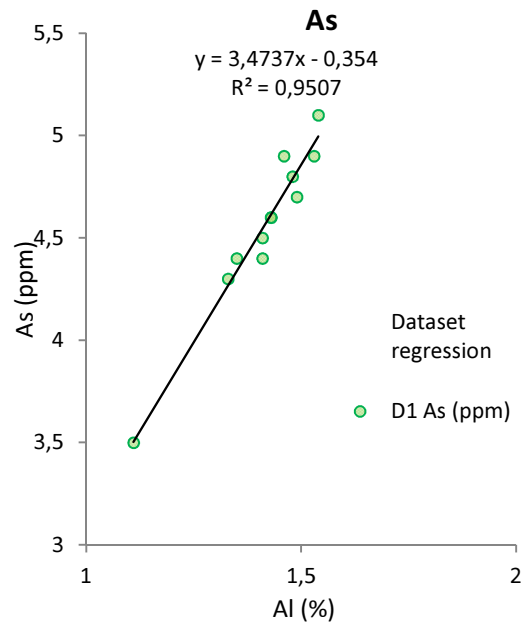
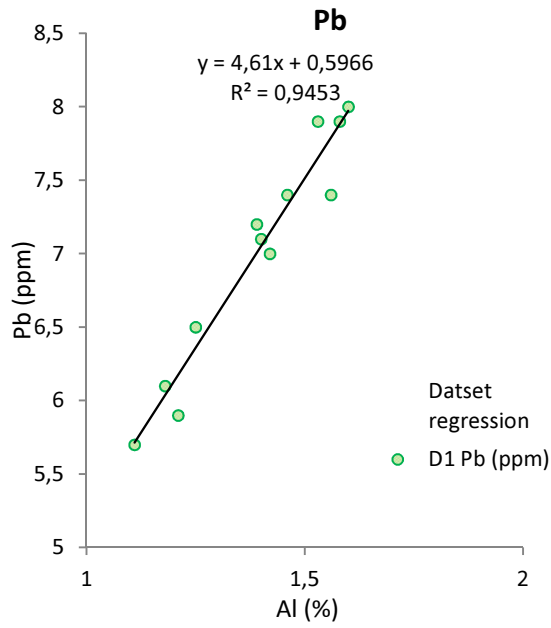
Depth (cm)	As (ppm)	Al (%)
2	8,5	1,82
1	5,2	1,35
2	5,7	1,39
3	5,8	1,44
4	6	1,48
5	6	1,49
6	6,4	1,54
7	6,2	1,52
8	6,5	1,55
9	6,5	1,53
10	6,5	1,53
11	6,9	1,57
12	7,2	1,6
14	7,6	1,61
15	7,4	1,61
19	7,4	1,56
44	7,9	1,85
46	7,8	1,83
48	9,5	2,19
52	9,6	2,15
54	10,5	2,25
56	10,1	2,33
58	8,6	2,38
60	10,9	2,59

The delta core (D1)



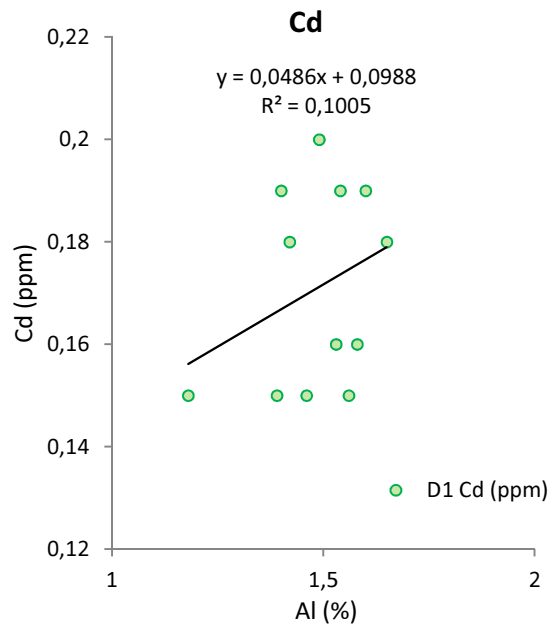
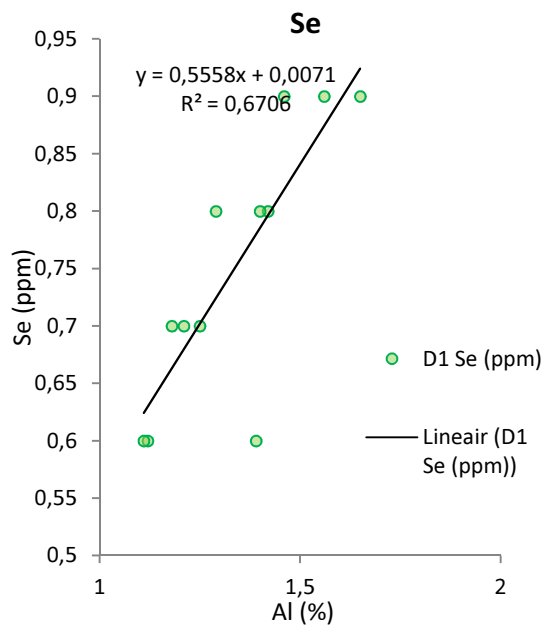
Depth (cm)	Cu (ppm)	Al (%)
25	28,9	1,41
26	25,4	1,41
27	26,7	1,43
28	23,3	1,43
29	24,1	1,46
30	24,8	1,48
32	25,2	1,43
34	25,4	1,49
36	30,2	1,54
38	28	1,53
40	29,9	1,58
42	29,4	1,46

Depth (cm)	Zn (ppm)	Al (%)
34	86	1,49
36	88	1,54
38	80	1,53
40	81	1,58
42	73	1,46
44	74	1,39
46	87	1,65
48	78	1,56
50	82	1,6
52	66	1,21
54	75	1,42
56	77	1,4



Depth (cm)	Pb (ppm)	Al (%)
38	7,9	1,53
40	7,9	1,58
42	7,4	1,46
44	7,2	1,39
48	7,4	1,56
50	8	1,6
52	5,9	1,21
54	7	1,42
56	7,1	1,4
58	6,1	1,18
62	6,5	1,25
66	5,7	1,11

Depth (cm)	As (ppm)	Al (%)
20	4,4	1,35
23	4,6	1,43
24	4,3	1,33
25	4,5	1,41
26	4,4	1,41
28	4,6	1,43
29	4,9	1,46
30	4,8	1,48
34	4,7	1,49
36	5,1	1,54
38	4,9	1,53
66	3,5	1,11



Depth (cm)	Se (ppm)	Al (%)
42	0,9	1,46
44	0,6	1,39
46	0,9	1,65
48	0,9	1,56
52	0,7	1,21
54	0,8	1,42
56	0,8	1,4
58	0,7	1,18
60	0,6	1,12
62	0,7	1,25
64	0,8	1,29
66	0,6	1,11

Depth (cm)	Cd (ppm)	Al (%)
34	0,2	1,49
36	0,19	1,54
38	0,16	1,53
40	0,16	1,58
42	0,15	1,46
44	0,15	1,39
46	0,18	1,65
48	0,15	1,56
50	0,19	1,6
54	0,18	1,42
56	0,19	1,4
58	0,15	1,18

A3 Qualitative descriptions of core E1, B1 and D1

Qualitative description core B1

The top 10 cm contains the majority of the roots and this slowly diminishes until around 20 cm depth. The roots alter the texture and the sediment in this upper part is more airy. The top 55 cm is characterized to be more sandy and contains little iron- and manganese (hydr)oxides (red spots). Below 55 cm depth the clay content increases and so does the amount of iron- and manganese (hydr)oxides, which makes sense as these prefer the finer fraction. Below 80 cm the cores starts to get sandier again and black dots indicating organic matter appear. The sandy parts are also characterized by the presence of mica. The core itself is 88 cm long. Only the upper 64 cm were analyzed for organic matter, radionuclides and geochemistry. When cutting the core, the core split in half. A ruler was drawn on both cores to assure the similarity between the centimeters.



Qualitative description core E1

The lower 30 cm of the core was split in half after cutting. The majority of the bigger roots was located in the upper 10 cm. This did alter the structure causing the sediment to be more airy. The first iron- and manganese (hydr)oxides started to appear at a depth of 10 cm together with black spots indicating organic matter degradation. Also from this depth on, the slices are characterized by little holes, probably as a result of biological activity. This continues until a depth of 55 cm. The texture stays consistent below the root zone and consists mainly of clay. This core was the most clayey of all cores. The total length of this core is 66 cm.

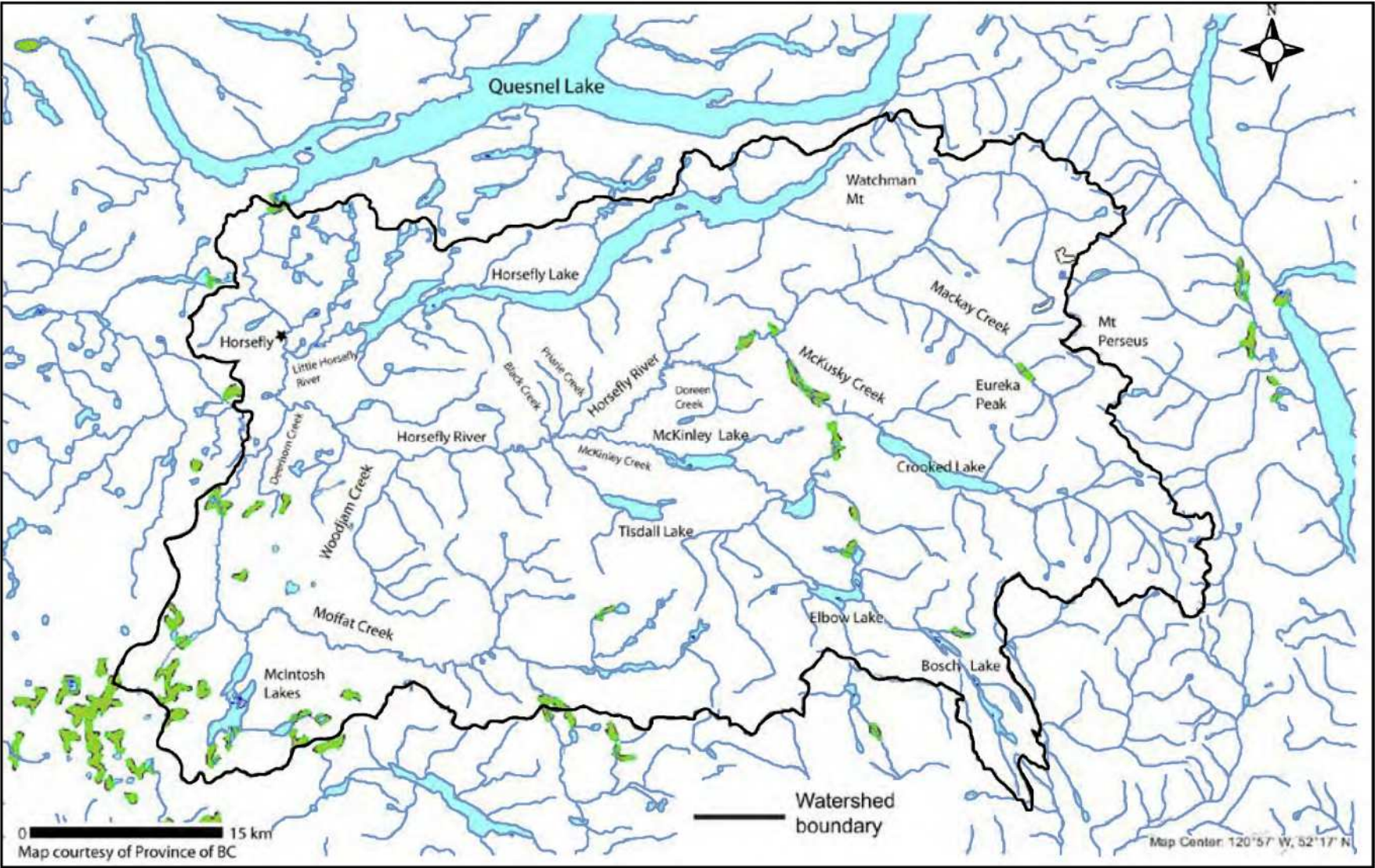


Qualitative description core D1

This core has a somewhat larger root zone of 15 cm. Probably because the delta is a more wet environment and is characterized by different kinds of vegetation. The upper 15 cm contains very small amounts of mica below 5 cm depth. Small pieces of rusty steel are found at a depth of 15 cm, which were already degraded for a large part. A vast number of black spots and little holes appear from 30 cm onwards, indicating organic matter and biological activity. This continues until a depth of 60 cm. Also, a considerable amount of iron- and manganese oxides arises below 30 cm. At 62 cm the core's texture switches from clayey to considerably more sandy, although there is still presence of amounts of iron- and manganese oxides. Pebbles are present from a depth of 56 cm and below, which range in size from 3 mm to 4.5 cm. The total length of this core is 66 cm.



A4 Horsefly watershed map



A5 Geology of the Central Quesnel Belt map



Geological Survey Branch

BULLETIN 97

Map 1

GEOLOGY OF THE CENTRAL QUESNEL BELT BRITISH COLUMBIA

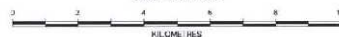
NTS 93A/5, 6, 7, 11, 12, 13;
93B/8, 16; 93G/1; 93H/4

Geology by D.G. Bailey (1976, 1978, 1988, 1989, 1990);

M.A. Bloodgood (1987, 1990); R.B. Campbell (1978); A. Panteleyev and

K.D. Hancock (1989); L. C. Struik (1988, 1984)

Scale 1:100 000



MAPPING SOURCES

- Bailey, D.G. (1976) Geology of the Morehead Lake Area, Central British Columbia, B.C. Ministry of Energy, Mines and Petroleum Resources, Preliminary Map 20 with notes, 1:91 680.
- Bailey, D.G. (1978) The Geology of the Morehead Lake Area, unpublished Ph.D. Thesis, Queen's University, 199 pages.
- Bailey, D.G. (1988) Geology of the Morehead Lake Area, NTS 93A/12, 13; 93B/16; 93G/1; B.C. Ministry of Energy, Mines and Petroleum Resources, Open File 1988-02, 1:50 000 map.
- Bailey, D.G. (1989) Geology of the Swift River Map Area, NTS 93A/5, 6, 7, 11, 12, 13; B.C. Ministry of Energy, Mines and Petroleum Resources, Open File 1989-02, 1:50 000 map.
- Bailey, D.G. (1990) Geology of the Central Quesnel Belt, British Columbia (Part of NTS 93A, 93B, 93G, and 93H); B.C. Ministry of Energy, Mines and Petroleum Resources, Open File 1990-31, 1:50 000 map with notes.
- Bloodgood, M.A. (1987) Delineation History: Stratigraphic Correlations and Geochronology of Eastern Quesnel Terrane Rocks in the Crooked Lake Area, Central British Columbia, Unpublished M. Sc. Thesis, The University of British Columbia, 166 pages.
- Bloodgood, M.A. (1989) Geology of the Lunenburg and Spanish Lake Map Areas, British Columbia, B.C. Ministry of Energy, Mines and Petroleum Resources, Paper 1989-3, 28 pages.
- Campbell, R.B. (1978) Quesnel Lake (89A) Map Area, Geological Survey of Canada, Open File Map 974.
- Panteleyev, A. and Hancock, K.D. (1989) Geology of the Beaver Creek - Hornsby River Map Area, NTS 93A/6; B.C. Ministry of Energy, Mines and Petroleum Resources, Open File 1989-14, 1:50 000 map.
- Struik, L.C. (1984) Geology of Spanish Lake (93A/11) and Parts of Adjacent Map Areas, Central British Columbia, Geological Survey of Canada, Open File Map 922, 1:50 000.
- Struik, L.C. (1984) Geology of Quesnel Lake and Part of Mitchell Lake, British Columbia, Geological Survey of Canada, Open File Map 952, 1:50 000.

SYMBOLS

- Geological contact
- Fold axis: antiform, synform
- Fold axis - overturned: antiform, synform
- Fault, generally high-angle and inferred
- Fault, lateral movement
- Thrust fault
- bedding
- Fracture: steep, not ind., measured
- Jointing: steep, inclined
- Minor fold axis and direction of plunge
- Lineation: plunge, trend
- Glacial striae
- Radiometric date in Ma
- Fossil locality
- Mines prospect: number in legend tabulation
- Placer workings: abandoned, active
- Pyrite, chalcopyrite, native copper, malachite
- Dred body
- Contour interval 200m

SELECTED MINERAL OCCURRENCES

(Refer to text table 5 for full listing)

MAP No	NAME	MINIFILE NUMBER	COMMODITY	TYPE
1	Morehead Mountain	OSB-033	Cu Au	Alluvial porphyry copper
2	M	OSB-036	Cu Au	& related veins
5	Crooked Creek	OSB-038	Cu	siliceous
6	Geron	OSB-119	Cu Au	
17	Morehead	OSB-091	Au Cu	
18	Dillon Lodge	OSB-041	Cu Au	
20	Lively Magnetite	OSB-094	Cu	
22	Morehead	OSB-094	Cu	
24	Cariboo-Bell (Bell, Pelly)	OSB-058	Cu Au	
27	Bayshore	OSB-096	Cu	
33	Brilo	OSB-028	Cu Au	
35	Hood	OSB-112	Cu	
36	BIT	OSB-116	Cu	
37	Finch	OSB-177	Cu Au	
38	Beaverfoot	OSB-155	Cu Ag Au (Pt)	
41	Pyrite	OSB-032	Cu	
-10	Terr	OSB-027	Cu Au Ag Mo	Veins and porphyry copper
-11	Myland Lake	OSB-059	Cu Mo	epithermal
-26	FR	OSB-076	Cu Mo	(calcalkalic porphyry)
-42	Melastache	OSB-078	Cu Au	
-48	DDR	OSB-117	Cu Au	
7	Lyrina	OSB-025	Cu Ag	Limestone-hosted veins
-12	Mitzy	OSB-048	Ag Cu Au Zn	(may be related to alkalic stock)
-14	Site	OSB-049	Cu	
-23	ML	OSB-118	Cu	
6	KB	OSB-027	Pb Zn	Metothermal veins
-28	Jay	OSB-072	Cu Pb Ag Au	
-30	CPW	OSB-043	Ag Pb Zn Ag Cu	
-31	Terr	OSB-147	Ag Pb	
-32	IGN	OSB-132	Au Ag Pb	
-47	Fraserfold	OSB-150	Au Ag	
-29	J	OSB-066	Cu	Volcanic-hosted native copper
-42	Red	OSB-084	Cu	
-44	Mallet	OSB-075	Cu	
3	Cottonwood	OSB-026	Au	Placer gold
4	Macleod	OSB-028	Au	
5	Aravorth	OSB-022	Au	
-15	Quartz Canyon	OSB-018	Au	
-18	Burton Creek	OSB-137	Au	
-19	Bullion Pt	OSB-225	Au	
-21	Morehead Creek	OSB-093	Au	
-29	Crooked Creek	OSB-141	Au	
-35	War's Horn	OSB-015	Au	
-40	Modere	OSB-014	Au	
-48	Horseshoe Hornsby	OSB-042	Au	
-49	Peak Creek	OSB-016	Au	
-54	Antona Creek	OSB-017	Au	

Many other occurrences, marked *

LEGEND

SEDIMENTARY AND VOLCANIC ROCKS

PLEISTOCENE - RECENT

- Qs1 Unconsolidated glacial, fluvio-glacial sediments (gravel, sand, silt and clay)

TERTIARY

MIOCENE (may include some younger)

- 11 Maroon and gray volcanic: alkali olivine basalt flows, breccia
- 11a Conglomerate, sandstone

Eocene

- 10 Gray, massive trachyandesite, trachyte, tuffe flows, breccia, ash flow tuffs, tuff
- 10a Gray and cream sandstone, mudstone, siltsone; minor conglomerate and tuff

CRETACEOUS

- 9 Gray polytypic cobble conglomerate, dark grey mudstone, sandstone and conglomerate (fine-up sequence); distinctive orange-weathering carbonate matrix

JURASSIC

AALENIAN

- 6 Gray and maroon polytypic cobble and pebble conglomerate, shale, siltstone, sandstone, minor redbeds

PLEINSBACHAL-TOJARCANT

- 5 Gray siltstone and sandstone, massive to well bedded; commonly pyritic; calcareous

PLEINSBACHIAN?

- 4 Maroon argillaceous and vesicular, uncaliche-bearing olivine pyroxene basalt, breccias and flows

SINEMUKHAN-PLEINSBACHIAN

- 3c Feldspathic, luffaceous siltstone, sandstone; minor volcanic breccia
- 3b Latice crystal tuff, tuff breccia and tuffaceous sandstone, minor ash flow breccia
- 3a Maroon and gray polytypic volcanic breccias, characterized by the presence of feldspar clasts
- 3 Polytypic breccias - undifferentiated 3a, 3b, 3c. Coarse to medium-grained plagioclase-pyroxene basaltic to intermediate, feldspathic ('felsic') volcaniclastic rocks, flows, low-dome complexes, loc of unit has conglomerate, sandstone and limestone beds

TRIASSIC

CARIBUAN-NORMAN

- 2g Melagolose latite and pyroxene-phyric basalt flows, breccia and lithic tuffs. In Beaver Creek Valley mainly polytypic conglomerate with abundant feldspathic clasts and rare porphyroclastic - diastrophite and
- 2f Dark brown to grey and grey-green mafic sandstone, siltstone, calcareous siltstone and sandstone. Limestone
- 2e Dark green and maroon andesitic-bearing pyroxene basalt flows and breccia, locally crystal and lithic tuffs. Vol - apophytic plug with rare plagioclase lenses
- 2d Greenish-grey to maroon hornblende-bearing pyroxene basalt; locally dark green pyroxene crystal wafers
- 2c Polytypic maroon and grey basaltic breccia with rare to absent leucite crystals, basaltic lithic tuff, pyroxene grain wafers
- 2b Maroon and grey pyroxene-phyric and plagioclase microcline alkali basalt flows, breccia, minor maroon and dark green basaltic lithic tuff and sandstone
- 2a Green and grey pyroxene-phyric alkali olivine and aphantic alkali basalt flows, breccia, minor pillow basalt; interbedded mudstone, limestone breccia

ANISIAN-CARNIAN

- 1 Dark grey and brown sandstone (pyroxene grain wafers), siltstone, shale, micaceous, phyllitic rocks in the eastern map area. Minor mafic tuffaceous unit

1A

- Dark green pyroxene-hornblende-plagioclase microcline to phyllic basalt flows, breccia, tuff, breccia and conglomerate calcareous siltstone aprons around volcanic centres interfingering with unit 1

PENNSYLVANIAN - PERMIAN

- DTS Serpentine, amoncholate, sheared ultramafic rock; talc schist

MISSISSIPPIAN - UPPER TRIASSIC

- MTQ Hobbit chert, agillite, greenstone, mafic volcanic rocks; lesser limestone, basalt and andesite; includes minor serpenitized porphyrite and other ultramafic rocks
- PROTEROZOIC - MISSISSIPPIAN
- DWqD Megacrystic gneissite to granite super orthogneiss
- PP Schist, gneiss, echistose quartzite, phyllite, marble, amoncholate; minor quartzite clast conglomerate, siltite

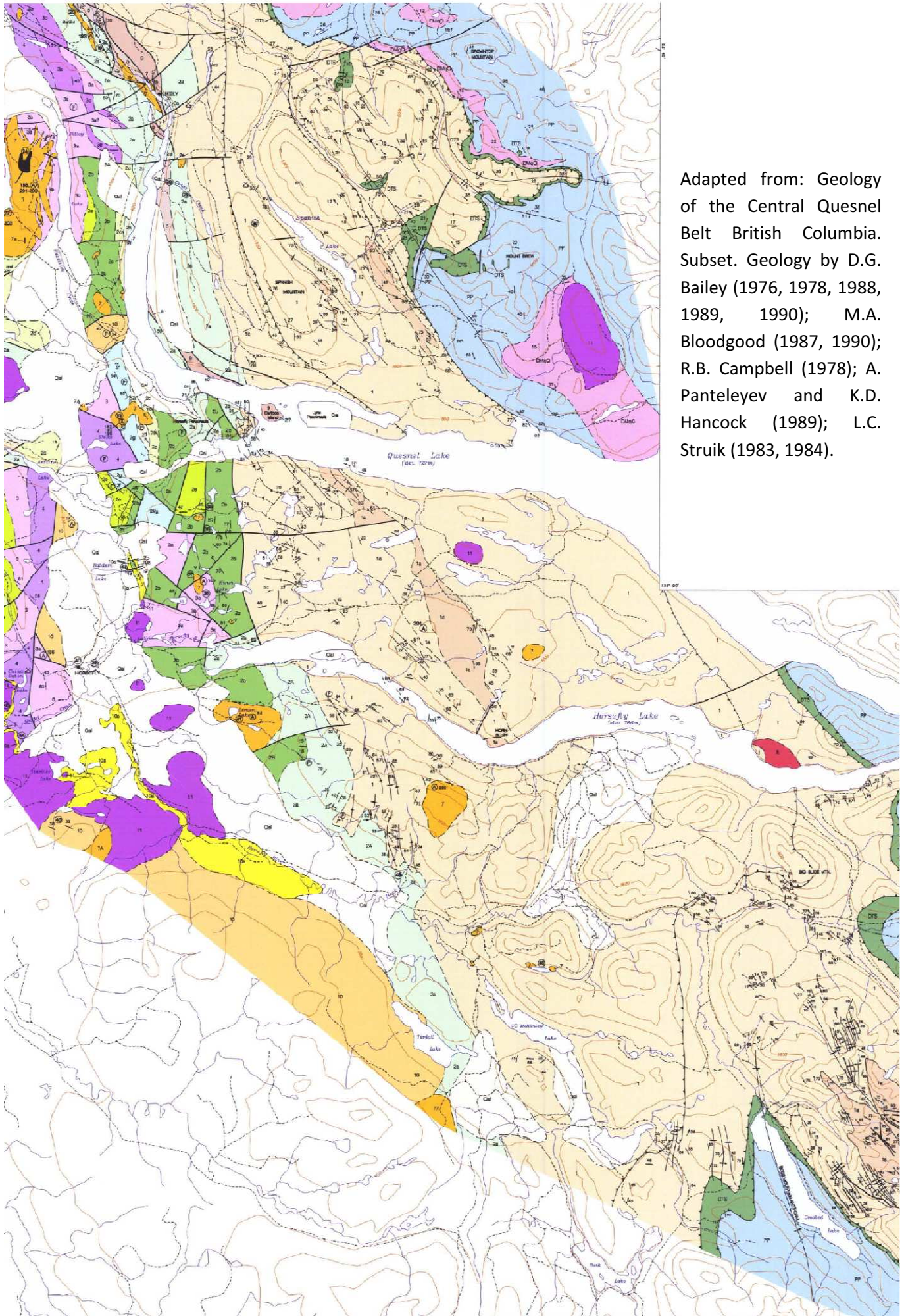
INTRUSIVE ROCKS

- 6 Medium to coarse-grained, hornblende granodiorite and quartz monzonite, leucocratic quartz monzonite and diorite

- 7b Medium to coarse-grained, hornblende and/or pyroxene-bearing, nepheline syenite, orbicular in part

- 7 Pink and grey medium to fine-grained diorite, monzonite syenite; minor plagioclase and hornblende phenocrysts; rare olivopyroxene gabbro and peridotite

- 7a Grey, medium-grained equigranular to porphyritic quartz diorite, granodiorite (laxominite barometer in part)



Adapted from: Geology of the Central Quesnel Belt British Columbia. Subset. Geology by D.G. Bailey (1976, 1978, 1988, 1989, 1990); M.A. Bloodgood (1987, 1990); R.B. Campbell (1978); A. Panteleyev and K.D. Hancock (1989); L.C. Struik (1983, 1984).

A6 Grain size dataset

Depth (cm) <2µm (%) Al (%)			Depth (cm) <2µm (%) Al (%)			Depth (cm) <2µm (%) Al (%)		
0,5	8,41	1,82	0,5	6,67	1,35	1	1,23	8,73
1,5	6,88	1,82	1,5	5,74	1,39	2,5	1,24	7,75
2,5	7,10	1,85	2,5	6,04	1,44	3,5	1,3	8,35
3,5	6,66	1,87	3,5	6,38	1,48	4,5	1,28	7,69
4,5	7,74	1,97	4,5	7,27	1,49	5,5	1,28	9,68
5,5	7,26	1,99	5,5	6,76	1,54	6,5	1,38	6,31
6,5	7,52	2,02	6,5	7,27	1,52	7,5	1,35	9,08
7,5	6,21	2,01	7,5	7,82	1,55	8,5	1,35	7,84
8,5	6,28	2,07	8,5	6,88	1,53	9,5	1,34	9,48
9,5	6,13	2,1	9,5	6,31	1,53	10,5	1,35	7,72
10,5	6,36	2,11	10,5	6,99	1,57	11,5	1,37	6,84
11,5	6,90	2,1	11,5	7,45	1,6	12,5	1,34	7,85
12,5	6,87	1,91	12,5	6,37	1,57	13,5	1,46	9,31
13,5	7,04	1,9	13,5	7,74	1,61	14,5	1,36	7,02
14,5	4,66	1,78	14,5	5,64	1,61	15,5	1,31	9,84
15,5	4,09	1,72	15,5	6,00	1,58	16,5	1,36	8,81
16,5	4,37	1,67	16,5	7,31	1,58	17,5	1,24	8,83
17,5	3,65	1,58	17,5	6,62	1,57	18,5	1,35	7,53
18,5	4,71	1,52	18,5	5,45	1,56	19,5	1,35	6,15
19,5	5,98	1,48	19,5	5,91	1,69	20,5	1,37	6,75
20,5	5,07	1,44	20,5	5,90	1,59	21,5	1,36	6,88
21,5	4,33	1,5	21,5	5,02	1,75	22,5	1,43	6,39
22,5	4,43	1,61	22,5	6,26	1,83	23,5	1,33	7,21
23,5	3,77	1,64	23,5	6,13	1,74	24,5	1,41	5,79
24,5	4,63	1,57	24,5	6,86	1,84	25,5	1,41	6,48
25,5	4,10	1,55	25,5	6,64	1,8	26,5	1,43	9,74
26,5	4,57	1,61	26,5	6,30	1,67	27,5	1,43	8,03
27,5	5,47	1,62	27,5	5,42	1,58	28,5	1,46	5,16
28,5	5,82	1,64	28,5	7,35	1,4	29,5	1,48	7,24
29,5	4,72	1,54	29,5	6,05	1,52	31,5	1,43	7,32
31,5	4,84	1,42	31,5	7,04	1,63	33,5	1,49	8,17
33,5	5,44	1,58	33,5	8,42	2,01	35,5	1,54	9,37
35,5	5,60	1,39	35,5	7,96	2,11	37,5	1,53	8,42
37,5	6,32	1,52	37,5	8,29	2,23	39,5	1,58	9,14
39,5	3,62	1,31	39,5	9,83	2,42	41,5	1,46	6,41
41,5	5,55	1,69	41,5	11,34	2,51	43,5	1,39	7,26
43,5	6,33	1,65	43,5	7,32	1,85	45,5	1,65	8,99
45,5	5,05	1,61	45,5	6,55	1,83	47,5	1,56	7,01
47,5	4,18	1,56	47,5	7,88	2,19	49,5	1,6	6,24
49,5	4,43	1,63	49,5	6,85	2,09	51,5	1,21	6,83
51,5	5,32	1,78	51,5	4,76	2,15	53,5	1,42	6,14
53,5	6,65	1,67	53,5	9,84	2,25	55,5	1,4	8,86
55,5	5,70	1,68	55,5	7,47	2,33	57,5	1,18	6,33
57,5	5,17	1,68	57,5	7,98	2,38	59,5	1,12	9,96
61,5	6,32	1,65	59,5	10,77	2,59	61,5	1,25	8,27
63,5	5,66	1,64	61,5	8,78	2,16	63,5	1,29	8,73
			63,5	8,01	1,85	65,5	1,11	8,82
			65,5	7,47	1,76			

A7 Organic matter dataset

sample nr.	OM (%)	sample nr.	OM (%)	sample nr.	OM (%)
0-1/9-12B1	12,5	0-1/9-12E1	13,1	0-2/9-12D1	14,3
1-2/9-12B1	12,6	1-2/9-12E1	12,8	2-3/9-12D1	13,4
2-3/9-12B1	11,3	2-3/9-12E1	12,2	3-4/9-12D1	13,4
3-4/9-12B1	10,3	3-4/9-12E1	11,5	4-5/9-12D1	13,5
4-5/9-12B1	9,9	4-5/9-12E1	11,6	5-6/9-12D1	12,8
5-6/9-12B1	9,5	5-6/9-12E1	11,1	6-7/9-12D1	13,2
6-7/9-12B1	9,0	6-7/9-12E1	10,2	7-8/9-12D1	13,0
7-8/9-12B1	8,5	7-8/9-12E1	10,4	8-9/9-12D1	12,0
8-9/9-12B1	7,8	8-9/9-12E1	10,7	9-10/9-12D1	12,7
9-10/9-12B1	6,8	9-10/9-12E1	10,4	10-11/912D1	12,8
10-11/9-12B1	6,5	10-11/9-12E1	9,9	11-12/912D1	13,4
11-12/9-12B1	6,7	11-12/9-12E1	9,4	12-13/912D1	13,1
12-13/9-12B1	6,8	12-13/9-12E1	9,1	13-14/912D1	13,0
13-14/9-12B1	6,9	13-14/9-12E1	9,0	14-15/912D1	12,8
14-15/9-12B1	5,9	14-15/9-12E1	8,8	15-16/912D1	13,7
15-16/9-12B1	5,2	15-16/9-12E1	8,3	16-17/912D1	15,2
16-17/9-12B1	5,0	16-17/9-12E1	8,0	17-18/912D1	14,2
17-18/9-12B1	4,5	17-18/9-12E1	8,2	18-19/912D1	13,9
18-19/9-12B1	4,4	18-19/9-12E1	7,8	19-20/912D1	13,0
19-20/9-12B1	4,1	19-20/9-12E1	5,4	20-21/912D1	13,9
20-21/9-12B1	3,8	20-21/9-12E1	4,5	21-22/912D1	13,5
21-22/9-12B1	9,6	21-22/9-12E1	5,0	22-23/912D1	13,1
22-23/9-12B1	4,7	22-23/9-12E1	5,3	23-24/9-2D1	12,3
23-24/9-12B1	4,4	23-24/9-12E1	4,5	24-25/912D1	11,4
24-25/9-12B1	-	24-25/9-12E1	5,4	25-26/912D1	10,4
25-26/9-12B1	4,0	25-26/9-12E1	5,6	26-27/912D1	9,1
26-27/9-12B1	4,2	26-27/9-12E1	4,5	27-28/912D1	8,0
27-28/9-12B1	4,0	27-28/9-12E1	4,2	28-29/912D1	7,4
28-29/9-12B1	4,0	28-29/9-12E1	4,0	29-30/912D1	7,3
29-30/9-12B1	3,8	29-30/9-12E1	3,8	30-31/912D1	7,3
30-31/9-12B1	3,4	30-31/9-12E1	3,8	31-32/912D1	6,4
31-32/9-12B1	3,4	31-32/9-12E1	4,0	32-33/912D1	6,7
32-33/9-12B1	4,7	32-33/9-12E1	4,9	33-34/912D1	6,1
33-34/9-12B1	3,9	33-34/9-12E1	7,1	34-35/912D1	6,4
34-35/9-12B1	3,8	34-35/9-12E1	8,0	35-36/912D1	5,7
35-36/9-12B1	3,1	35-36/9-12E1	7,7	36-37/912D1	5,2
36-37/9-12B1	3,6	36-37/9-12E1	7,2	37-38/912D1	-
37-38/9-12B1	3,7	37-38/9-12E1	6,8	38-39/912D1	5,8
38-39/9-12B1	3,5	38-39/9-12E1	5,8	39-40/912D1	5,2
39-40/9-12B1	2,9	39-40/9-12E1	6,2	40-41/912D1	-
40-41/9-12B1	4,2	40-41/9-12E1	7,4	41-42/912D1	4,8
41-42/9-12B1	4,1	41-42/9-12E1	7,5	42-43/912D1	4,4
42-43/9-12B1	4,2	42-43/9-12E1	5,8	43-44/912D1	4,7
43-44/9-12B1	4,0	43-44/9-12E1	4,2	44-45/912D1	5,2

44-45/9-12B1	3,8	44-45/9-12E1	4,6	45-46/912D1	5,4
45-46/9-12B1	4,1	45-46/9-12E1	4,0	46-47/912D1	5,3
46-47/9-12B1	3,6	46-47/9-12E1	4,5	47-48/912D1	4,9
47-48/9-12B1	3,6	47-48/9-12E1	5,7	48-49/912D1	5,2
48-49/9-12B1	3,8	48-49/9-12E1	5,3	49-50/912D1	5,6
49-50/9-12B1	3,7	49-50/9-12E1	4,6	50-51/912D1	4,7
50-51/9-12B1	4,0	50-51/9-12E1	4,5	51-52/912D1	4,0
51-52/9-12B1	4,6	51-52/9-12E1	4,2	52-53/912D1	4,2
52-53/9-12B1	4,2	52-53/9-12E1	5,4	53-54/912D1	4,6
53-54/9-12B1	3,9	53-54/9-12E1	5,5	54-55/912D1	4,6
54-55/9-12B1	4,0	54-55/9-12E1	5,3	55-56/912D1	6,1
55-56/9-12B1	4,2	55-56/9-12E1	5,0	56-57/912D1	3,9
56-57/9-12B1	4,4	56-57/9-12E1	4,9	57-58/912D1	3,4
57-58/9-12B1	4,2	57-58/9-12E1	5,4	58-59/912D1	-
58-59/9-12B1	3,9	58-59/9-12E1	5,9	59-60/912D1	-
59-60/9-12B1	3,8	59-60/9-12E1	-	60-61/912D1	4,1
60-61/9-12B1	4,2	60-61/9-12E1	5,3	61-62/912D1	3,8
61-62/9-12B1	4,0	61-62/9-12E1	4,8	62-63/912D1	-
62-63/9-12B1	3,9	62-63/9-12E1	4,2	63-64/912D1	4,0
63-64/9-12B1	4,1	63-64/9-12E1	4,2	64-65/912D1	4,2
64-65/9-12B1	4,3	64-65/9-12E1	4,5	65-66/912D1	-
		65-66/9-12E1	4,8		

A8 Radionuclide dataset

Core B1

Depth (cm)	Cs-137 (Bq/kg)	Pb(excess) (Bq/kg)
0,5	10,14	73,86
2,5	7,05	41,8
4,5	6,58	22,99
6,5	5,32	21,3
8,5	4,69	2,65
10,5	2,04	1,94
12,5	2,34	-4,95
14,5	1,36	-1,11
16,5	0	2,22
18,5	0	0,08
20,5	0	1,26
22,5	0	3,22
24,5	0	0,92
26,5	0	1,78
28,5	0	8,29

Core E1

Depth (cm)	Cs-137 (Bq/kg)	Pb(excess) (Bq/kg)
0,5	7,21	77,48
2,5	8,74	42,11
4,5	8,54	31,92
6,5	8,04	19,29
8,5	7,3	14,61
10,5	6,57	14,96
12,5	6,34	14,06
14,5	4,64	15,2
16,5	4,16	14,63
18,5	2,27	8,53
20,5	1,13	5,1
22,5	1,12	2,99
24,5	1,13	10,41
26,5	0,63	6,06
28,5	0,69	7,64

Core D1

Depth (cm)	Cs-137 (Bq/kg)	Pb(excess) (Bq/kg)
1	13,09	69,88
2,5	13,53	49,82
4,5	12,87	27,89
6,5	12,92	21,27
8,5	12,47	20,31
10,5	12,89	18,16
12,5	13,48	13,59
14,5	12,69	15,34
16,5	14,27	19,75
18,5	15,31	12,29
20,5	13,74	15,19
22,5	11,27	11,91
24,5	8,57	15,33
26,5	4,82	3,7
28,5	2,32	9,03

A9 Geochemical data



ALS Canada Ltd.
2103 Dollarton Hwy
North Vancouver BC V7H 0A7
Phone: 604 984 0221 Fax: 604 984 0218 www.alsglobal.com

To: UNIVERSITY OF NORTHERN BRITISH COLUMBIA
COLLEGE OF SCIENCE AND MANAGEMENT
3333 UNIVERSITY WAY
PRINCE GEORGE BC V2N 4Z9

Page: 1
Finalized Date: 4-DEC-2012
Account: UNBC

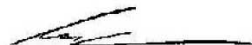
CERTIFICATE VA12282121
Project: Horsefly P.O. No.: VN 923277 This report is for 142 Pulp samples submitted to our lab in Vancouver, BC, Canada on 29-NOV-2012. The following have access to data associated with this certificate: PHIL OWENS

SAMPLE PREPARATION	
ALS CODE	DESCRIPTION
WEI-21	Received Sample Weight
LOG-24	Pulp Login - Rcd w/o Barcode
TRA-21	Transfer sample
ANALYTICAL PROCEDURES	
ALS CODE	DESCRIPTION
ME-MS41	51 anal. aqua regia ICPMS

To: UNIVERSITY OF NORTHERN BRITISH COLUMBIA
ATTN: PHIL OWENS
COLLEGE OF SCIENCE AND MANAGEMENT
3333 UNIVERSITY WAY
PRINCE GEORGE BC V2N 4Z9

This is the Final Report and supersedes any preliminary report with this certificate number. Results apply to samples as submitted. All pages of this report have been checked and approved for release.

***** See Appendix Page for comments regarding this certificate *****

Signature: 
Colin Ramshaw, Vancouver Laboratory Manager



ALS Canada Ltd.
2103 Dollarton Hwy
North Vancouver BC V7H 0A7
Phone: 604 984 0221 Fax: 604 984 0218 www.alsglobal.com

To: UNIVERSITY OF NORTHERN BRITISH COLUMBIA
COLLEGE OF SCIENCE AND MANAGEMENT
3333 UNIVERSITY WAY
PRINCE GEORGE BC V2N 4Z9

Page: 2 - A
Total # Pages: 5 (A - D)
Plus Appendix Pages
Finalized Date: 4-DEC-2012
Account: UNBC

Project: Horsefly

Sample Description	Method Analyte Units LOR	CERTIFICATE OF ANALYSIS VA12282121															
		WEI-21 Recvd Wt. kg	ME-MS41 Ag ppm	ME-MS41 Al ppm	ME-MS41 As ppm	ME-MS41 Au ppm	ME-MS41 B ppm	ME-MS41 Ba ppm	ME-MS41 Be ppm	ME-MS41 Bi ppm	ME-MS41 Ca ppm	ME-MS41 Cd ppm	ME-MS41 Ce ppm	ME-MS41 Co ppm	ME-MS41 Cr ppm	ME-MS41 Cs ppm	
B1 0-1	<0.02	0.78	1.82	9.0	<0.2	<10	140	0.47	0.22	0.68	0.57	37.1	16.7	58	1.28		
B1 1-2	<0.02	0.38	1.82	8.5	<0.2	<10	130	0.40	0.21	0.60	0.54	37.0	16.1	59	1.25		
B1 2-3	<0.02	0.34	1.85	9.0	<0.2	<10	140	0.47	0.23	0.57	0.53	37.7	16.1	59	1.31		
B1 3-4	<0.02	0.35	1.87	9.4	<0.2	<10	140	0.48	0.22	0.57	0.54	38.5	16.5	60	1.34		
B1 4-5	<0.02	0.37	1.97	10.3	<0.2	<10	150	0.46	0.23	0.59	0.50	41.8	17.8	62	1.45		
B1 5-6	<0.02	0.35	1.99	10.3	<0.2	<10	150	0.53	0.23	0.59	0.46	42.0	17.7	63	1.42		
B1 6-7	<0.02	0.35	2.02	10.5	<0.2	<10	150	0.53	0.25	0.60	0.45	43.0	17.6	63	1.49		
B1 7-8	<0.02	0.36	2.01	10.6	<0.2	<10	150	0.51	0.24	0.60	0.42	43.0	17.7	64	1.50		
B1 8-9	<0.02	0.35	2.07	11.3	<0.2	<10	150	0.51	0.24	0.60	0.40	45.6	17.9	65	1.54		
B1 9-10	<0.02	0.36	2.10	11.5	<0.2	<10	160	0.53	0.24	0.59	0.38	46.2	18.0	66	1.58		
B1 10-11	<0.02	0.43	2.11	11.9	<0.2	<10	160	0.55	0.26	0.60	0.38	46.8	18.1	67	1.63		
B1 11-12	<0.02	0.35	2.10	12.4	<0.2	<10	160	0.53	0.26	0.60	0.36	47.9	18.9	66	1.64		
B1 12-13	<0.02	0.35	1.91	11.4	<0.2	<10	150	0.51	0.24	0.54	0.34	42.1	17.7	63	1.69		
B1 13-14	<0.02	0.36	1.90	10.9	<0.2	<10	150	0.52	0.23	0.55	0.35	42.1	17.4	62	1.66		
B1 14-15	<0.02	0.36	1.78	12.6	<0.2	<10	140	0.49	0.24	0.51	0.36	45.6	17.4	61	1.75		
B1 15-16	<0.02	0.32	1.72	13.7	<0.2	<10	130	0.47	0.23	0.48	0.36	46.6	16.8	59	1.69		
B1 16-17	<0.02	0.33	1.67	15.5	<0.2	<10	120	0.47	0.24	0.47	0.37	47.6	16.8	57	1.77		
B1 17-18	<0.02	0.32	1.58	17.2	<0.2	<10	120	0.43	0.22	0.47	0.35	43.7	16.3	55	1.83		
B1 18-19	<0.02	0.32	1.52	15.9	<0.2	<10	110	0.39	0.22	0.47	0.37	43.8	15.8	53	1.59		
B1 19-20	<0.02	0.31	1.48	11.1	<0.2	<10	110	0.38	0.20	0.46	0.38	41.5	15.3	52	1.49		
B1 20-21	<0.02	0.28	1.44	9.0	<0.2	<10	100	0.38	0.19	0.48	0.37	40.5	14.3	50	1.45		
B1 21-22	<0.02	0.31	1.50	9.2	<0.2	<10	110	0.41	0.19	0.49	0.37	39.9	14.2	52	1.42		
B1 22-23	<0.02	0.35	1.61	10.0	<0.2	<10	120	0.44	0.21	0.49	0.43	45.0	15.7	55	1.60		
B1 23-24	<0.02	0.33	1.64	9.4	<0.2	<10	120	0.41	0.22	0.50	0.45	43.7	15.9	54	1.56		
B1 24-25	<0.02	0.32	1.57	9.1	<0.2	<10	120	0.40	0.19	0.51	0.44	42.7	15.2	52	1.47		
B1 25-26	<0.02	0.32	1.55	8.9	<0.2	<10	110	0.39	0.20	0.50	0.43	42.8	14.4	55	1.48		
B1 26-27	<0.02	0.35	1.61	10.0	<0.2	<10	120	0.44	0.22	0.49	0.45	43.7	15.8	56	1.57		
B1 27-28	<0.02	0.34	1.62	9.9	<0.2	<10	130	0.43	0.21	0.50	0.46	45.5	16.2	57	1.62		
B1 28-29	<0.02	0.35	1.64	9.6	<0.2	<10	130	0.43	0.22	0.52	0.40	48.3	16.0	58	1.59		
B1 29-30	<0.02	0.35	1.54	8.9	<0.2	<10	120	0.39	0.20	0.50	0.40	47.0	14.7	55	1.46		
B1 31-32	<0.02	0.26	1.42	7.9	<0.2	<10	110	0.36	0.17	0.50	0.33	38.5	13.4	49	1.26		
B1 33-34	<0.02	0.33	1.58	8.7	<0.2	<10	110	0.41	0.22	0.50	0.37	45.2	15.0	56	1.60		
B1 35-36	<0.02	0.29	1.39	6.8	<0.2	<10	100	0.37	0.18	0.49	0.33	43.3	12.5	50	1.38		
B1 37-38	<0.02	0.36	1.52	8.2	<0.2	<10	110	0.40	0.20	0.48	0.34	43.1	13.9	53	1.52		
B1 39-40	<0.02	0.22	1.31	7.3	<0.2	<10	90	0.33	0.18	0.49	0.36	40.3	12.8	46	1.31		
B1 41-42	<0.02	0.39	1.69	9.7	<0.2	<10	130	0.42	0.20	0.55	0.30	42.1	15.4	55	1.52		
B1 43-44	<0.02	0.38	1.65	9.2	<0.2	<10	120	0.44	0.22	0.50	0.29	45.2	15.8	58	1.61		
B1 45-46	<0.02	0.36	1.61	9.3	<0.2	<10	110	0.39	0.21	0.48	0.25	45.3	15.2	57	1.62		
B1 47-48	<0.02	0.37	1.56	8.9	<0.2	<10	110	0.40	0.22	0.47	0.24	47.6	15.2	54	1.66		
B1 49-50	<0.02	0.37	1.63	9.4	<0.2	<10	120	0.44	0.21	0.50	0.20	47.0	16.1	56	1.63		

***** See Appendix Page for comments regarding this certificate *****



ALS Canada Ltd.
 2103 Dollarton Hwy
 North Vancouver BC V7H 0A7
 Phone: 604 984 0221 Fax: 604 984 0218 www.alsglobal.com

To: UNIVERSITY OF NORTHERN BRITISH
 COLUMBIA
 COLLEGE OF SCIENCE AND MANAGEMENT
 3333 UNIVERSITY WAY
 PRINCE GEORGE BC V2N 4Z9

Page: 4 - D
 Total # Pages: 5 (A - D)
 Plus Appendix Pages
 Finalized Date: 4-DEC-2012
 Account: UNBC

Project: Horsefly

CERTIFICATE OF ANALYSIS VA12282121

Sample Description	Method Analyte Units LOR	ME-MS41	ME-MS41	ME-MS41	ME-MS41	ME-MS41	ME-MS41	ME-MS41
		Tl ppm 0.02	U ppm 0.05	V ppm 1	W ppm 0.05	Y ppm 0.05	Zn ppm 2	Zr ppm 0.5
E1 37-38		0.19	2.35	64	0.21	10.50	117	<0.5
E1 39-40		0.21	2.50	65	0.21	11.90	107	0.7
E1 41-42		0.26	4.01	69	0.24	18.60	105	0.7
E1 43-44		0.17	1.86	53	0.19	9.56	67	0.5
E1 45-46		0.18	2.01	51	0.22	10.75	68	0.6
E1 47-48		0.21	3.58	55	0.21	16.75	95	0.6
E1 49-50		0.21	2.48	55	0.20	12.85	90	0.8
E1 51-52		0.21	3.05	57	0.20	12.80	83	0.9
E1 53-54		0.21	2.64	68	0.20	14.10	90	0.6
E1 55-56		0.22	2.02	65	0.20	11.00	82	0.7
E1 57-58		0.22	2.03	64	0.19	10.70	89	0.7
E1 59-60		0.22	3.29	70	0.21	15.30	122	1.1
E1 61-62		0.20	2.54	63	0.18	13.85	99	1.2
E1 63-64		0.18	2.30	58	0.19	13.00	86	1.2
E1 65-66		0.16	2.82	53	0.45	14.25	81	1.0
D1 0-2		0.09	0.83	52	0.15	7.02	289	1.0
D1 2-3		0.10	0.85	52	0.11	6.89	291	1.0
D1 3-4		0.10	0.83	54	0.11	7.09	312	1.0
D1 4-5		0.11	0.84	53	0.15	7.26	307	1.1
D1 5-6		0.11	0.87	53	0.12	7.51	318	1.2
D1 6-7		0.10	0.87	57	0.11	7.38	359	1.3
D1 7-8		0.11	0.89	56	0.13	7.55	358	1.3
D1 8-9		0.11	0.90	56	0.13	7.52	332	1.2
D1 9-10		0.10	0.89	55	0.12	7.48	351	1.2
D1 10-11		0.11	0.89	55	0.11	7.25	361	1.2
D1 11-12		0.10	0.89	56	0.12	7.42	365	1.2
D1 12-13		0.10	0.87	55	0.12	7.38	338	1.2
D1 13-14		0.11	1.00	60	0.19	7.52	357	1.3
D1 14-15		0.10	0.93	56	0.14	7.34	325	1.3
D1 15-16		0.10	0.86	53	0.71	6.72	329	1.2
D1 16-17		0.09	0.87	56	0.22	6.81	352	1.2
D1 17-18		0.09	0.78	52	0.56	6.42	389	1.2
D1 18-19		0.11	0.86	55	0.14	7.11	388	1.2
D1 19-20		0.11	0.83	56	0.18	6.80	403	1.1
D1 20-21		0.10	0.86	56	0.13	7.08	408	1.2
D1 21-22		0.10	0.86	56	0.13	6.94	377	1.3
D1 22-23		0.10	0.87	59	0.13	7.08	365	1.3
D1 23-24		0.10	0.83	55	0.16	6.64	308	1.3
D1 24-25		0.10	0.88	58	0.15	6.67	276	1.3
D1 25-26		0.10	0.79	58	0.14	6.43	219	1.2

**** See Appendix Page for comments regarding this certificate ****



ALS Canada Ltd.
 2103 Dollarton Hwy
 North Vancouver BC V7H 0A7
 Phone: 604 984 0221 Fax: 604 984 0218 www.alsglobal.com

To: UNIVERSITY OF NORTHERN BRITISH
 COLUMBIA
 COLLEGE OF SCIENCE AND MANAGEMENT
 3333 UNIVERSITY WAY
 PRINCE GEORGE BC V2N 4Z9

Page: 5 - A
 Total # Pages: 5 (A - D)
 Plus Appendix Pages
 Finalized Date: 4-DEC-2012
 Account: UNBC

Project: Horsefly

CERTIFICATE OF ANALYSIS VA12282121

Sample Description	Method Analyte Units LOR	WB-21	ME-MS41	ME-MS41	ME-MS41	ME-MS41	ME-MS41	ME-MS41	ME-MS41	ME-MS41	ME-MS41	ME-MS41	ME-MS41	ME-MS41	ME-MS41	ME-MS41
		Revd Wt. kg 0.02	Ag ppm 0.01	Al % 0.01	As ppm 0.1	Au ppm 0.2	B ppm 10	Ba ppm 10	Be ppm 0.05	Bi ppm 0.01	Ca % 0.01	Cd ppm 0.01	Ce ppm 0.02	Co ppm 0.1	Cr ppm 1	Cs ppm 0.05
D1 26-27		<0.02	0.15	1.43	4.9	<0.2	<10	140	0.32	0.20	0.75	0.52	28.8	10.9	46	0.73
D1 27-28		<0.02	0.14	1.43	4.6	<0.2	<10	130	0.32	0.17	0.71	0.38	26.7	10.3	45	0.69
D1 28-29		<0.02	0.14	1.46	4.9	<0.2	<10	130	0.36	0.17	0.70	0.34	28.5	10.3	47	0.69
D1 29-30		<0.02	0.13	1.48	4.8	<0.2	<10	130	0.37	0.17	0.71	0.34	29.6	10.7	49	0.73
D1 31-32		<0.02	0.13	1.43	5.6	<0.2	<10	120	0.39	0.15	0.67	0.28	29.9	11.1	47	0.73
D1 33-34		<0.02	0.13	1.49	4.7	<0.2	<10	110	0.43	0.14	0.64	0.20	32.3	10.6	47	0.77
D1 35-36		<0.02	0.14	1.54	5.1	<0.2	<10	120	0.44	0.15	0.65	0.19	34.3	11.3	50	0.79
D1 37-38		<0.02	0.14	1.53	4.9	<0.2	<10	120	0.42	0.15	0.64	0.16	36.6	11.0	48	0.83
D1 39-40		<0.02	0.15	1.58	5.7	<0.2	<10	120	0.46	0.16	0.63	0.16	38.9	11.8	51	0.88
D1 41-42		<0.02	0.15	1.46	5.2	<0.2	<10	110	0.43	0.14	0.58	0.15	39.0	11.3	48	0.88
D1 43-44		<0.02	0.13	1.39	5.4	<0.2	<10	110	0.44	0.13	0.60	0.15	38.3	11.3	49	0.76
D1 45-46		<0.02	0.17	1.65	5.7	<0.2	<10	140	0.46	0.17	0.63	0.18	43.8	13.1	53	0.89
D1 47-48		<0.02	0.15	1.56	5.8	<0.2	<10	130	0.47	0.16	0.61	0.15	39.5	12.5	50	0.86
D1 49-50		<0.02	0.16	1.60	6.5	<0.2	<10	140	0.53	0.17	0.62	0.19	43.8	14.7	54	0.95
D1 51-52		<0.02	0.10	1.21	4.8	<0.2	<10	110	0.40	0.11	0.62	0.17	33.9	12.0	58	0.67
D1 53-54		<0.02	0.14	1.42	5.4	<0.2	<10	120	0.40	0.14	0.62	0.18	35.9	13.4	58	0.78
D1 55-56		<0.02	0.15	1.40	6.0	<0.2	<10	110	0.44	0.15	0.58	0.19	39.0	12.8	51	0.90
D1 57-58		<0.02	0.12	1.18	4.1	<0.2	<10	100	0.33	0.12	0.57	0.15	35.6	10.5	54	0.86
D1 59-60		<0.02	0.12	1.12	3.9	<0.2	<10	90	0.31	0.11	0.57	0.17	35.8	10.6	52	0.85
D1 61-62		<0.02	0.19	1.25	5.1	<0.2	<10	110	0.36	0.12	0.59	0.18	38.1	11.7	51	0.85
D1 63-64		<0.02	0.13	1.29	5.1	<0.2	<10	110	0.40	0.13	0.62	0.23	41.9	14.1	52	0.88
D1 65-66		<0.02	0.11	1.11	3.5	<0.2	<10	80	0.32	0.11	0.56	0.17	36.2	11.4	51	0.87

**** See Appendix Page for comments regarding this certificate ****



ALS Canada Ltd.
 2103 Dollarton Hwy
 North Vancouver BC V7H 0A7
 Phone: 604 984 0221 Fax: 604 984 0218 www.alsglobal.com

To: UNIVERSITY OF NORTHERN BRITISH
 COLUMBIA
 COLLEGE OF SCIENCE AND MANAGEMENT
 3333 UNIVERSITY WAY
 PRINCE GEORGE BC V2N 4Z9

Page: 5 - B
 Total # Pages: 5 (A - D)
 Plus Appendix Pages
 Finalized Date: 4-DEC-2012
 Account: UNBC

Project: Horsefly

CERTIFICATE OF ANALYSIS VA12282121

Sample Description	Method Analyte Units LOR	ME-MS41	ME-MS41	ME-MS41	ME-MS41	ME-MS41	ME-MS41	ME-MS41	ME-MS41	ME-MS41	ME-MS41	ME-MS41	ME-MS41	ME-MS41	ME-MS41	ME-MS41	ME-MS41
		Cu ppm	Fe %	Ga ppm	Ge ppm	Hf ppm	Hg ppm	In ppm	K %	La ppm	Li ppm	Mg %	Mn ppm	Mo ppm	Na %	Nb ppm	Ni %
D1 26-27		26.7	2.54	4.50	0.06	0.04	0.04	0.019	0.13	14.2	12.0	0.67	398	1.50	0.03	1.05	
D1 27-28		23.3	2.54	4.23	0.06	0.03	0.04	0.019	0.13	13.1	11.3	0.67	363	1.40	0.03	0.98	
D1 28-29		24.1	2.59	4.32	0.06	0.03	0.04	0.019	0.12	13.8	11.7	0.69	351	1.45	0.03	1.00	
D1 29-30		24.8	2.58	4.43	0.07	0.03	0.04	0.019	0.12	14.5	12.1	0.69	350	1.43	0.03	1.03	
D1 31-32		25.2	2.60	4.12	0.06	0.04	0.04	0.019	0.11	14.3	11.4	0.67	340	1.48	0.04	0.98	
D1 33-34		25.4	2.54	4.25	0.06	0.03	0.03	0.017	0.11	14.8	12.1	0.69	309	1.43	0.03	0.97	
D1 35-36		30.2	2.66	4.36	0.07	0.04	0.04	0.018	0.11	15.8	12.5	0.71	318	1.46	0.03	1.00	
D1 37-38		28.0	2.58	4.24	0.06	0.04	0.05	0.019	0.12	16.5	12.2	0.69	305	1.46	0.04	0.96	
D1 39-40		29.9	2.74	4.38	0.07	0.04	0.03	0.020	0.12	17.5	13.1	0.73	325	1.51	0.04	0.98	
D1 41-42		29.4	2.51	4.19	0.07	0.03	0.03	0.020	0.10	18.2	12.4	0.67	296	1.50	0.04	0.96	
D1 43-44		28.6	2.49	4.04	0.06	0.04	0.03	0.018	0.10	17.7	11.7	0.65	319	1.44	0.03	0.93	
D1 45-46		36.5	2.84	4.69	0.07	0.04	0.03	0.020	0.12	20.9	14.3	0.76	371	1.80	0.03	0.96	
D1 47-48		34.6	2.70	4.24	0.07	0.04	0.03	0.019	0.12	19.9	12.4	0.70	404	1.82	0.03	0.86	
D1 49-50		38.4	2.87	4.66	0.07	0.04	0.04	0.021	0.13	22.4	13.4	0.72	455	2.11	0.04	0.98	
D1 51-52		28.2	2.45	3.64	0.06	0.04	0.03	0.016	0.10	18.3	8.7	0.55	426	1.47	0.04	0.75	
D1 53-54		36.8	2.69	4.04	0.07	0.04	0.04	0.019	0.11	19.8	11.2	0.65	454	1.88	0.04	0.78	
D1 55-56		37.6	2.62	4.13	0.07	0.04	0.04	0.018	0.11	21.3	12.8	0.64	361	2.04	0.03	0.86	
D1 57-58		29.1	2.28	3.58	0.07	0.04	0.04	0.016	0.10	18.6	10.2	0.54	326	1.31	0.04	0.81	
D1 59-60		28.4	2.21	3.56	0.07	0.04	0.03	0.015	0.09	18.7	9.7	0.52	343	1.25	0.04	0.80	
D1 61-62		30.3	2.37	3.67	0.08	0.04	0.03	0.016	0.11	19.6	10.7	0.57	421	1.54	0.04	0.82	
D1 63-64		36.6	2.46	3.84	0.08	0.05	0.04	0.017	0.11	22.0	11.2	0.60	554	1.49	0.04	0.82	
D1 65-66		27.9	2.26	3.49	0.08	0.04	0.03	0.016	0.09	18.4	10.2	0.53	382	1.00	0.04	0.78	

**** See Appendix Page for comments regarding this certificate ****



ALS Canada Ltd.
 2103 Dollarton Hwy
 North Vancouver BC V7H 0A7
 Phone: 604 984 0221 Fax: 604 984 0218 www.alsglobal.com

To: UNIVERSITY OF NORTHERN BRITISH
 COLUMBIA
 COLLEGE OF SCIENCE AND MANAGEMENT
 3333 UNIVERSITY WAY
 PRINCE GEORGE BC V2N 4Z9

Page: 5 - C
 Total # Pages: 5 (A - D)
 Plus Appendix Pages
 Finalized Date: 4-DEC-2012
 Account: UNBC

Project: Horsefly

CERTIFICATE OF ANALYSIS VA12282121

Sample Description	Method Analyte Units LOR	ME-MS41	ME-MS41	ME-MS41	ME-MS41	ME-MS41	ME-MS41	ME-MS41	ME-MS41	ME-MS41	ME-MS41	ME-MS41	ME-MS41	ME-MS41	ME-MS41	ME-MS41	ME-MS41
		Ni ppm	P ppm	Pb ppm	Rb ppm	Re ppm	S %	Sb ppm	Sc ppm	Se ppm	Si ppm	Sr ppm	Ta ppm	Tb ppm	Th ppm	Ti ppm	Tl ppm
D1 26-27		29.7	1290	14.5	30.3	0.001	0.02	0.87	3.8	1.4	0.5	60.6	<0.01	0.02	1.7	0.091	
D1 27-28		27.0	1260	11.2	25.9	0.001	0.02	0.74	3.6	1.2	0.4	54.6	<0.01	0.03	1.8	0.091	
D1 28-29		28.3	1250	10.5	23.5	0.001	0.02	0.68	3.8	1.0	0.4	54.5	<0.01	0.02	1.9	0.093	
D1 29-30		28.4	1260	10.4	22.9	0.001	0.02	0.68	3.9	1.2	0.4	54.9	<0.01	0.02	2.1	0.096	
D1 31-32		28.2	1270	9.1	19.2	0.001	0.01	0.62	3.9	1.1	0.4	51.3	<0.01	0.02	2.2	0.092	
D1 33-34		28.4	1230	7.9	18.0	0.001	0.01	0.54	4.0	1.0	0.4	49.8	<0.01	0.03	2.3	0.093	
D1 35-36		30.9	1290	9.6	17.7	0.001	0.01	0.57	4.2	1.2	0.4	49.4	<0.01	0.04	2.4	0.096	
D1 37-38		28.9	1280	7.9	17.2	0.001	0.01	0.49	4.4	1.1	0.4	48.6	<0.01	0.03	2.6	0.097	
D1 39-40		30.7	1280	7.9	16.6	0.001	0.01	0.53	4.6	1.0	0.4	47.3	<0.01	0.03	3.0	0.099	
D1 41-42		29.8	1260	7.4	16.6	0.001	0.01	0.51	4.5	0.9	0.4	45.4	<0.01	0.02	2.8	0.091	
D1 43-44		28.8	1280	7.2	14.9	0.001	<0.01	0.47	4.5	0.6	0.4	45.2	<0.01	0.03	3.1	0.091	
D1 45-46		34.0	1340	8.6	18.6	0.001	0.01	0.49	5.2	0.9	0.4	48.9	<0.01	0.04	3.2	0.098	
D1 47-48		30.7	1260	7.4	19.3	<0.001	0.01	0.51	4.8	0.9	0.3	45.4	<0.01	0.03	3.2	0.097	
D1 49-50		34.0	1330	8.0	22.7	0.001	0.01	0.60	5.6	1.0	0.4	49.5	<0.01	0.03	3.4	0.101	
D1 51-52		26.8	1420	5.9	16.3	0.001	0.01	0.52	4.6	0.7	0.3	45.4	<0.01	0.02	2.9	0.097	
D1 53-54		30.7	1400	7.0	19.9	0.001	0.01	0.55	5.1	0.8	0.3	46.6	<0.01	0.03	3.0	0.096	
D1 55-56		31.8	1390	7.1	21.4	0.001	0.01	0.57	5.1	0.8	0.4	44.5	<0.01	0.04	3.3	0.092	
D1 57-58		26.9	1440	6.1	18.5	<0.001	0.01	0.48	4.1	0.7	0.4	41.5	<0.01	0.03	3.5	0.096	
D1 59-60		26.6	1490	5.9	20.1	<0.001	0.01	0.44	4.1	0.6	0.4	41.7	<0.01	0.02	3.6	0.095	
D1 61-62		28.1	1520	6.5	18.5	<0.001	0.01	0.48	4.4	0.7	0.3	41.9	<0.01	0.03	3.6	0.097	
D1 63-64		30.5	1510	7.1	19.4	0.001	0.01	0.61	4.8	0.8	0.3	45.2	<0.01	0.03	3.5	0.096	
D1 65-66		26.5	1370	5.7	16.8	<0.001	0.01	0.47	4.2	0.6	0.3	41.5	<0.01	0.02	3.7	0.094	

**** See Appendix Page for comments regarding this certificate ****



ALS Canada Ltd.
 2103 Dollarton Hwy
 North Vancouver BC V7H 0A7
 Phone: 604 984 0221 Fax: 604 984 0218 www.alsglobal.com

To: UNIVERSITY OF NORTHERN BRITISH
 COLUMBIA
 COLLEGE OF SCIENCE AND MANAGEMENT
 3333 UNIVERSITY WAY
 PRINCE GEORGE BC V2N 4Z9

Page: 5 - D
 Total # Pages: 5 (A - D)
 Plus Appendix Pages
 Finalized Date: 4-DEC-2012
 Account: UNBC

Project: Horsefly

CERTIFICATE OF ANALYSIS VA12282121

Sample Description	Method Analyte Units LOR	ME-MS41	ME-MS41	ME-MS41	ME-MS41	ME-MS41	ME-MS41	ME-MS41
		Tl ppm	U ppm	V ppm	W ppm	Y ppm	Zn ppm	Zr ppm
D1 26-27		0.09	0.80	60	0.13	6.52	184	1.6
D1 27-28		0.09	0.76	60	0.15	6.30	147	1.4
D1 28-29		0.09	0.79	61	0.12	6.49	132	1.5
D1 29-30		0.09	0.80	62	0.15	6.77	126	1.5
D1 31-32		0.08	0.81	61	0.21	6.86	101	1.7
D1 33-34		0.10	0.87	59	0.22	7.26	86	1.5
D1 35-36		0.10	0.94	62	0.12	7.88	88	1.8
D1 37-38		0.11	1.00	60	0.15	8.37	80	1.8
D1 39-40		0.11	1.10	61	0.13	8.84	81	1.9
D1 41-42		0.11	1.15	56	0.17	9.37	73	1.7
D1 43-44		0.10	1.16	58	0.12	9.60	74	1.9
D1 45-46		0.12	1.44	61	0.54	11.20	87	1.9
D1 47-48		0.12	1.40	60	0.15	11.15	78	1.9
D1 49-50		0.13	1.62	64	0.13	12.85	82	2.0
D1 51-52		0.09	1.31	67	0.10	11.15	66	2.2
D1 53-54		0.10	1.52	66	0.12	12.25	75	1.9
D1 55-56		0.11	1.63	59	0.13	12.60	77	1.7
D1 57-58		0.10	1.37	60	0.64	10.60	72	1.8
D1 59-60		0.11	1.30	59	1.82	10.40	82	1.7
D1 61-62		0.10	1.39	57	0.52	11.00	95	1.8
D1 63-64		0.12	1.59	59	0.18	12.60	148	2.1
D1 65-66		0.10	1.25	57	0.21	10.35	121	1.9

***** See Appendix Page for comments regarding this certificate *****



ALS Canada Ltd.
 2103 Dollarton Hwy
 North Vancouver BC V7H 0A7
 Phone: 604 984 0221 Fax: 604 984 0218 www.alsglobal.com

To: UNIVERSITY OF NORTHERN BRITISH
 COLUMBIA
 COLLEGE OF SCIENCE AND MANAGEMENT
 3333 UNIVERSITY WAY
 PRINCE GEORGE BC V2N 4Z9

Page: Appendix 1
 Total # Appendix Pages: 1
 Finalized Date: 4-DEC-2012
 Account: UNBC

Project: Horsefly

CERTIFICATE OF ANALYSIS VA12282121

Method	CERTIFICATE COMMENTS
ME-MS41	Gold determinations by this method are semi-quantitative due to the small sample weight used (0.5g).